NOVEL VIRAL AND ASTROCYTIC CONTRIBUTORS TO EPILEPSY

Julie Chen

A DISSERTATION

in

Neuroscience

Presented to the Faculties of the University of Pennsylvania

in

Partial Fulfillment of the Requirements for the

Degree of Doctor of Philosophy

2015

_____

Stewart A. Anderson, Associate Professor of Psychiatry
Supervisor of Dissertation

_____

Joshua I. Gold, Professor of Neuroscience
Graduate Group Chairperson

Dissertation Committee:
Eric D. Marsh, Assistant Professor of Neurology
Michael B. Robinson, Professor of Pediatrics (Committee Chairperson)
Douglas C. Wallace, Professor of Pathology and Laboratory Medicine
Zhaolan Zhou, Assistant Professor of Genetics

ACKNOWLEDGEMENT

I would like to thank Dr. Stewart Anderson for providing the stimulating lab environment I was seeking in my third year and recognizing my potential when I so often failed to see it. To the members of the Anderson lab, past and present, as well as our collaborators – a fun and diverse group of people who have been instrumental in shaping my development as a scientist from helpful discussions on my project, to tips on public speaking, and fun times outside of the lab – thank you. I would also like to thank my thesis committee members: Drs. Eric Marsh, Mike Robinson, Doug Wallace, and Zhaolan Zhou for their contributions in fostering ideas that are now a part of this dissertation, as well as their kind support, both professional and personal.

My thanks go out to the administrative team and faculty of the BGS NGG program and beyond. My journey through graduate school would not have been as smooth were it not for the organization of Jane Hoshi, Christine Clay, Chloe Newsome, Sherri Ghee, and the help and support of Dr. Josh Gold.

To my Penn friends for all the board games, nerdy TV shows, music, pop culture education, and life advice: life as a graduate student would not have been the same without you! A shout out to my special friend Lee Dietterich, who witnessed me undergo cycles of insanity and helped me through it all with adventures in music, international travel, food, love, and patience. Lastly, to my family, for being there every step of the way (and never asking me when I was going to graduate), and my sister Catherine Chen, Ph.D., who best understood what this journey was all about and provided endless nuggets of wisdom, humor, and support. Thank you.

ABSTRACT

NOVEL VIRAL AND ASTROCYTIC CONTRIBUTORS TO EPILEPSY

Julie Chen

Stewart A. Anderson

Epilepsy is a neurological seizure disorder affecting approximately 1% of the world's population. Seizure disorders are numerous, heterogeneous, and can develop from a multitude of physiological conditions including but not limited to interneuron dysfunction, ion channel mutations, irregular development and layering of the cerebral cortex, abnormalities in cell signaling pathways, brain tumors, traumatic brain injuries, and mitochondrial diseases. In many seizure disorders, gene mutations (primary) cause physiological abnormalities (secondary) that result in seizures. In some cases, the primary cause of epilepsy remains unknown, and in other cases, the secondary cause remains to be determined. My thesis research identified a novel, exogenous primary contributor to epilepsy in a specific subtype of cortical malformation disorders, as well as a secondary astrocytic irregularity resulting from a mitochondria-related nuclear gene mutation that may contribute to epilepsy. In Chapter 1, I briefly introduce the relationship between cortical malformation disorders, mitochondrial disease, and epilepsy. In Chapter 2, I present data supporting the idea that the cortical dyslamination and resultant epilepsy in focal cortical dysplasia type IIB is caused by the human papillomavirus oncoprotein E6. In Chapter 3, I present data on astrocyte-specific irregularities resulting from mitochondrial

aspartate glutamate carrier loss of function and its effects on glutamatergic neurotransmission, and speculate on the role and importance of astrocytes in seizure genesis and propagation.

Table of Contents

List of Tables

List of Figures

Chapter 1
Introduction

Epilepsy is a neurological seizure disorder defined by the recurrence of two or more unprovoked seizures more than 24 hours apart (Fisher et al., 2014). The first reports of epileptic patients can be traced back to Assyrian texts from 2,000 B.C., making epilepsy one of the oldest medical conditions described (Magiorkinis et al., 2014). Today, more than 50 million people worldwide (approximately 1%) suffer from epilepsy, with the incidence on the rise (Banerjee et al., 2009). The study of epilepsy poses a unique challenge because it is a disorder with a singular set of symptoms (seizures) that can be caused by a multitude of physiological conditions, each of which may have their own causes. A PubMed search on causes of epilepsy yields numerous results: interneuron dysfunction, sodium channel mutations, cortical dyslamination, cellular signaling abnormalities, brain tumors, traumatic brain injury, and metabolic and/or mitochondrial dysregulation (Figure 1.1). My thesis research focused on identifying novel contributors to epilepsy and is divided into two chapters: 1) identification of a viral element that causes cortical dyslamination; and 2) identification of an astrocytic irregularity resulting from mitochondrial dysfunction, which may contribute to abnormal glutamate neurotransmission underlying epilepsy. In the first part of this chapter, I introduce cortical lamination disorders and the role that hyperactivated mammalian target of rapamycin (mTOR) signaling plays in the development of these disorders, and subsequently, of epilepsy. In the second part of this chapter, I discuss the neurologic effects of mitochondrial and metabolic dysfunction and how they result in epilepsy.

Cortical lamination disorders, mTOR signaling, and epilepsy

Malformations of cortical development are one of the most common causes of intractable epilepsy (Blumcke et al., 2009; Aronica et al., 2012), and can be categorized into three groups with considerable overlap based on their causes. Group I consists of malformations that result from abnormal neuronal and glial proliferation or apoptosis, and includes conditions such as the megalencephalies, tuberous sclerosis complex, and the focal cortical dysplasias. Group II describes malformations resulting from abnormal neuronal migration, such as Pretzel Syndrome and lissencephaly. Finally, Group III consists of malformations from abnormal postmigrational development, such as the focal cortical dysplasias. A commonality among cortical malformation disorders is that many of them result from the dysregulation of signaling pathways that regulate cell size, neuronal migration, and cortical development. One such signaling pathway that is commonly dysregulated is the mammalian target of rapamycin (mTOR) signaling complex (Figure 1.2).

mTOR is a highly conserved, cytosolic serine/threonine kinase that is a member of the phosphatidylinositol-3-kinase (PI3K-related protein kinase, or PIKK) family (Abraham, 2004). First identified in 1991 in a genetic screen to identify the protein target of the drug rapamycin (Heitman et al., 1991), mTOR functions as part of the AMPK metabolic signaling complex to sense a cell's nutrient, energy, and growth factor availability to ultimately regulate its protein expression, growth, and, in the nervous system, migration (Potter et al., 2001; Loewith et al., 2002; Potter et al., 2002; Hahn-Windgassen et al., 2005; Ruvinsky et al., 2005). mTOR exists and

functions in two distinct multi-protein complexes, aptly named mTORC1 and mTORC2 (Sarbassov et al., 2004). mTORC1 is sensitive to rapamycin and regulates cell growth and proliferation in response to nutrient signaling and sensing. The majority of the literature published on mTOR is focused on mTORC1, as rictor, a protein component in mTORC2, is not conserved across species, rendering the study of mTORC2 regulators and targets less extensive and less well understood.

Because of the role of mTOR in cell growth, proliferation, and migration, it is essential for the development of the brain. Knocking out mTOR in the mouse results in a defect in the formation of the telencephalon and embryonic lethality (Murakami et al., 2004). The ablation of other proteins along the mTOR pathway also results in embryonic or early lethality. Using nestin-Cre to create a conditional raptor knockout mouse to study the effects of mTOR knockout on brain development, researchers discovered that even the raptor conditional knockout mice died at early ages, with a pronounced microcephalic phenotype underscored by reductions in cell size and cell number (Cloëtta et al., 2013). Besides development, mTOR conditional knockout mice have also revealed roles for mTOR in dendrite formation (Jaworski et al., 2005) and axon elongation (Campbell and Holt, 2001).

In addition to regulating cell growth and proliferation, mTORC1 also regulates protein translation and ribosome biogenesis through the phosphorylation of ribosomal S6 kinase 1 and suppression of elongation factor 4E binding protein 1 (4EBP1), respectively (Pause et al., 1994; Pearson et al., 1995; Saitoh et al., 2002). Phosphorylated S6K1 then goes on to phosphorylate the 40S ribosomal protein S6.

Phosphorylated S6 is a commonly used readout for mTORC1 activation, and we employ this readout in the studies conducted in Chapter 2.

Recently, researchers have identified numerous genetic mutations in mTORC1 that underlie neurological seizure conditions. The first demonstration of an epilepsy syndrome directly related to enhanced mTORC1 activation was tuberous sclerosis complex (TSC), an autosomal dominant, multisystemic disorder resulting from the loss of function of one or both negative regulators of mTOR TSC1 and TSC2 (Baybis et al., 2004; Crino et al., 2006). TSC has been identified in all ethnic groups, with no gender bias. It is estimated that approximately 2 million people worldwide are affected with TSC, with 65-75% of patients harboring spontaneous *de novo* mutations (Hyman et al., 2000). Patients with TSC develop benign tumors in multiple organ systems, and brain tubers consisting of neuroglial cells exhibiting a loss of hexalaminar organization in the brain. Over 80% of TSC patients suffer from seizures, and it has been demonstrated that the cortical tubers are highly correlated with epileptic foci (Evans et al., 2012).

A second example of hyperactivated mTOR signaling in seizures occurs in the rare, neurodevelopmental disorder polyhydramnios, megalencephaly, and symptomatic epilepsy syndrome (PMSE), or Pretzel Syndrome (Orlova et al., 2010). Pretzel Syndrome, so named because of characteristic body posture displayed by affected patients, results from a loss of function mutation in STE20-related kinase adaptor alpha (STRADA), an upstream inhibitor of mTORC1. Patients with Pretzel Syndrome display heterotopic neurons in the subcortical white matter and subependymal regions. A recent study demonstrated STRADA loss of function-

induced deficits in neuronal migration, path finding, and polarity *in vitro* and altered cortical lamination *in vivo* in an acute, inducible mouse model of Pretzel Syndrome, demonstrating another link between hyperactive mTORC1 signaling, cortical dyslamination, and epilepsy (Parker et al., 2013).

Although TSC, Pretzel Syndrome, and a number of other cortical lamination disorders have now been associated with identifiable mutations in mTORC1, the genetic cause for other mTORC1 hyperactive cortical malformation disorders remains elusive. One example of this is the Group I/III disorder focal cortical dysplasia type IIB (FCDIIB). Focal cortical dysplasia type IIB is characterized by the presence of balloon cells – multinucleated cells with enlarged cytoplasms – which display hyperactive mTOR signaling. In Chapter 2, I will discuss the discovery of a viral mTOR-activating agent present only in FCDIIB brain specimens that we believe underlies the pathogenesis of cortical dyslamination and seizures.

Mitochondrial and metabolic dysfunction and epilepsy

Mitochondrial diseases are multisystemic disorders caused by abnormal metabolic pathways within the mitochondria, which result in decreased energy production. Mitochondrial diseases can result from either an inherited gene mutation, or through *de novo* mutations in mitochondrial proteins (inborn errors of metabolism). There are now over 500 identified inborn errors of metabolism (Saudubray et al., 2006), with an overall incidence 1:1000 (Campeau et al., 2008). The most common presentation of mitochondrial disease, inherited or congenital, is encephalomyopathy (Schmiedel et al., 2003), which is highly co-morbid with seizures and epilepsy.

Different epilepsy phenotypes have been described that result from inborn errors of metabolism or *de novo* or inherited mutations in mitochondrial DNA (most often in the enzymatic complexes that comprise the oxidative phosphorylation machinery) or mitochondria-related nuclear gene mutations (Khurana et al., 2013).

The most well-known mitochondrial DNA-related epilepsy syndromes is mitochondrial encephalomyopathy, lactic acidosis, and stroke-like episodes (MELAS), which can result from mutations in complex I, V, or the mitochondrially encoded transfer RNAs histidine, leucine 1, or valine. First characterized in 1984 (Pavlakis et al., 1984), mutations that cause MELAS often result in a build up of lactic acid, which results in muscle weakness, headaches, gastrointestinal issues, and seizures (Hirano and Pavlakis, 1994). Another mitochondrial DNA-related epilepsy syndrome is myoclonic epilepsy and ragged red fibers (MERRF), a condition resulting most often from mutations in mitochondrial transfer RNA lysine, as well as in leucine 1, histidine, and serine 1. Epilepsy is the defining characteristic of MERRF (Fukuhara et al., 1980), with patients presenting with progressive myoclonus or generalized tonic-clonic seizures (Berkovic et al., 1989). Lastly, Kearns-Sayre syndrome is a multisystemic disorder resulting from large mitochondrial DNA mutations that affects approximately 3 in 100,000 individuals. Mitochondrial DNA mutation deletions that cause Kearns-Sayre are often associated with proteins involved in oxidative phosphorylation. Epileptic seizures in MELAS, MERRF, and Kearns-Sayre syndrome can include myoclonic, tonic-clonic, absence, or status-like seizures, and patients frequently display more than one seizure type.

Though complex II is the only member of the enzymatic oxidative phosphorylation machinery fully encoded by nuclear DNA, the fact is nuclear DNA also encodes many other mitochondrial proteins, including components of the other oxidative phosphorylation complexes. The most common nuclear-encoded mitochondrial gene mutation occurs in the *POLG* gene, which encodes the catalytic subunit of the mitochondrial DNA polymerase. Mutations in *POLG* result in Alpers' disease, a condition of severe intractable seizures occurring early in life with intellectual disability and hypotonia, ataxic neuropathies, and chronic progressive external ophthalmoplegia (Naviaux and Nguyen, 2004; Van Goethem et al., 2003; Van Goethem et al., 2001). Other mutations in nuclear-encoded mitochondrial proteins often result in the deletion of large segments of mitochondrial DNA or damage of mitochondrial DNA due to defective nucleotide exchange across the mitochondrial membrane. The encoded nuclear proteins include but are not limited to thymidine phosphorylase, adenine nucleotide translocator 1, and TWINKLE (Nishino et al., 1999; Kaukonen et al., 2000; Spelbrink et al., 2001).

Despite the knowledge that patients with mitochondrial mutations have epilepsy, the cause and effect relationship between mitochondrial mutations and epilepsy is highly debated. On the one hand, mitochondrial dysfunction results in diminished ATP output and altered calcium homeostasis, both of which have effects on neuronal excitability and seizure susceptibility. On the other hand, prolonged seizures can result in mitochondrial oxidative stress and free radical production. In a whole genome mitochondrial DNA sequencing study of temporal lobe epilepsy patients, researchers found that the majority of heteroplasmic mitochondrial DNA

mutations was highly congregated to the epileptic region of the hippocampus, suggesting that mitochondrial mutations are the underlying pathology for seizures in temporal lobe epilepsy (Azakli et al., 2013). In Chapter 3, I will discuss the cell-specific effects contributing to seizures of the loss of function of a nuclear-encoded mitochondrial protein, Slc25a12.

Figure 1.1. Epilepsy is a seizure disorder resulting from many different physiological conditions.

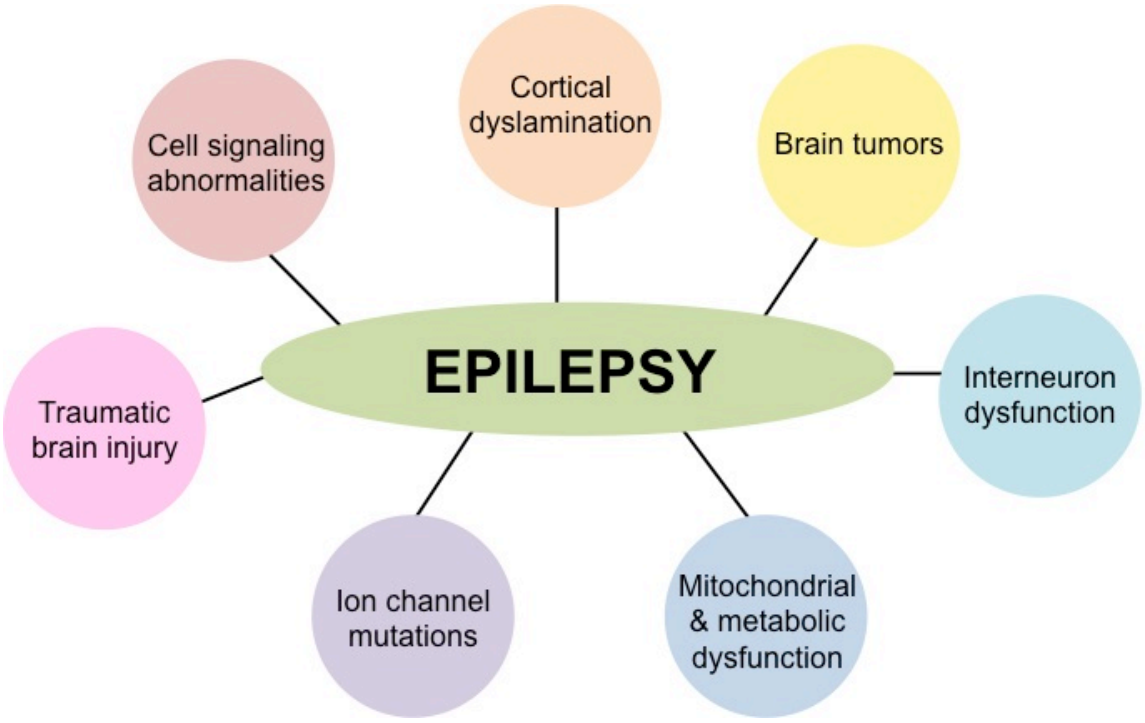

Figure 1.2. The mTOR signaling cascade.

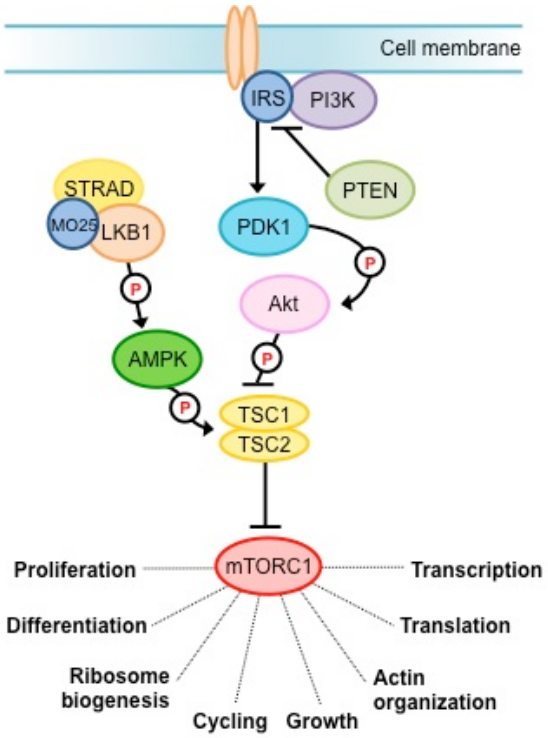

References

Abraham RT (2004) PI 3-kinase related kinases: 'big' players in stress-induced signaling pathways. DNA repair *3*:883-887.

Aronica E, Becker AJ, Spreafico R (2012) Malformations of cortical development. Brain pathology *22*:380-401.

Azakli H, Gurses C, Arikan M, Aydoseli A, Aras Y, Sencer A, Gokyigit A, Bilgic B, Ustek D (2013) Whole mitochondrial DNA variations in hippocampal surgical specimens and blood samples with high-throughput sequencing: a case of mesial temporal lobe epilepsy with hippocampal sclerosis. Gene *529*:190-194.

Banerjee PN, Filippi D, Allen Hauser W (2009) The descriptive epidemiology of epilepsy-a review. Epilepsy research *85*:31-45.

Baybis M, Yu J, Lee A, Golden JA, Weiner H, McKhann G, 2nd, Aronica E, Crino PB (2004) mTOR cascade activation distinguishes tubers from focal cortical dysplasia. Annals of neurology *56*:478-487.

Berkovic SF, Carpenter S, Evans A, Karpati G, Shoubridge EA, Andermann F, Meyer E, Tyler JL, Diksic M, Arnold D, et al. (1989) Myoclonus epilepsy and ragged-red fibres (MERRF). 1. A clinical, pathological, biochemical, magnetic resonance spectrographic and positron emission tomographic study. Brain : a journal of neurology *112* (Pt 5):1231-1260.

Blumcke I, Vinters HV, Armstrong D, Aronica E, Thom M, Spreafico R (2009) Malformations of cortical development and epilepsies: neuropathological findings with emphasis on focal cortical dysplasia. Epileptic disorders : international epilepsy journal with videotape *11*:181-193.

Campbell, D. S., and Holt, C. E. (2001). Chemotropic responses of retinal growth cones mediated by rapid local protein synthesis and degradation. Neuron *32*, 1013–1026.

Campeau PM, Scriver CR, Mitchell JJ (2008) A 25-year longitudinal analysis of treatment efficacy in inborn errors of metabolism. Molecular genetics and metabolism *95*:11-16.

Cloetta D, Thomanetz V, Baranek C, Lustenberger RM, Lin S, Oliveri F, Atanasoski S, Ruegg MA (2013) Inactivation of mTORC1 in the developing brain causes microcephaly and affects gliogenesis. The Journal of neuroscience : the official journal of the Society for Neuroscience *33*:7799-7810.

Crino PB, Nathanson KL, Henske EP (2006) The tuberous sclerosis complex. The New England journal of medicine *355*:1345-1356.

Evans LT, Morse R, Roberts DW (2012) Epilepsy surgery in tuberous sclerosis: a review. Neurosurgical focus *32*:E5.

Fisher RS, Acevedo C, Arzimanoglou A, Bogacz A, Cross JH, Elger CE, Engel J, Jr., Forsgren L, French JA, Glynn M, Hesdorffer DC, Lee BI, Mathern GW, Moshe SL, Perucca E, Scheffer IE, Tomson T, Watanabe M, Wiebe S (2014) ILAE official report: a practical clinical definition of epilepsy. Epilepsia *55*:475-482.

Fukuhara N, Tokiguchi S, Shirakawa K, Tsubaki T (1980) Myoclonus epilepsy associated with ragged-red fibres (mitochondrial abnormalities): disease entity or a syndrome? Light-and electron-microscopic studies of two cases and review of literature. Journal of the neurological sciences *47*:117-133.

Hahn-Windgassen A, Nogueira V, Chen CC, Skeen JE, Sonenberg N, Hay N (2005) Akt activates the mammalian target of rapamycin by regulating cellular ATP level and AMPK activity. The Journal of biological chemistry *280*:32081-32089.

Heitman J, Movva NR, Hall MN (1991) Targets for cell cycle arrest by the immunosuppressant rapamycin in yeast. Science *253*:905-909.

Hirano M, Pavlakis SG (1994) Mitochondrial myopathy, encephalopathy, lactic acidosis, and strokelike episodes (MELAS): current concepts. Journal of child neurology *9*:4-13.

Hyman MH, Whittemore VH (2000) National Institutes of Health consensus conference: tuberous sclerosis complex. Archives of neurology *57*:662-665.

Jaworski J, Spangler S, Seeburg DP, Hoogenraad CC, Sheng M (2005) Control of dendritic arborization by the phosphoinositide-3'-kinase-Akt-mammalian target of rapamycin pathway. The Journal of neuroscience : the official journal of the Society for Neuroscience *25*:11300-11312.

Kaukonen J, Juselius JK, Tiranti V, Kyttala A, Zeviani M, Comi GP, Keranen S, Peltonen L, Suomalainen A (2000) Role of adenine nucleotide translocator 1 in mtDNA maintenance. Science *289*:782-785.

Khurana DS, Valencia I, Goldenthal MJ, Legido A (2013) Mitochondrial dysfunction in epilepsy. Seminars in pediatric neurology *20*:176-187.

Loewith R, Jacinto E, Wullschleger S, Lorberg A, Crespo JL, Bonenfant D, Oppliger W, Jenoe P, Hall MN (2002) Two TOR complexes, only one of which is rapamycin sensitive, have distinct roles in cell growth control. Molecular cell *10*:457-468.

Magiorkinis E, Diamantis A, Sidiropoulou K, Panteliadis C (2014) Highights in the history of epilepsy: the last 200 years. Epilepsy research and treatment *2014*:582039.

Murakami M, Ichisaka T, Maeda M, Oshiro N, Hara K, Edenhofer F, Kiyama H, Yonezawa K, Yamanaka S (2004) mTOR is essential for growth and proliferation in early mouse embryos and embryonic stem cells. Molecular and cellular biology *24*:6710-6718.

Naviaux RK, Nguyen KV (2004) POLG mutations associated with Alpers' syndrome and mitochondrial DNA depletion. Annals of neurology *55*:706-712.

Nishino I, Spinazzola A, Hirano M (1999) Thymidine phosphorylase gene mutations in MNGIE, a human mitochondrial disorder. Science *283*:689-692.

Orlova KA, Parker WE, Heuer GG, Tsai V, Yoon J, Baybis M, Fenning RS, Strauss K, Crino PB (2010) STRADalpha deficiency results in aberrant mTORC1 signaling during corticogenesis in humans and mice. The Journal of clinical investigation *120*:1591-1602.

Parker WE, Orlova KA, Parker WH, Birnbaum JF, Krymskaya VP, Goncharov DA, Baybis M, Helfferich J, Okochi K, Strauss KA, Crino PB (2013) Rapamycin prevents seizures after depletion of STRADA in a rare neurodevelopmental disorder. Science translational medicine *5*:182ra153.

Pause A, Belsham GJ, Gingras AC, Donze O, Lin TA, Lawrence JC, Jr., Sonenberg N (1994) Insulin-dependent stimulation of protein synthesis by phosphorylation of a regulator of 5'-cap function. Nature *371*:762-767.

Pavlakis SG, Phillips PC, DiMauro S, De Vivo DC, Rowland LP (1984) Mitochondrial myopathy, encephalopathy, lactic acidosis, and strokelike episodes: a distinctive clinical syndrome. Annals of neurology *16*:481-488.

Pearson RB, Dennis PB, Han JW, Williamson NA, Kozma SC, Wettenhall RE, Thomas G (1995) The principal target of rapamycin-induced p70s6k inactivation is a novel phosphorylation site within a conserved hydrophobic domain. The EMBO journal *14*:5279-5287.

Potter CJ, Huang H, Xu T (2001) Drosophila Tsc1 functions with Tsc2 to antagonize insulin signaling in regulating cell growth, cell proliferation, and organ size. Cell *105*:357-368.

Potter CJ, Pedraza LG, Xu T (2002) Akt regulates growth by directly phosphorylating Tsc2. Nature cell biology *4*:658-665.

Ruvinsky I, Sharon N, Lerer T, Cohen H, Stolovich-Rain M, Nir T, Dor Y, Zisman P, Meyuhas O (2005) Ribosomal protein S6 phosphorylation is a determinant of cell size and glucose homeostasis. Genes & development *19*:2199-2211.

Saitoh M, Pullen N, Brennan P, Cantrell D, Dennis PB, Thomas G (2002) Regulation of an activated S6 kinase 1 variant reveals a novel mammalian target of rapamycin phosphorylation site. The Journal of biological chemistry *277*:20104-20112.

Sarbassov DD, Ali SM, Kim DH, Guertin DA, Latek RR, Erdjument-Bromage H, Tempst P, Sabatini DM (2004) Rictor, a novel binding partner of mTOR, defines a rapamycin-insensitive and raptor-independent pathway that regulates the cytoskeleton. Current biology : CB *14*:1296-1302.

Saudubray JM, Sedel F, Walter JH (2006) Clinical approach to treatable inborn metabolic diseases: an introduction. Journal of inherited metabolic disease *29*:261-274.

Schmiedel J, Jackson S, Schafer J, Reichmann H (2003) Mitochondrial cytopathies. Journal of neurology *250*:267-277.

Spelbrink JN, Li FY, Tiranti V, Nikali K, Yuan QP, Tariq M, Wanrooij S, Garrido N, Comi G, Morandi L, Santoro L, Toscano A, Fabrizi GM, Somer H, Croxen R, Beeson D, Poulton J, Suomalainen A, Jacobs HT, Zeviani M, Larsson C (2001) Human mitochondrial DNA deletions associated with mutations in the gene encoding Twinkle, a phage T7 gene 4-like protein localized in mitochondria. Nature genetics *28*:223-231.

Van Goethem G, Dermaut B, Lofgren A, Martin JJ, Van Broeckhoven C (2001) Mutation of POLG is associated with progressive external ophthalmoplegia characterized by mtDNA deletions. Nature genetics *28*:211-212.

Van Goethem G, Martin JJ, Dermaut B, Lofgren A, Wibail A, Ververken D, Tack P, Dehaene I, Van Zandijcke M, Moonen M, Ceuterick C, De Jonghe P, Van Broeckhoven C (2003) Recessive POLG mutations presenting with sensory and ataxic neuropathy in compound heterozygote patients with progressive external ophthalmoplegia. Neuromuscular disorders : NMD *13*:133-142.

Chapter 2
Detection of human papillomavirus in human focal cortical dysplasia type IIB

Julie Chen, BA,[1] Victoria Tsai, MS,[1] Whitney E. Parker, BA,[1] Eleonora Aronica, MD, PhD,[2,3] Marianna Baybis, MS,[1] and Peter B. Crino, MD, PhD[1,4]

[1] PENN Epilepsy Center and Department of Neurology, Perelman School of Medicine, University of Pennsylvania, Philadelphia, PA
[2] Department of (Neuro)Pathology, Academic Medical Center, University of Amsterdam, Amsterdam, the Netherlands
[3] Epilepsy Institute in the Netherlands Foundation, Heemstede, the Netherlands
[4] Shriner's Hospitals Pediatric Research Center, Department of Neurology, Temple University School of Medicine, Philadelphia, PA

Annals of Neurology. 2012 Dec 31;72(6):881-92.

Focal cortical dysplasia type IIB (FCDIIB) is a sporadic developmental malformation of the cerebral cortex highly associated with pediatric epilepsy. Balloon cells (BCs) in FCDIIB exhibit constitutive activation of the mammalian target of rapamycin complex 1 (mTORC1) signaling pathway. Recently, the high-risk human papillomavirus type 16 oncoprotein E6 was identified as a potent activator of mTORC1 signaling. Here, we test the hypothesis that HPV16 E6 is present in human FCDIIB specimens. HPV16 E6 protein was robustly expressed in all FCDIIB specimens in BCs, but not in regions without BCs or in control tissue specimens including normal brain, lymphoblasts, fibroblasts, cortical tubers, and u87 glioma cells. E6 expression in FCDIIB colocalized with phosphactivated S6 protein, a known mTORC1 substrate. HPV16 E6 DNA and mRNA were detected in representative specimens of FCDIIB but not control cortex, and were confirmed by sequencing. Transfection of E6 into fetal mouse brains caused a focal cortical malformation in

association with enhanced mTORC1 signaling. Our results indicate a new association between HPV16 E6 and FCDIIB and demonstrate for the first time HPV16 E6 in the human brain. We propose a novel etiology for FCDIIB based on HPV16 E6 expression during fetal brain development.

Introduction

Focal cortical dysplasia type IIB (FCDIIB) is a sporadic developmental malformation of the cerebral cortex that is a common cause of pediatric epilepsy. FCDIIB is characterized by disorganized laminar architecture and enlarged, dysmorphic cells called balloon cells (BCs) (Blumcke et al., 2011), which exhibit constitutive activation of the mammalian target of rapamycin complex 1 (mTORC1) signaling pathway (Crino, 2011). Although aberrant mTORC1 activation can be caused by genetic mutations in upstream mTOR effectors, the etiology of mTORC1 activation in BCs is unknown. We have previously proposed that FCDIIB is part of a pathological spectrum of developmental disorders (mTORopathies) associated with abnormal cortical architecture, seizures, and enhanced mTOR signaling that includes tuberous sclerosis complex (TSC), hemimegalencephaly, and ganglioglioma (GG) (Crino, 2011; Crino 2007).

High-risk human papillomavirus type 16 (HPV16) is the most common cause of cervical cancer (Faridi et al., 2011) in women and has been linked to a growing number of cases of oropharyngeal cancer (Bishop and Westra, 2011). Interestingly, the cytopathic effect of HPV16 infection on cervical epithelium results in the formation of koilocytes—enlarged cells with multilobulated nuclei—also called BCs (McLeod, 1987). The E6 oncoprotein encoded by HPV16 can be detected in clinical samples, and detection of HPV16 E6 DNA and mRNA by polymerase chain reaction (PCR), reverse transcriptase PCR (RT-PCR), or *in situ* hybridization (ISH) is considered diagnostic of HPV16 infection (Zaravinos et al., 2009). Recent work has shown that the HPV16 E6 oncoprotein activates mTORC1 signaling at distinct steps:

first by binding to TSC2 and targeting it for ubiquitin-mediated degradation (Lu et al., 2004), and second by activating PDK1 and Akt (Spangle and Munger, 2010) upstream of TSC1/TSC2. In both mechanisms, mTORC1 activation is evidenced by enhanced phosphorylation of the ribosomal S6 protein (phospho-S6), as in cervical cancer (Zhou et al., 2007). We found the effects of HPV16 E6 on mTORC1 signaling to be strikingly similar to previous reports demonstrating reduced levels of TSC2 (Grajkowska et al., 2008), enhanced phospho-PDK1 and phospho-Akt levels (Schick et al., 2007), and enhanced mTORC1 signaling in BCs (Crino, 2011) in FCDIIB. To date, there is no evidence that HPV16 can infect the brain, although HPV16 has been detected in peripheral nerves adjacent to oropharyngeal cancers (Fule et al., 2006) and transgenic mice expressing E6 and E7 oncoproteins develop anaplastic brain tumors (Arbeit et al., 1993). However, based on the cytopathic and cell signaling similarities between cervical dysplasia and FCDIIB, we hypothesized that HPV16 E6 DNA, mRNA, and protein are present in human FCDIIB brain specimens and could serve as a pathogenic agent in FCDIIB. We further hypothesized that expression of E6 would overlap with markers of mTORC1 hyperactivation and that introduction of E6 into fetal mouse brain would cause alteration of cortical architecture.

Results

Detection of HPV16 E6

Antibodies recognized HPV16 E6 by immunocytochemistry in the CaSki HPV16 cervical cancer cell line, known to contain E6 (Figure 2.1A, B), as demonstrated previously (Herfs et al., 2012). In contrast, Western assay of fibroblast

and immortalized lymphoblastoid cell lines generated from normal control individuals and patients with TSC—an autosomal dominant disorder with brain histopathology similar to FCDIIB—did not express E6 protein, nor did U87 and U87vIII glioma lines (Figure 2.1C). E6 protein was not detected in normal human postmortem brain tissue (n=4) using 3 E6 antibodies (Figure 2.1D, E).

In all 50 histopathologically confirmed specimens of FCDIIB (20 females, 30 males; see Table 2.1; Supplementary Figure 2.1; Supplementary Table 2.1), there was robust cytoplasmic expression of E6 primarily in BCs in the subcortical white matter and cortical mantle that was detected by E6 ab70 and confirmed with 2 additional antibodies (Figure 2.2). In accordance with varying degrees of pathological heterogeneity in FCDIIB, subregions of some specimens did not contain BCs, and these regions did not exhibit E6 expression. However, regions with high BC numbers showed extensive E6 expression (Figure 2.1A, border zone, arrows). Similar to quantification of other established BC protein markers (Lamparello et al., 2007), cell count analyses in 10 representative FCDIIB specimens revealed that on average, 79% of morphologically defined BCs expressed E6 (Supplementary Figure 2.2). E6 expression was highly specific for and exclusively linked to FCDIIB histopathology and was not detected in 36 control brain specimens including temporal lobe epilepsy specimens with no evidence of FCD (n=9), or in 5 other types of epilepsy-associated brain malformations including tuberous sclerosis complex (see Table 2.2; Supplementary Figure 2.3). “No primary’’ antibody and ubiquitous IgG1 isotype immunohistochemical controls did not yield an immunohistochemical reaction (Supplementary Figure 2.4). Interestingly, as has been demonstrated in many cervical

dysplasia specimens (Gatta et al., 2011) and peripheral nerve adjacent to oropharyngeal cancer (Fule et al., 2006), the L1 capsid protein was not detected by immunohistochemistry (data not shown).

p16INK4a, a cyclin-dependent kinase inhibitor highly associated with HPV infection in cervical and oropharyngeal cancers (Kostopoulou et al., 2011), was detected immunohistochemically within BCs in all FCDIIB cases analyzed (n=20), but not in surrounding brain tissue without BCs (Figure 2.3) or in control brains. Additionally, because p53 degradation occurs in cervical cancers (Gatta et al., 2011) and is promoted by E6 (Doorbar, 2006; Scheffner et al., 1990), we examined p53 expression. Contrary to previous reports (Chamberlain and Prayson, 2008), we found low p53 expression in astrocytes within the lesions and no expression in BCs (Supplementary Figure 2.5).

Colocalization of E6 and Phosphoactivated mTORC1 Substrates in FCDIIB

Next we hypothesized that E6 expression, if pathogenic through enhanced mTORC1 signaling, should colocalize in cells exhibiting mTORC1 activation. Double fluorescence immunohistochemistry was performed on FCDIIB specimens using antibodies against E6 and phospho-S6 (Ser235/236), a robust biomarker for mTORC1 activation in FCDIIB (Orlova et al., 2010). Phospho-S6 and E6 proteins were highly coexpressed in BCs (Figure 2.4A–C). A few cells expressing E6 did not exhibit phospho-S6 (see Figure 2.4D, arrow), but virtually all of the phospho-S6 labeled cells expressed E6. In further support of our data, cortical tubers, which exhibit mTORC1 activation as a consequence of either mutations in TSC1 or TSC2

(but not E6 expression), did not exhibit E6 immunoreactivity. mTORC1 activation is not a feature of control brain tissue, FCDI, and MCD; this was supported by the absence of E6 in these tissues.

HPV16 E6 DNA

Template DNA was extracted in blinded fashion from 11 randomly selected FCDIIB specimens containing E6-labeled BCs and 19 control brain specimens with no E6 detection (see Supplementary Table 2.1). Viral cross-contamination of tissue blocks was unlikely, as specimens were sectioned in 3 different pathology laboratories. From equal quantities of template DNA, HPV16 E6-specific primers amplified a 477bp amplicon, confirmed by sequencing to be HPV16 E6 (homology, 97–99%; National Center for Biotechnology Information #U34127), in all FCDIIB specimens but not in control brain specimens, an HPV-negative cervical cancer cell line, C33A, or in a no template control reaction (Figure 2.5A, top). The sequences amplified from our patient samples contain variations that are distinct from published E6 sequence (Seedorf et al., 1985), suggesting that our amplicons were distinct and not a uniform contaminant. As most of our sample was from individuals of Northern European decent, it is not surprising that we find European prototype variant E-G350 (T350G) as the uniform isotype. As further corroboration of HPV16 infection, the HPV16 E7 gene, an oncogene directly adjacent to E6 in the HPV16 genome, and upstream long control region were also detected in FCDIIB cases by PCR (Supplementary Figure 2.6).

We then show that HPV16 viral DNA can be visualized in the FCDIIB

specimens by ISH. FCDIIB specimens (n=7) were probed with a biotinylated HPV DNA probe that hybridizes robustly to HPV16 DNA in CaSki and SiHa cells (Montag et al., 2011), and visualized with DAB (Evans et al., 2003). HPV16 DNA was detected in BCs of all FCDIIB specimens, but it was not present in regions of FCDIIB with no BCs, or in control brain tissue (n=6, see Figure 2.5B–H and Supplementary Figure 2.7) (Montag et al., 2011).

mRNA

Total RNA was extracted in a blinded fashion from 12 randomly selected FCDIIB specimens containing E6-labeled BCs and 17 controls. RT-PCR using specific primer pairs designed to detect full-length HPV16 E6 and its known splice variants (E6*I and E6*II) detected E6 mRNA in all selected representative FCDIIB specimens (see Figure 2.5A, bottom) but not in any of the controls. Whereas E6 splice variants were detected in CaSki cells, only full-length E6 transcript was detected in FCDIIB tissue. The detection of E6 transcript by RT-PCR provides a critical diagnostic link between detection of viral DNA and encoded protein and strongly supports the presence of HPV16 E6 in FCDIIB.

HPV16 E6 Expression in Neuroglial Progenitor Cells Disrupts Cortical Lamination

To functionally link E6 expression with the development of cortical malformations, we next tested the hypothesis that expression of E6 protein in neuroglial progenitor cells during fetal brain development disrupts cortical lamination. A plasmid encoding E6 was cotransfected with an RFP reporter plasmid

into fetal mouse brains (n=3) at embryonic day 14 (ED14) by *in utero* electroporation (Saito, 2006). Progenitor cells born on ED14 achieve a cortical laminar destination of layer II–III by ED19, and brains transfected with RFP plasmid alone exhibited RFP+ cells in layer II–III at ED19 (Figure 2.6A; Supplementary Figure 2.8). Histological examination of the cotransfected brains on ED19 by fluorescence microscopy revealed a focal cortical malformation where 74% of RFP+ cells—all of which were E6 immunoreactive—failed to reach their appropriate layer II–III destination and accumulated in the subcortical white matter and ventricular/subventricular (VZ/SVZ) zones (see Figure 2.6B, C). Overt cytomegaly was not observed. In cotransfected brains, RFP+ neurons that reached cortical layer II–III were not E6 immunoreactive (Figure 2.6D). Colabeling with phospho-S6 revealed that most transfected RFP+ cells within the focal malformation in the VZ/SVZ zones expressed phospho-S6 (Supplementary Figure 2.9). These results demonstrate that E6 expression in neural progenitor cells during fetal brain development alters cortical lamination in association with enhanced mTORC1 activation.

Conclusions and Discussion

We demonstrate the presence of HPV16 E6 DNA, mRNA, and protein in BCs in FCDIIB. There was a high concordance between the localization of E6 protein and the phosphoactivated mTORC1 substrate S6 in BCs, suggesting a functional link between HPV16 E6 and mTORC1 activation in FCDIIB. Indeed, introduction of E6 into fetal mouse brain at ED14 causes a developmental malformation of the brain, associated with enhanced mTORC1 signaling. Although further investigation is

warranted to understand how FCDIIB causes epilepsy, our findings suggest a new pathogenesis for FCDIIB based on localized central nervous system HPV16 infection during fetal brain development that accounts for many of the known features of FCDIIB, including sporadic occurrence, enhanced mTORC1 signaling (Crino, 2011), and altered brain cytoarchitecture. Our study is the first to provide an association between HPV16 infection and a neurological disorder and the first to detect HPV16 in human brain.

The standard detection methods for HPV16 in cervical dysplasia and cancer as well as oropharyngeal cancer include PCR, RT-PCR, ISH, and proprietary, commercially available capture assays. For example, the landmark paper reporting HPV16 in head and neck cancer detected HPV16 by PCR and ISH (Gillison et al., 2000). Our approach included PCR, RT-PCR, ISH, and immunohistochemistry and thus implemented methodologies that are widely believed to represent the gold standards for HPV16 detection (Zaravinos et al., 2009). The E6 antibodies detected E6 protein in a well-described cervical cancer cell line (CaSki cells), but not in a variety of human lymphoblast, fibroblast, or glioma cell lines as well as normal control brain and several other types of brain malformation associated with epilepsy. We further find that pINK4a, a cell-signaling protein that is activated by E7 (also detected in our samples), is expressed in FCDIIB. Taken together, these data provide strong support for the presence of HPV16 E6 in FCDIIB. HPV16 E6 is commonly detected in the nucleus and cytoplasm; E6 DNA has been reported in the cytoplasm, nucleus, or both in cervical dysplasia (Gatta et al., 2011; Montag et al., 2011; Burns et al., 1987; Pillai et al., 1999) and in peripheral nerves adjacent to oropharyngeal

cancer (Fule et al., 2006).

Our findings in human FCDIIB tissue are supported by expression of E6 in fetal mouse brain causing disruption of cortical architecture. Although BCs were not detected, a limitation of *in utero* electroporation assay is the duration of the transfection effect, with E6 being expressed for only 4 to 5 days (from ED14 to ED19). In human patients, the genesis of BCs may take much longer to occur. We acknowledge that a transient transfection of E6 in the mouse brain for 5 days likely cannot fully replicate human FCDIIB, and clearly future studies will be needed to examine the cellular phenotype, lineage, and excitability of the transfected cells. Nonetheless, our data demonstrate that expression of E6 in the fetal mouse brain leads to aberrant cortical lamination and supports the hypothesis that E6 may be a pathogenic agent in FCDIIB.

We submit that it is highly unlikely that our results reflect artifactual contamination of the resected specimens or laboratory reagents. For example, the FCDIIB brain tissue specimens were resected under sterile surgical conditions during epilepsy surgery and taken immediately from the operating room to the pathology area in designated sterile tubes, where they were immediately fixed in formalin. HPV is not known to be an aerosolized virus and, for example, is not detected outside of areas in which gynecological procedures are performed (Strauss et al., 2002). We did not detect HPV16 in control specimens under blinded conditions, and HPV16 was not detected in a known cancer cell line (C33A) that does not contain HPV16. We did not detect the capsid protein L1 in our samples using immunohistochemistry; however, in mid to later stage cervical dysplasia, L1 is often not detected (Gatta et al., 2011). The

absence of L1 in FCDIIB is similar to results in peripheral nerves expressing E6 adjacent to oropharyngeal carcinoma (Fule et al., 2006). Other genomic components of HPV16 such as E1 and E4 may not be detected in middle to late stage cervical dysplasia (Doorbar, 2006). Interestingly, severe cervical dysplasia and cervical cancer contain integrated HPV genomes expressing exclusively E6 and E7 rather than episomes capable of producing more assembled virus.

One pivotal unresolved issue is the mode of HPV16 transmission in FCDIIB. Because it is believed that FCDIIB forms during embryonic brain development, a possibility is transplacental HPV16 infection of progenitor cells in the developing brain. Typically, HPV16 infects basal epithelial cells in the cervix to initiate the viral life-cycle and infection via putative interactions with cell surface heparan sulfate proteoglycans such as syndecan-1 and glypican, which are widely expressed on squamous epithelial cells. However, syndecan-1 is highly expressed on neural progenitor cells in the embryonic mouse brain (Ford-Perriss et al., 2003), thus providing a potential mechanism for viral entry. The transplacental HPV transmission rate among women with either known HPV infection, an abnormal Papanicolaou smear, or genital warts has been reported as 12.2% (Rombaldi et al., 2008). Thus, because the prevalence of HPV infection is estimated at 26.8% (Dunne et al., 2007) among females aged 14 to 59 years in the United States, and in many women HPV16 infection is asymptomatic (Tota et al., 2011), transplacental spread of HPV16 is a plausible mechanism for entry into the brain during early fetal cortical development, even in the absence of overt clinical infection. Indeed, a recent study demonstrated that sporadic fetal brain malformations (e.g., dysplasias) could be detected as early as

24 weeks gestation by magnetic resonance imaging (Righini et al., 2012). Alternatively, it is conceivable that the effects of HPV16 E6 could lead to FCDIIB formation in the early neonatal period.

Although the detection of E6 in FCDIIB provides a new insight into the pathogenesis of this brain malformation, the mechanism by which HPV16 might cause epilepsy remains to be defined. Furthermore, although we sampled a small number of additional brain malformation subtypes and did not detect E6, it remains possible that HPV16 may be pathogenic in other forms of cortical malformation. Clearly, future epidemiological investigation will be necessary to define the extent, modes, and temporal course of HPV16 transmission into the developing brain.

Experimental Procedures

Brain Specimens

FCDIB, FCDIIA, FCDIIB, GG, mild malformation of cortical development (mMCD), temporal lobe epilepsy, and TSC brain tissues (Tables 2.1 and 2.2) were obtained following surgical resection (Academic Medical Center, Amsterdam, the Netherlands; University College London, London, UK, courtesy of S. Sisodiya; University of Pennsylvania Medical Center, Philadelphia, PA) for intractable epilepsy. Normal control brain tissues were obtained at postmortem examination (National Disease Research Interchange, Philadelphia, PA; Developmental Tissue Bank, University of Maryland, Baltimore, MD). Specimens were fixed in 4% paraformaldehyde, embedded in paraffin, and sectioned at 6 to 10 μm in 3 distinct pathology laboratories. All human tissue was obtained in accordance with an

approved institutional review board protocol.

Cell Culture

Immortalized lymphoblasts and fibroblasts derived from normal control individuals, and patients with known mutations in either TSC1 or TSC2, were obtained from Coriell (Camden, NJ). CaSki (CRL-1550) and C33A (CRM-HTB-31) cervical cancer cell lines were obtained from the American Type Culture Collection (Manassas, VA). Immortalized lymphoblasts were cultured in RPMI-1640 media (Invitrogen, Grand Island, NY), 15% fetal bovine serum (FBS), 2mM L-glutamine. Immortalized fibroblasts were cultured in modified Eagle medium (MEM; Invitrogen, Grand Island, NY) supplemented with 15% FBS and 2 mM L-glutamine. U87 glioma cells were obtained courtesy of D. O'Rourke, Perelman School of Medicine and were cultured in Dulbecco MEM supplemented with 1% FBS and 1% penicillin/streptomycin. CaSki cells were cultured in RPMI-1640 media (Invitrogen) supplemented with 10% FBS and 1% penicillin/streptomycin. C33A cells were cultured in MEM supplemented with 10% FBS.

Immunohistochemistry

Brain sections were probed with antibodies recognizing E6 (ab70, Abcam, Cambridge, MA; MA1-46057, Thermo Scientific, Waltham, MA; sc-1583, Santa Cruz Biotechnology, Santa Cruz, CA), phospho-S6 (108D2; Cell Signaling Technology, Danvers, MA), p16INK4a (ab54210, Abcam), or p53 (ab26, Abcam) overnight at 4 degrees in TRIS buffer pH 7.4/2% fetal bovine serum), incubated in

biotinylated secondary antibody, and visualized using avidin–biotin conjugation (Vectastain ABC Elite, Vector Laboratories, Burlingame, CA or Powervision Kit, Immunologic, Duiven, the Netherlands) with 3,3'-diaminobenzidine under light microscopy. For double-labeling studies, after incubation with primary antibodies, sections were incubated for 2 hours with Alexa Fluor 568 and Alexa Fluor 488 (antirabbit immunoglobulin G [IgG] or antimouse IgG; 1:200; Molecular Probes, Eugene, OR) and visualized with a laser scanning confocal microscope (SP2, argon-ion laser; Leica, Wetzlar, Germany). All immunostained sections were assessed in a blinded fashion independently by 2 observers.

PCR

DNA was extracted from FCDIIB specimens exhibiting E6 expression (see Results) and from control sections without evidence of E6 expression (QIAamp DNA FFPE Tissue Kit; QIA- GEN, Valencia, CA). Equal amounts of template genomic DNA were used for PCR in designated PCR-safe, contaminant-free stations. Primers amplifying the entire HPV16 E6 coding regions (5'-ATGCACCCAAAGAGAACTGCA-3' forward; 5'-ATTACAGCTGGGTTTCTCTACG-3' reverse) were used to detect viral genomic DNA brain specimens. DNA was subjected to 35 cycles of PCR amplification. Amplicons were resolved on a 1.5% agarose gel and were sequenced at the PENN Sequencing Facility.

In Situ Hybridization

Detection of HPV DNA *in situ* in resected tissue sections was accomplished using GenPoint HPV Biotinylated DNA Probe recognizing genomic clones of several HPV isotypes, including HPV16 and 18, that account for >90% of cervical cancers (Dako, Carpinteria, CA) and GenPoint Tyramide Signal Amplification System for Biotinylated Probes (Dako). *In situ* hybridization was achieved as previously described[15] with the addition of 200 μg/ml proteinase K in water and 1:50 diaminobenzidine (DAB) for 5 minutes, and visualized under light microscopy. Assessment of the sections was performed in a blinded fashion by 2 investigators.

RT-PCR

RNA was extracted from tissue sections (RNeasy FFPE Kit; QIAGEN). Synthesis of cDNA and RT-PCR were performed (OneStep RT-PCR Kit; QIAGEN). RT-PCR primers amplifying full-length HPV16 E6 cDNA and known splice variants E6*I and E6*II were used (5'-AATGTTTCAGGACCCAC AGG-3' forward; 5'-CAGCTGGGTTTCTCTACGTGTTC-3' reverse). RNA was subjected to 40 rounds of PCR amplification after cDNA synthesis. Amplicons were resolved on a 1.5% agarose gel and were sequenced at the PENN Sequencing Facility.

In Utero Electroporation

Introduction of plasmid cDNAs by *in utero* electroporation into fetal C5BL/6 mice (Charles River, Wilmington, MA) on embryonic day (ED) 14 was achieved as reported previously.[16] E6 (plasmid 8641; Addgene, Cambridge, MA) and red fluorescent protein (RFP) plasmids (5 μl each) were microinjected into the lateral

ventricle of fetal mouse brains (n=3). In control mice, an RFP-only plasmid was injected (n=5). Following microinjection, the lateral aspects of the brain were exposed to a brief electrical field pulse (40V) by a forceps-type electrode (CUY21EDIT Square Wave Electroporator; Sonidel, Dublin, Ireland) to effect passage of the plasmid into cells. Embryos were euthanized at ED19. Brains were flash frozen on dry ice, and 10 μm sections were probed with E6 and phospho-S6 antibodies. Sections were visualized by fluorescence (DM4000 B microscope, Leica) or confocal (LSM510; Zeiss, Thornwood, NY) microscopy. Animal experiments were performed in accordance with an approved institutional animal care and use committee protocol.

Figure 2.1. E6 is detected in CaSki cervical cancer cells.

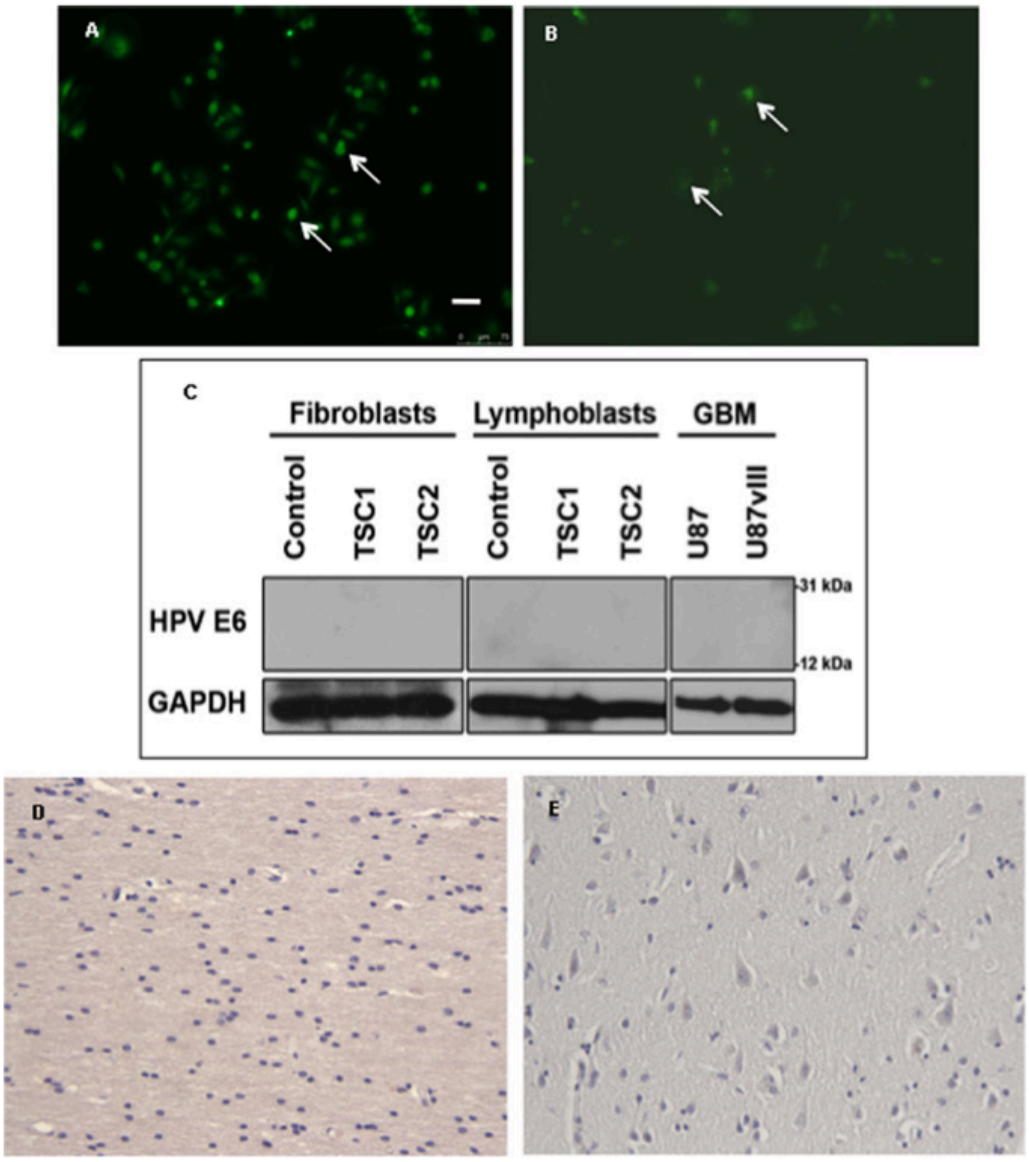

Figure 2.1. E6 is detected in CaSki cervical cancer cells.

A) With ab70 antibody

B) With sc-1583 antibody. Cytoplasmic staining can be seen as well. Scale bar = 50 μm.

C) Western assay depicting absence of E6 protein expression in immortalized lymphoblasts and cultured fibroblasts from normal control individuals and patients with tuberous sclerosis complex (TSC), as well as U87 glioma cell lines. Protein loading was confirmed with glyceraldehyde-3-phosphate dehydrogenase (GAPDH). GBM indicates glioblastoma multiforme.

D) Absence of E6 expression in control brain specimens.

E) Absence of E6 expression in control brain specimens.

Figure 2.2. E6 immunoreactivity in 6 distinct focal cortical dysplasia type IIB specimens.

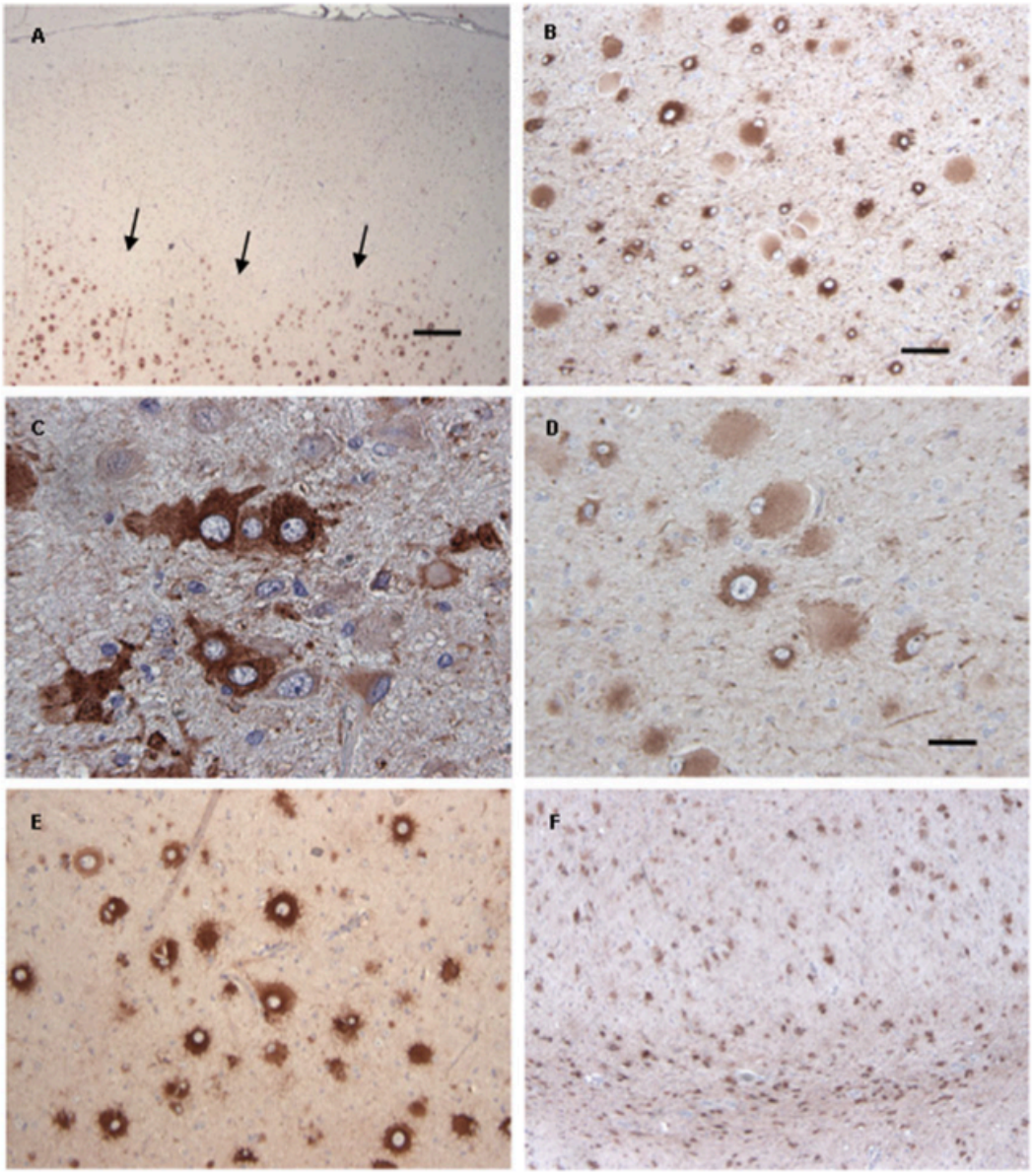

Figure 2.2. E6 immunoreactivity in 6 distinct focal cortical dysplasia type IIB specimens.

A) E6 expression in balloon cells, but not overlying cortex (border zone, arrows). Scale bar = 250 μm.

B) E6 expression in balloon cells. Scale bar = 100 μm.

C) E6 detected and visualized with high magnification. Scale bar = 75 μm.

D) E6 detected and visualized with high magnification. Scale bar = 75 μm.

E) E6 detected and visualized with high magnification. Scale bar = 100 μm.

F) E6 detected and visualized with high magnification. Scale bar = 75 μm.

Figure 2.3. p16INK4a immunoreactivity in focal cortical dysplasia type IIB (FCDIIB) balloon cells (BCs).

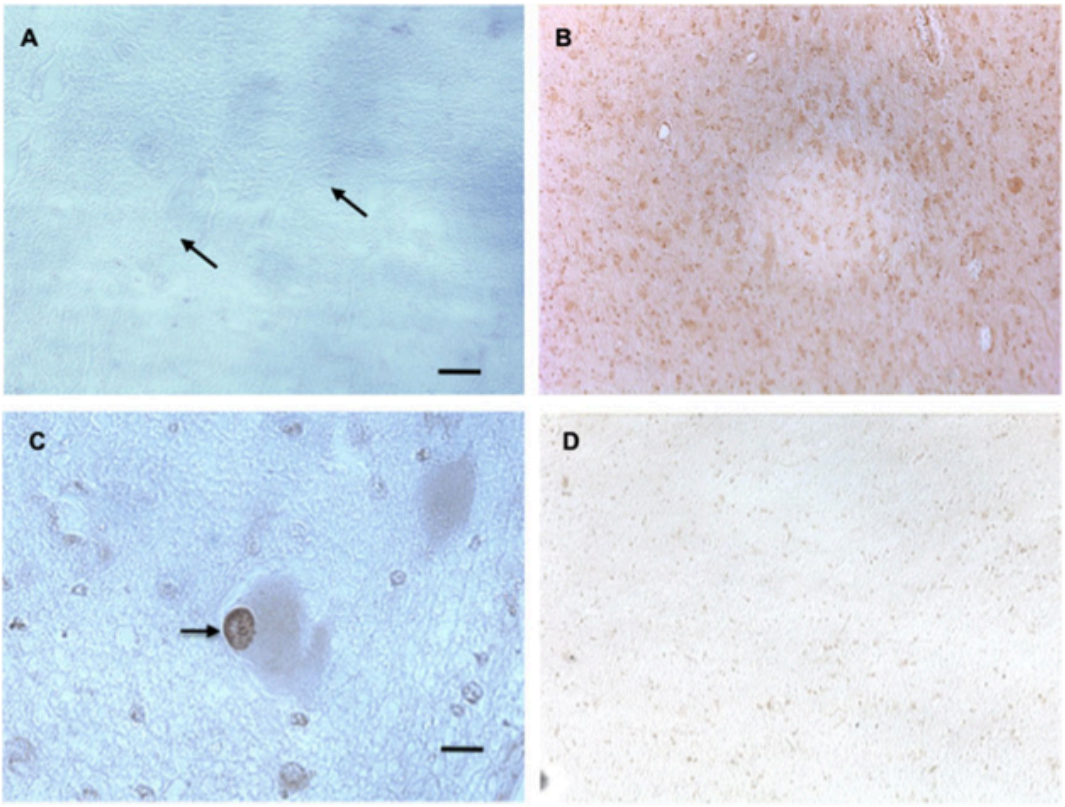

Figure 2.3. p16INK4a immunoreactivity in focal cortical dysplasia type IIB (FCDIIB) balloon cells (BCs).

A) Phase contrast light microscopy depicting absent p16INK4a immunoreactivity in control cerebral cortex. Neurons in A can be seen without p16INK4a labeling (arrows). Scale bar = 100 μm.

B) p16INK4a immunoreactivity in FCDIIB BCs. Scale bar = 100 μm.

C) p16INK4a in nucleus of BC (arrow). Scale bar = 200 μm.

D) Minimal p16INK4a expression in cortex surrounding FCDIIB with no BCs. Scale bar = 100 μm.

Figure 2.4. Coexpression of E6 and phosphorylated S6 proteins in focal cortical dysplasia type IIB (FCDIIB).

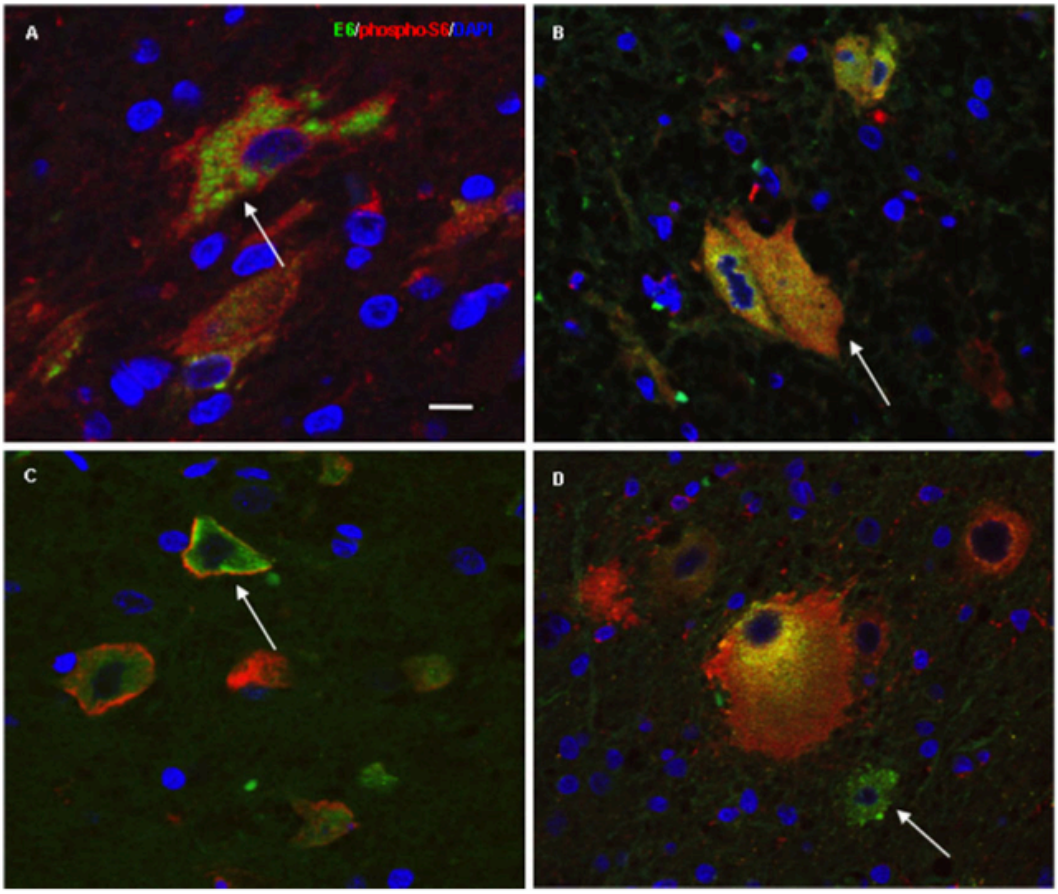

Figure 2.4. Coexpression of E6 and phosphorylated S6 proteins in focal cortical dysplasia type IIB (FCDIIB).

A) Balloon cells in FCDIIB express both E6 (green) and phosphor-S6 (red) proteins (arrows). DAPI nuclear stain is shown in blue. Scale bar = 25 μm.

B) Balloon cells in FCDIIB express both E6 (green) and phosphor-S6 (red) proteins (arrows). DAPI nuclear stain is shown in blue. Scale bar = 25 μm.

C) Balloon cells in FCDIIB express both E6 (green) and phosphor-S6 (red) proteins (arrows). DAPI nuclear stain is shown in blue. Scale bar = 25 μm.

D) Rare cells express E6 only within minimal phosphor-S6 colabeling (arrow). Scale bar = 25 μm.

Figure 2.5. E6 DNA and mRNA detection in focal cortical dysplasia type IIB (FCDIIB) specimens by polymerase chain reaction (PCR), reverse transcriptase PCR (RT-PCR), and in situ hybridization.

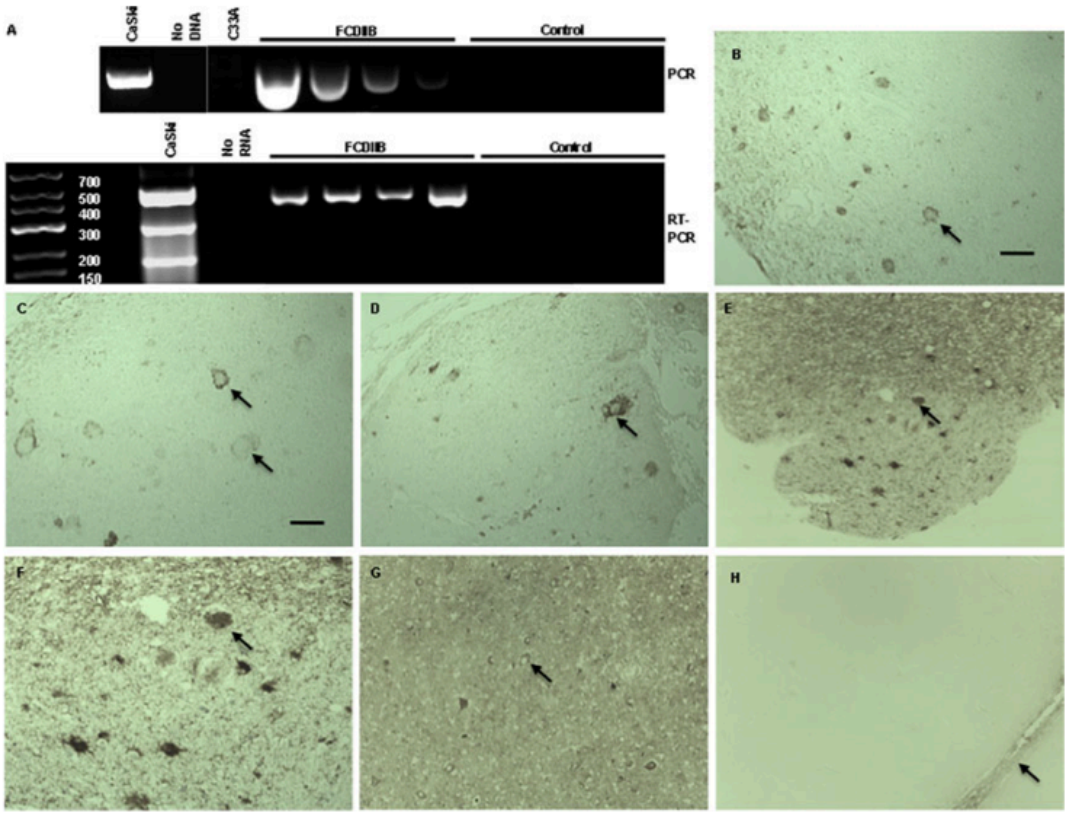

Figure 2.5. E6 DNA and mRNA detection in focal cortical dysplasia type IIB (FCDIIB) specimens by polymerase chain reaction (PCR), reverse transcriptase PCR (RT-PCR), and in situ hybridization.

A) E6 DNA and mRNA are detected by PCR and RT-PCR in CaSki cells (lower molecular weight bands in RT-PCR represent E6 splice variants) and 8 different representative FCDIIB specimens, but not in control brain, C33A cells, or no template control.

B) E6 detection by in situ hybridization in nuclei and cytoplasm of balloon cells. Scale bar = 125 μm.

C) E6 detection by in situ hybridization in nuclei and cytoplasm of balloon cells. Scale bar = 80 μm.

D) E6 detection by in situ hybridization in nuclei and cytoplasm of balloon cells. Scale bar = 80 μm.

E) E6 detection by in situ hybridization in nuclei and cytoplasm of balloon cells. Scale bar = 125 μm.

F) E6 detection by in situ hybridization in nuclei and cytoplasm of balloon cells. Scale bar = 80 μm.

G) E6 detection by in situ hybridization in nuclei and cytoplasm of balloon cells. Scale bar = 125 μm.

H) Absent hybridization signal in control cortex. Pial surface is depicted by arrow. Scale bar = 125 μm.

Figure 2.6. E6 transfection in utero causes a focal cortical malformation.

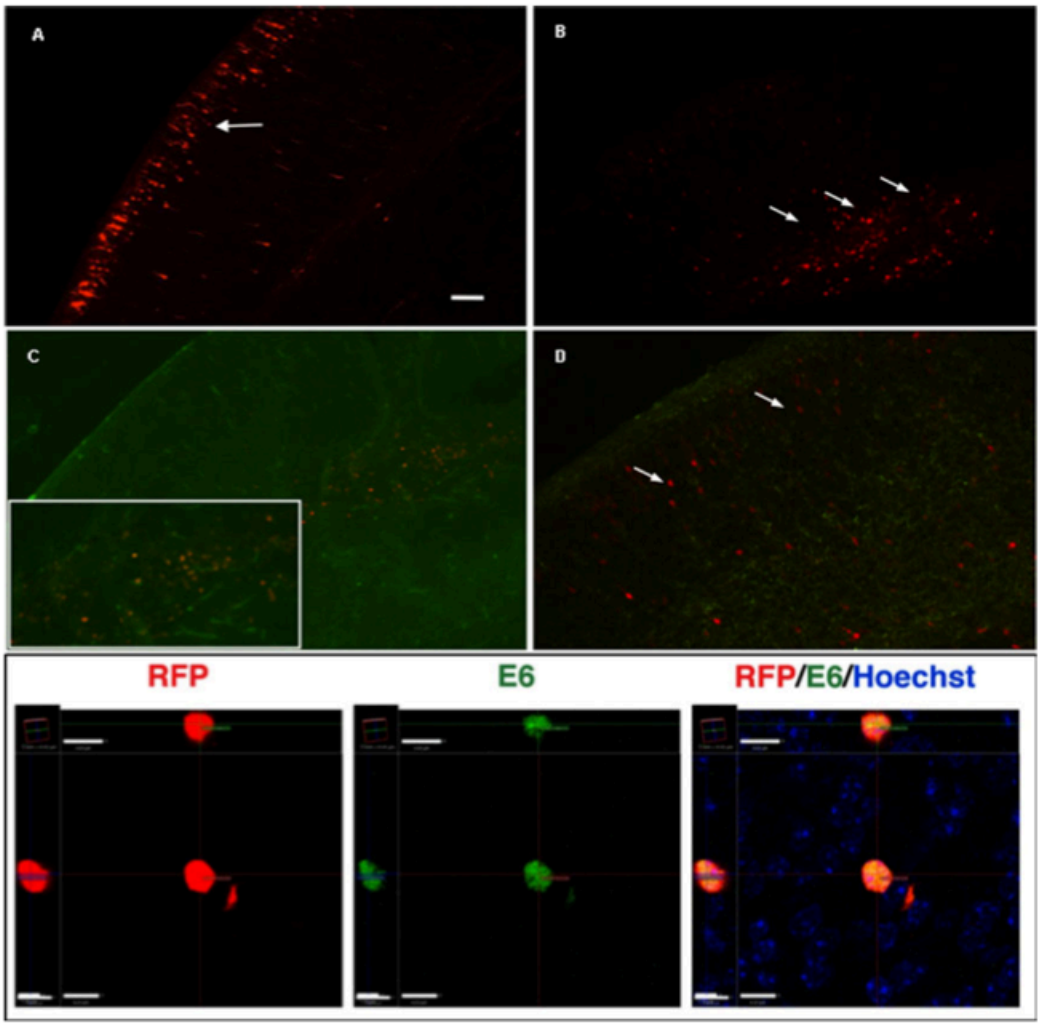

Figure 2.6. E6 transfection in utero causes a focal cortical malformation.

A) Red fluorescent protein (RFP)+ cells achieve appropriate laminar destination (layer II/III) following in utero electroporation with RFP plasmid alone (see also Supplementary Figure 2.8). Scale bar = 100 μm.

B) Focal cortical malformation at embryonic day 19 following in utero electroporation of E6 and RFP plasmids (arrows). Scale bar = 100 μm.

C) Cells retained within the ventricular/subventricular zones coexpress RFP and E6 (inset, higher magnification). Scale bar = 100 μm.

D) In cotransfected brains, cells reaching the cortical plate do not express E6. In bottom panel, confocal microscopy demonstrating cellular colocalization of E6 and RFP within the focal malformation depicted in C. Scale bar = 100 μm.

Table 2.1. HPV E6 protein is detected in 50 FCDIIB specimens.

Case	Diagnosis	Gender	Age at Surgery	Location	HPV, +/−
1	FCDIIB	M	10 years	Frontal	+
2	FCDIIB	M	14 years	Frontal	+
3	FCDIIB	F	9 years	Frontal	+
4	FCDIIB	F	41 years	Temporal	+
5	FCDIIB	M	14 years	Frontal	+
6	FCDIIB	F	13 years	Frontal	+
7	FCDIIB	F	33 years	Frontal	+
8	FCDIIB	F	37 years	Temporal	+
9	FCDIIB	F	1 year	Frontal	+
10	FCDIIB	F	12 years	Frontal	+
11	FCDIIB	M	23 years	Temporal	+
12	FCDIIB	M	29 years	Temporal	+
13	FCDIIB	M	1 year	Frontal	+
14	FCDIIB	F	7 months	Temporal	+
15	FCDIIB	M	1 year	Temporal	+
16	FCDIIB	M	5 years	Temporal	+
17	FCDIIB	M	14 years	Frontal	+
18	FCDIIB	M	15 years	Temporal	+
19	FCDIIB	M	21 years	Temporal	+
20	FCDIIB	F	17 years	Frontal	+
21	FCDIIB	M	3 years	Temporal	+
22	FCDIIB	F	23 years	Frontal	+
23	FCDIIB	F	12 years	Frontal	+
24	FCDIIB	M	12 years	Frontal	+
25	FCDIIB	M	1 year	Frontal	+
26	FCDIIB	M	26 years	Frontal	+
27	FCDIIB	M	30 years	Frontal	+
28	FCDIIB	M	44 years	Temporal	+
29	FCDIIB	F	52 years	Frontal	+
30	FCDIIB	M	59 years	Temporal	+
31	FCDIIB	F	22 years	Frontal	+
32	FCDIIB	M	52 years	Cingulate	+
33	FCDIIB	M	26 years	Frontal	+
34	FCDIIB	M	14 years	Temporal	+
35	FCDIIB	M	23 years	Frontal	+
36	FCDIIB	F	18 years	Temporal	+
37	FCDIIB	F	31 years	Temporal	+
38	FCDIIB	M	14 years	Frontal	+
39	FCDIIB	M	35 years	Frontal	+
40	FCDIIB	M	21 years	Frontal	+
41	FCDIIB	F	15 years	Parietal	+
42	FCDIIB	M	29 years	Temporal	+
43	FCDIIB	M	5 years	Frontal	+
44	FCDIIB	F	37 years	Temporal	+
45	FCDIIB	M	24 years	Frontal	+
46	FCDIIB	F	23 years	Temporal	+
47	FCDIIB	M	17 years	Frontal	+
48	FCDIIB	F	25 years	Frontal	+
49	FCDIIB	F	15 years	Frontal	+
50	FCDIIB	M	23 years	Frontal	+

Table details diagnosis, gender, age at epilepsy surgery, brain location of resected specimen, and presence (+) of E6 protein.
F = female; FCDIIB = focal cortical dysplasia type IIB; HPV = human papillomavirus; M = male.

Table 2.2. Absence of E6 in non-FCDIIB cases.

Case	Diagnosis	Gender	Age at Surgery, yr	Location	HPV, +/−
1	MCD	F	4	Parietal	−
2	FCDIB	M	19	Frontal	−
3	FCDIB	M	23	Temporal	−
4	FCDIB	F	16	Frontal	−
5	FCDIB	M	24	Temporal	−
1	FCDIIA	M	5	Frontal	−
2	FCDIIA	M	1	Frontal	−
3	FCDIIA	M	3	Frontal	−
4	FCDIIA	M	13	Temporal	−
5	FCDIIA	F	1	Parietal	−
6	FCDIIA	F	22	Temporal	−
7	FCDIIA	M	17	Frontal	−
1	TSC	M	32	Parietal	−
2	TSC	F	42	Frontal	−
3	TSC	M	16	Temporal	−
4	TSC	M	1	Temporal	−
5	TSC	F	14	SEGA	−
1	Control	F	73	Temporal	−
2	Control	M	44	Frontal	−
3	Control	F	46	Frontal	−
4	Control	M	59	Frontal	−
1	GG	M	27	Temporal	−
2	GG	F	19	Temporal	−
3	GG	M	34	Temporal	−
4	GG	M	31	Frontal	−
5	GG	M	19	Temporal	−
6	GG	F	22	Temporal	−
1	TLE	M	36	Temporal	−
2	TLE	F	19	Temporal	−
3	TLE	M	35	Temporal	−
4	TLE	M	24	Temporal	−
5	TLE	F	29	Temporal	−
6	TLE	M	30	Temporal	−
7	TLE	F	31	Temporal	−
8	TLE	F	45	Temporal	−
9	TLE	F	43	Temporal	−

E6 expression was not detected in postmortem control, TLE, mild MCD, FCD types IB and IIA, TSC, or GG specimens.
F = female; FCD = focal cortical dysplasia; GG = ganglioglioma; HPV = human papillomavirus; M = male; MCD = mild malformation of cortical development; SEGA = subependymal giant cell astrocytoma; TLE = temporal lobe epilepsy; TSC = tuberous sclerosis complex.

Supplemental Figure 2.1. FCDIIB specimens exhibiting nestin **(a-b)** and vimentin **(c)** immunoreactivity. Note that most BCs exhibit robust nestin and vimentin expression. Scale bar: 150 µm (a,c); 100 µm (b).

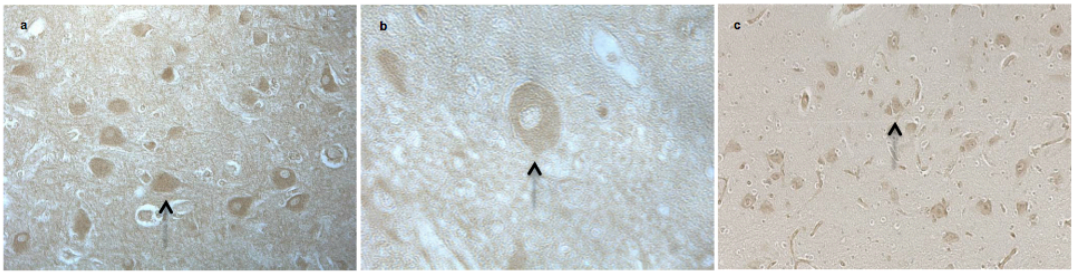

Supplemental Figure 2.2. Percentage of BCs that express E6. Morphologically dlefined BCs from 10 representative cases were examined at high magnification (40x) for total BC counts. E6 expression in each BC was determined as present or absent and the percentage of morphologically identified BCs that expressed E6 protein was calculated.

FCDIIB Case	Total # BCs	% BCs Expressing E6
1	110	75%
2	95	94%
3	115	86%
4	96	87%
5	100	70%
6	112	71%
7	90	65%
8	111	81%
9	112	77%
10	98	86%

Supplemental Figure 2.3. Absent E6 immunoreactivity in human TSC speciments. Cortical tubers **(a-c),** subependymal giant cell astrocytoma **(d).** Scale bar: 150 µm (a, c), 100 µm (b, d).

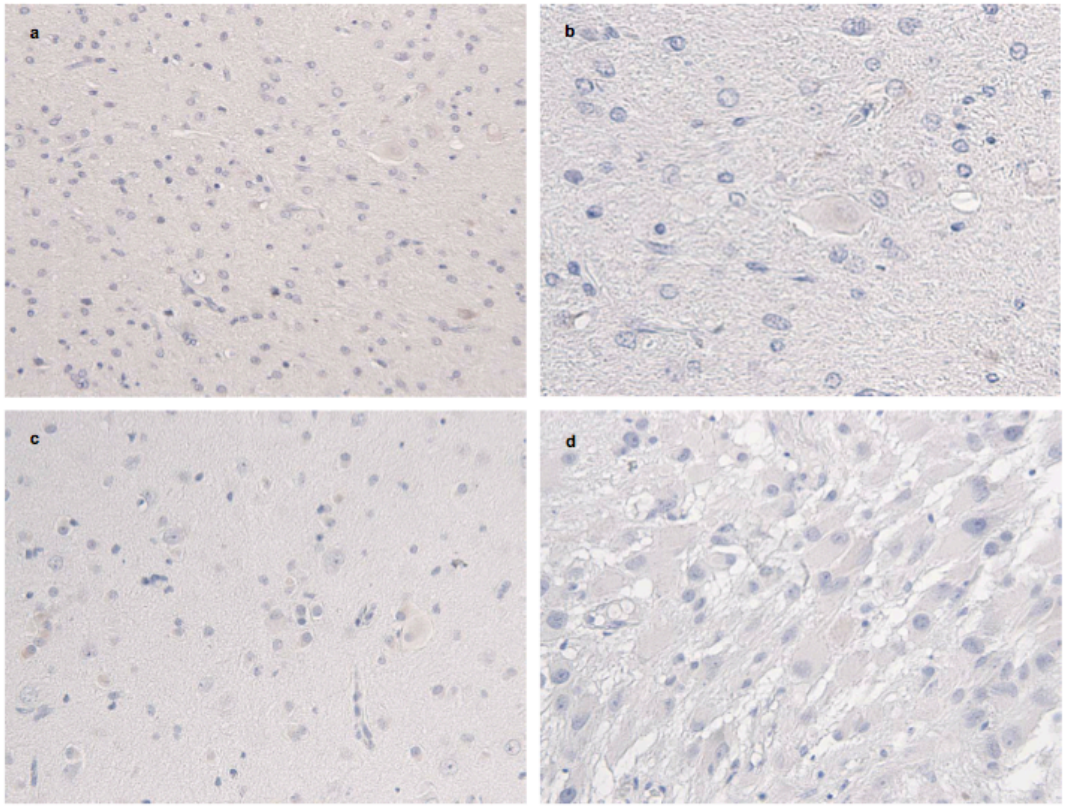

Supplemental Figure 2.4. Immunohistochemistry control experiments. No primary (E6) antibody controls **(a-b).** Isotype IgG antibody with no primary (E6) added **(c-d).** Note absence of immunolabeling in balloon cells (arrows). Scale bar = 150 µm.

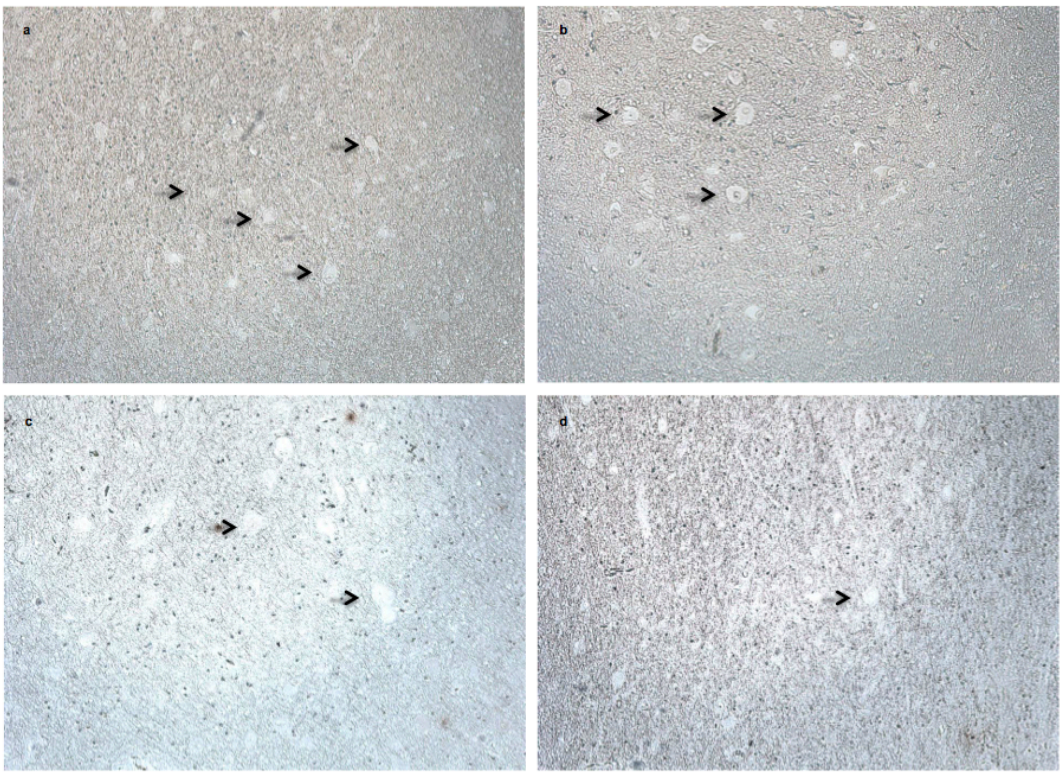

Supplemental Figure 2.5. p53 expression in FCDIIB. p53 immunoreactive astrocytes in FCDIIB specimens **(a).** Absence of p53 immunoreactivity in BCs **(b, arrow).** Scale bar: 200 μm.

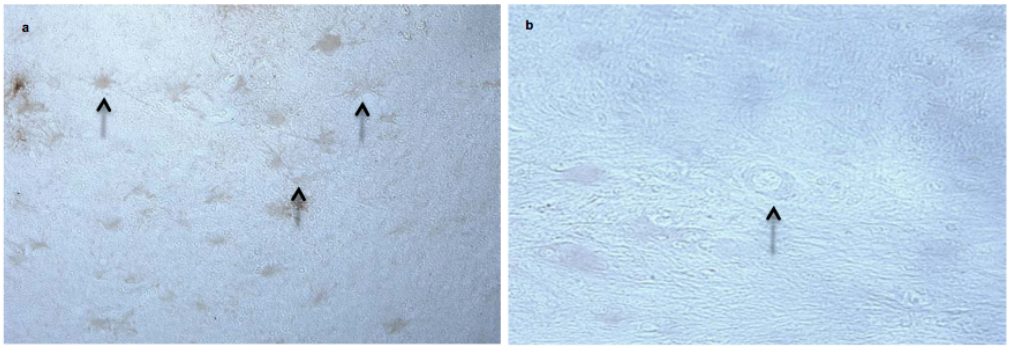

Supplemental Figure 2.6. PCR in representative FCDIIB cases for HPV16 E7 and HPV16 LCR revealed 297bp and 439bp amplicons. DNA sequencing confirmed the identity of viral elements and BLAST against HPV16 E7 and LCR sequence revealed 98% sequence similarity.

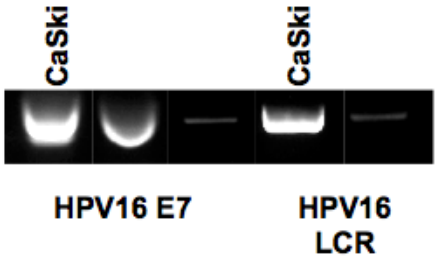

Supplemental Figure 2.7. HPV DNA is not present in control brain **(a)** and regions of FCDIIB specimens with no balloon cells **(b-c)** by *in situ* hybridization. Note single neuron **(b**; arrow). Small arrows in a and c depict the pial surface.

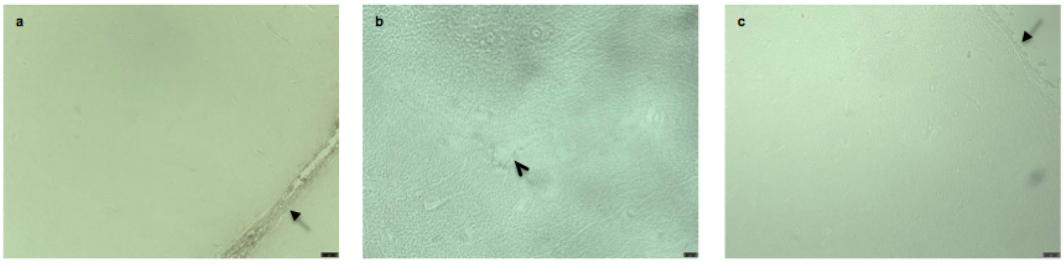

Supplemental Figure 2.8. *In utero* electroporation of RFP plasmid does not disrupt normal cortical lamination. Transfection of RFP plasmid on embryonic day 14 by *in utero* electroporation labels a population of cells destined for layer II-III **(a).** Co-labeling with Cux1 antibody reveals normal expression of Cux1 protein in transfected layer II-III cells **(b).** Hoechst labeling demonstrates laminar organization of the cortex **(c).** Composite photomicrograph showing direct overlay of RFP and Cux1 in layer II-III **(d).** Scale: 100 μm.

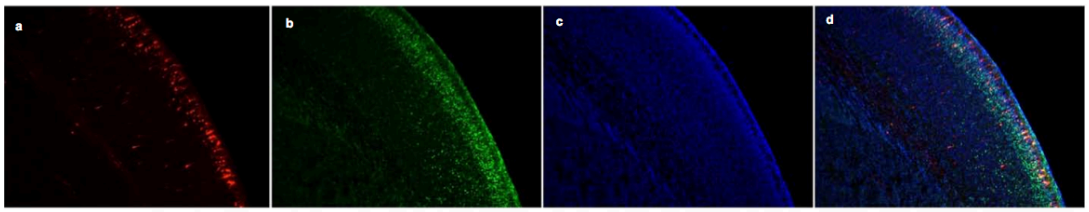

Supplemental Figure 2.9. Three dimensional confocal microscopy demonstrates co-localization of RFP and phosphor-S6 (P-S6) protein in cells within the subventricuar zone following electroporation with RFP and E6 plasmids. Three RFP transfected cells are shown. The cells at right and left exhibit P-S6 immunoreactivity (green), shown in overlay on far right; the center cell does not show phosphor-S6 labeling. Cross sectional image for this cell is depicted in left panels (L); apical view of both cells represented in top panels (T).

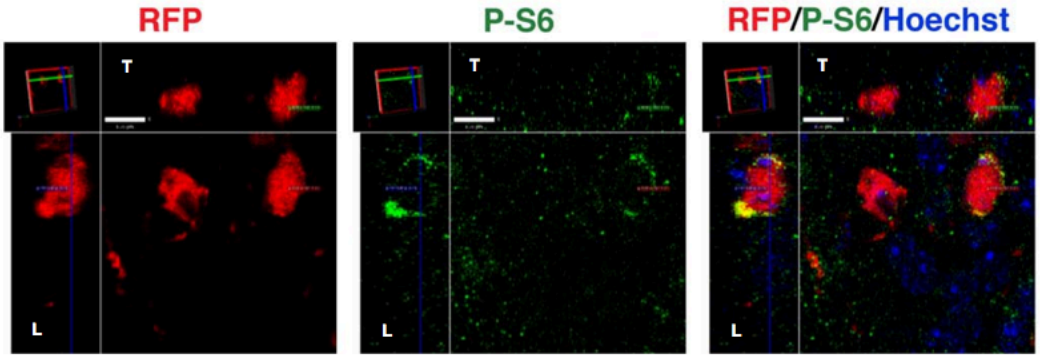

Supplemental Table 2.1. Table detailing detection assays conducted on FCDIIB or control cases. Check mark denotes assay was performed.

FCDIIB	PCR	ISH	RT-PCR	IHC	Controls	PCR	ISH	RT-PCR	IHC
T86-9864	✓		✓	✓	CL009	✓	✓		✓
975276 3F	✓			✓	CL010	✓			✓
975276 3B	✓			✓	CL011	✓	✓	✓	✓
02952135 IC	✓			✓	CL106	✓	✓		✓
02952996 I	✓			✓	CL1366.2	✓			✓
EA_03	✓		✓	✓	CL102	✓			✓
EA_06	✓		✓	✓	CL105	✓			✓
EA_09	✓		✓	✓	CL425	✓			✓
EA_10	✓		✓	✓	CL408	✓			✓
HS11010672	✓			✓	CL001	✓			✓
H20205	✓		✓	✓	EA_01	✓		✓	✓
NP0764			✓	✓	EA_02	✓		✓	✓
NH0669-1			✓	✓	EA_04	✓		✓	✓
NH0669-2			✓	✓	EA_05	✓		✓	✓
H1262-05			✓	✓	EA_07	✓		✓	✓
H789-96			✓	✓	EA_08	✓		✓	✓
H-1022-96			✓	✓	CL002	✓			✓
06-21145 2B		✓		✓	CL005	✓			✓
06-18426 VE		✓		✓	CL006				✓
06-20144		✓		✓	CL007				✓
07-12578		✓		✓	CL008				✓
79-02426		✓		✓	CL600		✓	✓	✓
97-15099		✓		✓	CL602		✓	✓	✓
TOP-07786		✓		✓	CL138		✓	✓	✓
					CL427			✓	✓
					CL1878			✓	✓
					CL100			✓	✓
					CL1878			✓	✓
					CL504			✓	✓
					MPSIII			✓	✓
					WI92-79			✓	✓

References

Arbeit JM, Munger K, Howley PM, Hanahan D (1993) Neuroepithelial carcinomas in mice transgenic with human papillomavirus type 16 E6/E7 ORFs. The American journal of pathology *142*:1187-1197.

Bishop JA, Westra WH (2011) Human papillomavirus-related small cell carcinoma of the oropharynx. The American journal of surgical pathology *35*:1679-1684.

Blumcke I, Thom M, Aronica E, Armstrong DD, Vinters HV, Palmini A, Jacques TS, Avanzini G, Barkovich AJ, Battaglia G, Becker A, Cepeda C, Cendes F, Colombo N, Crino P, Cross JH, Delalande O, Dubeau F, Duncan J, Guerrini R, Kahane P, Mathern G, Najm I, Ozkara C, Raybaud C, Represa A, Roper SN, Salamon N, Schulze-Bonhage A, Tassi L, Vezzani A, Spreafico R (2011) The clinicopathologic spectrum of focal cortical dysplasias: a consensus classification proposed by an ad hoc Task Force of the ILAE Diagnostic Methods Commission. Epilepsia *52*:158-174.

Burns J, Graham AK, Frank C, Fleming KA, Evans MF, McGee JO (1987) Detection of low copy human papilloma virus DNA and mRNA in routine paraffin sections of cervix by non-isotopic in situ hybridisation. Journal of clinical pathology *40*:858-864.

Chamberlain WA, Prayson RA (2008) Focal cortical dysplasia type II (malformations of cortical development) aberrantly expresses apoptotic proteins. Applied immunohistochemistry & molecular morphology : AIMM / official publication of the Society for Applied Immunohistochemistry *16*:471-476.

Crino PB (2007) Focal brain malformations: a spectrum of disorders along the mTOR cascade. Novartis Foundation symposium *288*:260-272; discussion 272-281.

Crino PB (2011) mTOR: A pathogenic signaling pathway in developmental brain malformations. Trends in molecular medicine *17*:734-742.

Doorbar J (2006) Molecular biology of human papillomavirus infection and cervical cancer. Clinical science *110*:525-541.

Dunne EF, Unger ER, Sternberg M, McQuillan G, Swan DC, Patel SS, Markowitz LE (2007) Prevalence of HPV infection among females in the United States. Jama *297*:813-819.

Evans MF, Aliesky HA, Cooper K (2003) Optimization of biotinyl-tyramide-based in situ hybridization for sensitive background-free applications on formalin-fixed, paraffin-embedded tissue specimens. BMC clinical pathology *3*:2.

Faridi R, Zahra A, Khan K, Idrees M (2011) Oncogenic potential of Human Papillomavirus (HPV) and its relation with cervical cancer. Virology journal *8*:269.

Ford-Perriss M, Turner K, Guimond S, Apedaile A, Haubeck HD, Turnbull J, Murphy M (2003) Localisation of specific heparan sulfate proteoglycans during the proliferative phase of brain development. Developmental dynamics : an official publication of the American Association of Anatomists *227*:170-184.

Fule T, Mathe M, Suba Z, Csapo Z, Szarvas T, Tatrai P, Paku S, Kovalszky I (2006) The presence of human papillomavirus 16 in neural structures and vascular endothelial cells. Virology *348*:289-296.

Gatta LB, Berenzi A, Balzarini P, Dessy E, Angiero F, Alessandri G, Gambino A, Grigolato P, Benetti A (2011) Diagnostic implications of L1, p16, and Ki-67 proteins and HPV DNA in low-grade cervical intraepithelial neoplasia. International journal of gynecological pathology : official journal of the International Society of Gynecological Pathologists *30*:597-604.

Gillison ML, Koch WM, Capone RB, Spafford M, Westra WH, Wu L, Zahurak ML, Daniel RW, Viglione M, Symer DE, Shah KV, Sidransky D (2000) Evidence for a causal association between human papillomavirus and a subset of head and neck cancers. Journal of the National Cancer Institute *92*:709-720.

Grajkowska W, Kotulska K, Matyja E, Larysz-Brysz M, Mandera M, Roszkowski M, Domanska-Pakiela D, Lewik-Kowalik J, Jozwiak S (2008) Expression of tuberin and hamartin in tuberous sclerosis complex-associated and sporadic cortical dysplasia of Taylor's balloon cell type. Folia neuropathologica / Association of Polish Neuropathologists and Medical Research Centre, Polish Academy of Sciences *46*:43-48.

Herfs M, Yamamoto Y, Laury A, Wang X, Nucci MR, McLaughlin-Drubin ME, Munger K, Feldman S, McKeon FD, Xian W, Crum CP (2012) A discrete population of squamocolumnar junction cells implicated in the pathogenesis of cervical cancer. Proceedings of the National Academy of Sciences of the United States of America *109*:10516-10521.

Kostopoulou E, Samara M, Kollia P, Zacharouli K, Mademtzis I, Daponte A, Messinis IE, Koukoulis G (2011) Different patterns of p16 immunoreactivity in cervical biopsies: correlation to lesion grade and HPV detection, with a review of the literature. European journal of gynaecological oncology *32*:54-61.

Lamparello P, Baybis M, Pollard J, Hol EM, Eisenstat DD, Aronica E, Crino PB (2007) Developmental lineage of cell types in cortical dysplasia with balloon cells. Brain : a journal of neurology *130*:2267-2276.

Lu Z, Hu X, Li Y, Zheng L, Zhou Y, Jiang H, Ning T, Basang Z, Zhang C, Ke Y (2004) Human papillomavirus 16 E6 oncoprotein interferences with insulin signaling

pathway by binding to tuberin. The Journal of biological chemistry *279*:35664-35670.

McLeod K (1987) Prediction of human papilloma virus antigen in cervical squamous epithelium by koilocyte nuclear morphology and "wart scores": confirmation by immunoperoxidase. Journal of clinical pathology *40*:323-328.

Montag M, Blankenstein TJ, Shabani N, Bruning A, Mylonas I (2011) Evaluation of two commercialised in situ hybridisation assays for detecting HPV-DNA in formalin-fixed, paraffin-embedded tissue. Archives of gynecology and obstetrics *284*:999-1005.

Orlova KA, Tsai V, Baybis M, Heuer GG, Sisodiya S, Thom M, Strauss K, Aronica E, Storm PB, Crino PB (2010) Early progenitor cell marker expression distinguishes type II from type I focal cortical dysplasias. Journal of neuropathology and experimental neurology *69*:850-863.

Pillai MR, Phanidhara A, Kesari AL, Nair P, Nair MK (1999) Cellular manifestations of human papillomavirus infection in the oral mucosa. Journal of surgical oncology *71*:10-15.

Righini A, Parazzini C, Doneda C, Avagliano L, Arrigoni F, Rustico M, Consonni D, Re TJ, Bulfamante G, Triulzi F (2012) Early formative stage of human focal cortical gyration anomalies: fetal MRI. AJR American journal of roentgenology *198*:439-447.

Rombaldi RL, Serafini EP, Mandelli J, Zimmermann E, Losquiavo KP (2008) Transplacental transmission of Human Papillomavirus. Virology journal *5*:106.

Saito T (2006) In vivo electroporation in the embryonic mouse central nervous system. Nature protocols *1*:1552-1558.

Scheffner M, Werness BA, Huibregtse JM, Levine AJ, Howley PM (1990) The E6 oncoprotein encoded by human papillomavirus types 16 and 18 promotes the degradation of p53. Cell *63*:1129-1136.

Schick V, Majores M, Engels G, Hartmann W, Elger CE, Schramm J, Schoch S, Becker AJ (2007) Differential Pi3K-pathway activation in cortical tubers and focal cortical dysplasias with balloon cells. Brain pathology *17*:165-173.

Seedorf K, Krammer G, Durst M, Suhai S, Rowekamp WG (1985) Human papillomavirus type 16 DNA sequence. Virology *145*:181-185.

Spangle JM, Munger K (2010) The human papillomavirus type 16 E6 oncoprotein activates mTORC1 signaling and increases protein synthesis. Journal of virology *84*:9398-9407.

Strauss S, Sastry P, Sonnex C, Edwards S, Gray J (2002) Contamination of environmental surfaces by genital human papillomaviruses. Sexually transmitted infections *78*:135-138.

Tota JE, Chevarie-Davis M, Richardson LA, Devries M, Franco EL (2011) Epidemiology and burden of HPV infection and related diseases: implications for prevention strategies. Preventive medicine *53* Suppl 1:S12-21.

Zaravinos A, Mammas IN, Sourvinos G, Spandidos DA (2009) Molecular detection methods of human papillomavirus (HPV). The International journal of biological markers *24*:215-222.

Zhou Y, Pan Y, Zhang S, Shi X, Ning T, Ke Y (2007) Increased phosphorylation of p70 S6 kinase is associated with HPV16 infection in cervical cancer and esophageal cancer. British journal of cancer *97*:218-222.

Chapter 3
Astrocytic apoptosis and contributions to seizures in Slc25a12 mutant mice

Slc25a12 is a mitochondrial aspartate-glutamate carrier that promotes the effective crossing of reducing equivalents into the mitochondria, which are then used as electron donors for the electron transport chain. Patients with Slc25a12 loss of function mutations develop autism-like neurological abnormalities and seizures early in life. In this study, we employ knock out (KO) mouse technology to study the effect of complete Slc25a12 KO on different neural cell types. We show that Slc25a12 KO hippocampal astrocytes undergo apoptosis, down-regulate their expression of glutamate reuptake transporters, and up-regulate the neuromodulatory protein adenosine kinase, all of which may contribute to the dysregulation of glutamatergic neurotransmission. Our data uncover an unexpected role for astrocytes in seizure genesis and continue to underscore the importance of studying the most abundant and underappreciated neural cell type to probe its contributions to seizures and other neurological disorders, as well as its potential for therapeutic interventions.

Introduction

The mitochondrial aspartate-glutamate carrier isoform 1, also known as aralar, or Slc25a12, is a calcium-binding protein localized to the inner mitochondrial membrane. As part of the malate-aspartate shuttle, it transfers reducing equivalents in the form of NADH from the cytosol to the mitochondria by catalyzing the exchange of intermitochondrial aspartate and cytosolic glutamate and a proton (Figure 3.1). Discovered and cloned in 1998 (del Arco and Satrústegui, 1998), Slc25a12 was later identified as an autism susceptibility gene after multiple genome wide association studies found Slc25a12 SNPs highly associated with autism spectrum disorders (Ramoz et al., 2004; Segurado et al., 2005; Silverman et al., 2008; Turunen et al., 2008; Chien et al., 2010; Kim et al., 2011; Anitha et al., 2012; Li et al., 2012; Prandini et al., 2012). Though the link between Slc25a12 and autism has been contested by a few (Blasi et al., 2006; Correia et al., 2006; Rabionet et al., 2006; Lepagnol-Bestel et al., 2008), two recent meta-analysis studies further substantiated the association (Aoki and Cortese, 2015; Liu et al., 2015). Recently, two independent case studies identified three patients with loss of function mutations in Slc25a12 (Wibom et al., 2009; Falk et al., 2014). These patients develop normally during the first few months of life after which they begin to develop psychomotor deficits and seizures. It is not currently known what changes in the brain resulting from Slc25a12 loss of function lead to seizures. Here, we use Slc25a12 KO mice to investigate the effect of Slc25a12 loss of function on different neural cell types to examine their role in seizure genesis.

The pathogenesis of astrocytes is increasingly being recognized as a major contributor to many neurological disorders. In seizure disorders, a number of astrocyte-specific deficiencies have now been identified in both human temporal lobe and animal models of epilepsy that contribute to seizure propensity (Bordey and Sontheimer, 1998; Das et al., 2012). The most well established astrocyte abnormality documented in seizure disorders is reactive astrocytosis, whereby astrocytes display hypertrophic morphology and increased expression of astrocytic intermediate filaments GFAP and vimentin. Other astrocyte deficiencies include changes in ion channel composition (Kir4.1) reflecting an inability of astrocytes to buffer extracellular potassium (Wallraff et al., 2006; Sicca et al., 2011); reduction in glutamate transporters (GLT-1, GLAST) (Mathern et al., 1999; Proper et al., 2012; Sarac et al., 2009; Takahashi et al., 2010) and glutamate degrading enzymes such as glutamine synthetase (Dennis et al., 1977; Eid et al., 2004; van der Hel et al., 2005), resulting in the inability to sequester and degrade synaptic glutamate into the astrocytic cytosol; and disrupted homeostasis of neurotransmitter precursors for both excitatory and inhibitory neurotransmission . In this study, we report a novel astrocytic deficiency that we believe may further contribute to the pathophysiology and exacerbation of seizures in Slc25a12 KO mice.

Results

Slc25a12 is expressed in neurons, interneurons, and astrocytes

Slc25a12 mRNA is expressed in pyramidal neurons in mouse cortex and hippocampus (del Arco et al., 2002; Ramos et al., 2003), prompting us to examine

whether the regional localization of its protein expression follows suit. We probed brain tissue from wild type mouse brain using antibodies recognizing Slc25a12. We found that Slc25a12 protein was highly expressed in cortical pyramidal neurons (Figure 3.2A), similar to mRNA *in situ* hybridization expression patterns. Here, we also demonstrated the specificity of the Slc25a12 antibody by using it on Slc25a12 KO brain tissue, where Slc25a12 protein is clearly not detected (Figure 3.2A). To determine whether Slc25a12 is expressed in inhibitory interneurons, we examined wild type mouse brain tissues using antibodies against parvalbumin (PV), the calcium-binding protein expressed in a subset of fast-spiking interneurons. Consistent with the high numbers of mitochondria in PV interneurons (Gulyás et al., 2006), we found that Slc25a12 protein was also detected in this cell type (Figure 3.2B).

The astrocytic expression of Slc25a12 has not been established and is highly debated. Some groups found that astrocytes do not express Slc25a12 protein (Ramos et al., 2003; Pardo et al., 2011), while others argued that astrocytes are metabolically compromised without Slc25a12, and demonstrated using the rigorous methodology of electron microscopy with immunogold labeling, that astrocytes do in fact express Slc25a12 (Li et al., 2012). Using a GLT-1-GFP transgenic BAC mouse, which expresses GFP in all astrocytes from P10 to adulthood (Regan et al., 2007), we found prominent Slc25a12 expression in astrocytes of both the cortex and the hippocampus (Figure 3.2C). This implies that Slc25a12 loss of function may have more diverse effects than previously realized, given the intermediary roles that astrocytes have, particularly in glutamatergic neurotransmission.

Loss of Slc25a12 does not adversely impact interneuron development and differentiation

Abnormal GABAergic signaling is known to underlie some seizure disorders, as evidenced by genetic mutations in interneuron development that lead to seizure states (McManus and Golden, 2005; Friocourt et al., 2008; Cobos et al., 2005). Interestingly, mitochondrial disease is also starting to gain recognition as a major contributor to seizures and epilepsy, as the incidence of seizures in patients with mitochondrial disease is greater than that of the general population and the fact that there is an increasing number of identified mitochondrial mutations that result in epilepsy (Khurana et al., 2008; Kang et al., 2013). Preliminary data from our lab has shown that interneurons rely on mitochondrial oxidative phosphorylation for tangential migration to the cortex (Lin-Hendel et al., unpublished), further substantiating, and establishing a precedent for the dual role that interneurons and mitochondria play in seizure disorders. This led us to investigate whether loss of Slc25a12 would result in a deficit in interneuron development.

We examined GABAergic interneuron numbers in wild type and Slc25a12 KO mice by probing tissues with an antibody against GABA. We focused our analysis on the hippocampus, since it is known to be a highly epileptogenic region, and it was previously demonstrated that loss of interneurons in the hippocampus led to a seizure-like state (Sloviter, 1987; de Lanerolle et al., 1989; Dudek, 2002; Cobos et al., 2005). To our surprise, the number of GABAergic interneurons in Slc25a12 KO hippocampus did not significantly differ from wild type (Figure 3.3A).

To investigate whether Slc25a12 KO affected interneuron differentiation, we induced interneuron differentiation on induced pluripotent stem cells (iPSCs) derived from patients with partial Slc25a12 loss of function (Falk et al., 2014). The differentiation protocol has been used in our lab to successfully differentiate iPSCs into interneurons (Maroof et al., 2013) and consists of exposing iPSCs to a variety of small molecules to first enhance forebrain differentiation and then achieve cell type ventralization, mimicking the environment of the medial ganglionic eminence where interneurons are naturally born (Figure 3.3B). After subjecting patient-derived iPSCs to this differentiation protocol, we showed that Slc25a12 loss of function iPSCs were able to successfully differentiate into cells that expressed Nkx2.1, a transcription factor critical for the determination and specification of inhibitory interneurons (Figure 3.3C), suggesting that Slc25a12 loss of function does not affect the initial development of GABAergic interneurons.

Though the investigation of interneuron numbers and differentiation does not shed light on the effect of Slc25a12 KO on interneuron function, it suggests that Slc25a12 is not required for interneuron migration and that insufficient interneuron numbers is most likely not the cause of seizures in Slc25a12 KO mice/patients.

Slc25a12 KO results in hippocampal selective astrocyte apoptosis with compensatory increase in astrocyte numbers

Despite the respiratory chain being functionally intact, patients with loss of function mutations in Slc25a12 have reduced ATP output (Wibom et al., 2009), most likely due to a reduction in reducing equivalents (used to fuel ATP synthesis) being

imported into the mitochondria by Slc25a12's actions as part of the malate aspartate shuttle. Cells that undergo metabolic stress and do not produce enough ATP can undergo apoptosis (Aito et al., 2002; Altman and Rathmell, 2012). The brain is one of the most energy-consuming organs in the body, using up to 20% of the body's basal metabolism despite being only 2% of the total body weight (Raichle and Gusnard, 2002). We reasoned that the high-energy demands of the brain would make it particularly susceptible to reduced ATP output, leading to cellular apoptosis across the board. To test this idea, we examined wild type and Slc25a12 KO brains with the apoptotic marker cleaved caspase 3.

To our surprise, we observed an astounding region-specific enrichment of cleaved caspase 3-expressing cells in the hippocampus of Slc25a12 KO mice (Figure 3.4A). Using double labeling with the astrocytic marker S100β, we also determined that the apoptosis was specific to astrocytes, with over 50% of S100β-expressing astrocytes also expressing apoptotic markers (Figure 3.4B). The statistical variance observed may be due to the small number of animals tested, but quite possibly also the heterogeneity in the developmental progression of the phenotype. This heterogeneity is also observed in the patients with loss of function Slc25a12 mutations, where the onset of seizures varies from 7-10 months. Though we observed apoptosis in all hippocampal CA fields, the phenotype was most pronounced and statistically significant in the hilus, and we confirmed this result using other apoptotic markers cleaved PARP and the TUNEL assay (Figure 3.4C).

In mouse, most astrocytes in the hippocampus are generated by P16 (Nixdorf-Bergweiler et al., 1994). Since astrocyte apoptosis is most pronounced at P16 in

Slc25a12 KO hippocampus, we wondered whether the putative loss of astrocytes to apoptosis in Slc25a12 KO hippocampus would lead to a compensatory increase in astrocytes. To test this question, we examined whether an increase in both immature and mature astrocytes would be apparent in Slc25a12 KO hippocampus. In wild type hippocampus, the immature astrocyte marker CD44 is expressed at low levels from P5-P7 and diminishes at P11, consistent with the developmental timeline of astrocyte proliferation (Bushong et al., 2004). In Slc25a12 KO hippocampus, CD44 was enriched from P5-P7, and particularly at P11 (Figure 3.5A), indicating either that astrocyte maturation is delayed, or that astrocytes proliferate to replenish apoptosing astrocytes. An analysis of total astrocyte numbers in Slc25a12 KO hippocampus at P16 indicates that there are significantly more astrocytes compared to wild type, suggesting that astrocyte proliferation may in fact be compensating for apoptotic cell loss (Figure 3.5B).

Hippocampal astrocyte apoptosis is not apparent in mice deficient in the transcription factor Arx

It had been previously demonstrated that kainic acid-induced status epilepticus resulted in robust cleaved caspase 3 expression in astrocytes (Narkilahti et al., 2003), suggestive of apoptosis. However, evidence for this occurring in a genetic seizure model other than Slc25a12 KO has been lacking. To determine whether astrocyte apoptosis could also result from non-chemically-induced persistent seizures, we examined Arx null mice for evidence of astrocyte apoptosis.

Arx is one of several homeodomain-containing transcription factors involved in GABAergic interneuron migration and maturation in the brain (McManus and Golden, 2005; Friocourt et al., 2008). Similar to patients with Slc25a12 loss of function mutations, patients with mutations in Arx exhibit spontaneous persistent seizures with developmental delay. Using mice with a GCG triplet repeat expansion in Arx ($Arx^{(GCG)10+7}$), which are viable and recapitulates the features of the human triplet repeat expansion (Price et al., 2009), we observed that astrocyte apoptosis was not apparent before or after the age of seizure onset (~P30) (Figure 3.6), suggesting that the phenotype is unique to Slc25a12 KO.

Hippocampal astrocyte apoptosis precedes onset of behavioral seizures

In many epilepsy models as well as in human epilepsy, prolonged seizures can result in neuronal cell death in the hippocampus (Zhang et al., 1998; Faherty et al., 1999; Henshall et al., 2004; Henshall 2007). In one study, kainic acid-induced status epilepticus also resulted in pronounced hippocampal astrocytic cell death (Narkilahti et al., 2003). To determine whether astrocyte cell death in Slc25a12 KO mice precedes seizures or is a result of them, we used video seizure monitoring to examine whether the onset of behavioral seizures precedes or follows the onset of astrocyte apoptosis at P11.

While behavioral seizures in Slc25a12 KO mice are entirely spontaneous, we found that a one-hour period of monitoring from ages P7-P16 was sufficient to document a spontaneous seizure. In this time period, 6 of 7 Slc25a12 KO mice exhibited behavioral seizures by P15, with the earliest occurring on P13, two days

after the onset of astrocyte apoptosis (Figure 3.5C). Unlike the kainic acid-induced seizure model where seizures resulted in astrocyte apoptosis, that astrocyte apoptosis in Slc25a12 KO precedes the onset of behavioral seizures suggests that astrocytes may contribute to seizure genesis.

Slc25a12 KO astrocytes down-regulate expression of glutamate transporters GLT-1 and GLAST

Astrocytes play an important role in the modulation of excitatory neurotransmission. They achieve this in part through the expression of the sodium-dependent glutamate reuptake transporters GLT-1 and GLAST, which clear glutamate from the synaptic cleft, thereby ceasing its effects on postsynaptic glutamate receptors. Our evidence refuting the notion that interneurons may be a driver of seizure genesis in Slc25a12 KO mice prompted us to examine whether Slc25a12 KO astrocytes exhibit other abnormalities that would contribute to seizures. Previous studies have shown that GLT-1 and GLAST protein expression is down-regulated in other seizure models (Miller et al., 1997; Tanaka et al., 1997; Dutuit et al., 2002; Zhang et al., 2004). To test this idea, we examined hippocampal glutamate levels and GLT-1 and GLAST protein expression from wild type and Slc25a12 KO mice.

Our findings indicate that the expression of astrocytic glutamate reuptake transporter GLT-1 is significantly decreased in the Slc25a12 KO hippocampus (Figure 3.7). 5-10% of GLT-1 protein is also expressed in neurons. We maintain that the loss of GLT-1 in Slc25a12 occurs in astrocytes, as a preliminary analysis of glutamate reuptake in P2 synaptosomes revealed that glutamate reuptake was not

different between Slc25a12 KO and wild type, an effect that can be explained by the recent finding that neuronal GLT-1 is the major contributor to glutamate uptake in P2 synaptosomes (Petr et al., 2015). Hippocampal GLAST was also shown to have a decreasing trend (Figure 3.7). The lack of glutamate reuptake transporters in Slc25a12 KO suggests a role for altered glutamate neurotransmission in seizure genesis.

Electrophysiology of Slc25a12 KO pyramidal cells indicate evidence of synaptic glutamate retention

We examined amplitude, frequency, area, and decay of mEPSPs in hippocampal CA3 excitatory pyramidal cells in wild type and Slc25a12 KO mice. We found the amplitude unchanged, suggesting that the amount of glutamate packaged and released by the pyramidal cells is not different between KO and wild types (Figure 3.8A). In addition to this, we found that there were more frequent glutamate release events in the KO, as evidenced by the leftward shift in the cumulative probability of Slc25a12 KO events, or the decrease in Slc25a12 KO inter-event interval (Figure 3.8B). This finding, coupled with the enhanced area under the mEPSP curve (Figure 3.8C) and longer delay towards signal decay (Figure 3.8D) in Slc25a12 KO animals supports the hypothesis that Slc25a12 KO animals have prolonged synaptic glutamate retention that may contribute to seizures. These electrophysiological data support the biochemical GLT-1 expression data. The glutamate reuptake transporters contribute directly to the amplitude of the mEPSPs by virtue of their kinetics. Glutamate reuptake transporter kinetics are known to be

considerably faster than the kinetics of post-synaptic glutamate receptors, and thus, their absence or down-regulation will cause an enhancement of the mEPSP amplitude. To determine how GABAergic neurotransmission is altered, we have measured mIPSPs; the analysis is forthcoming.

Slc25a12 KO astrocytes up-regulate expression of the neuromodulatory kinase ADK

Adenosine has been identified as an inhibitory neuromodulator through its effects on reducing glutamate release (Corradetti et al., 1984). Adenosine-modulated inhibitory tone can be disturbed, resulting in seizure states, through its phosphorylation into AMP by ADK. ADK exists in a long and short isoform, found in the nucleus and cytoplasm, respectively (Cui et al., 2009). In early postnatal development, ADK-L is expressed specifically in neuronal nuclei, and for reasons unknown, the ADK shifts its isoform and cellular expression to astrocytic ADK-S by P14 (Studer et al., 2006). Research from Detlev Boison's group has shown that ADK-S is up-regulated in hippocampal astrocytes in human temporal lobe epilepsy, and becomes up-regulated as a result of reactive astrocytosis in animal models of epilepsy (Gouder et al., 2004; Fedele et al., 2005; Li et al., 2008; Shen et al., 2014). Moreover, overexpressing ADK-S in a kainic acid model of epilepsy exacerbated seizures, suggesting that up-regulated ADK may play a role not only in genesis, but also in perseverance of seizures (Fedele et al., 2005). This prompted us to examine whether ADK was up-regulated in Slc25a12 KO mice, and whether seizures resulted from ADK-driven loss of inhibitory tone.

Our immunohistological examination of ADK revealed enhanced astrocytic ADK in Slc25a12 KO hippocampus (Figure 3.9A). However, unlike previously published reports on ADK expression levels in seizure models, we found that total ADK protein levels were unchanged between wild type and Slc25a12 KO (Figure 3.9B). Upon further examination, we observed that ADK in Slc25a12 KO astrocytes was localized to the nucleus. It is not known how ADK functions in the nucleus, and whether it affects the bioavailability of adenosine like cytoplasmic ADK. However, the aberrant localization of ADK in Slc25a12 KO astrocytes contributes to growing evidence of astrocytic abnormalities that may contribute to altered glutamate neurotransmission and seizure states.

Discussion

In this study, we identify a novel phenotype – hippocampal-specific astrocyte apoptosis occurring before the onset of behavioral seizures – that strongly implicates the astrocyte as a major contributor to seizure genesis in Slc25a12 KO mice. We further confirm the role of astrocytes in Slc25a12 KO seizure genesis by showing that astrocytes also down-regulate their expression of glutamate reuptake transporters GLT-1 and GLAST, and up-regulate the expression of ADK, resulting in glutamate excitotoxicity through glutamate retention in the synaptic cleft and an increase in glutamate release events, respectively. These effects are supported by the electrophysiological characteristics of hippocampal pyramidal cells.

Normal interneuron development in Slc25a12 KO mice

Mitochondrial ATP via oxidative phosphorylation is required for interneuron tangential migration (Lin-Hendel et al., unpublished), and interneurons, particularly the fast-spiking subset, contain large amounts of mitochondria (Gulyás et al., 2006). How might knocking out Slc25a12, a mitochondrial protein indirectly involved in ATP generation, lead to the normal development of interneurons? Postnatal expression of Slc25a12 is limited to only a few organs: the brain, heart, and skeletal muscle (del Arco et al., 2002). During development, Slc25a12 shares overlapping expression with its protein isoform Slc25a13, particularly in the brain (del Arco et al., 2002). This overlapping expression persists until the end of neurogenesis and interneuron migration, and suggests that Slc25a13 may provide functional compensation for neural development in Slc25a12 KO mice, leading to normal interneuron development.

Astrocyte apoptosis: Cell autonomy

Oligodendrocytes do not express Slc25a12, yet both Slc25a12 loss of function patients and Slc25a12 KO mice exhibit global central nervous system hypomyelination (Jalil et al., 2005; Wibom et al., 2009; Sakurai et al., 2009; Falk et al., 2014), a non-cell autonomous phenotype that was demonstrated to be a result of a lack of neuron-supplied N-acetylaspartate, which oligodendrocytes use to synthesize myelin. The astrocytic expression of Slc25a12 has been a subject of debate. We have shown that Slc25a12 is expressed in astrocytes, suggesting that global Slc25a12 KO may contribute to cell autonomous effects in astrocytes, though this does not rule out non-cell autonomous effects neuronal Slc25a12 KO may have on astrocytes.

One method we plan to use to determine cell autonomy is an *in vitro* system where neurons and astrocytes that are either both wild type, both Slc25a12 KO, or of mixed genotypes are co-cultured. These cultures can thereafter be assayed for astrocyte cell death. However, it is known that astrocytes *in vitro* substantially differ from their *in vivo* counterparts. To resolve this difference, we also plan to examine cell autonomy *in vivo* by transplanting doubly transgenic Slc25a12 KO; GLT-1-GFP astrocytes into wild type, neonatal mouse pups.

Despite the issue of cell autonomy, we have so far failed to observe Slc25a12 KO astrocyte cell death *in vitro* using both mixed primary neuron and astrocyte cultures and astrocyte only cultures. Moreover, it is not known whether the astrocytes of patients with Slc25a12 loss of function mutations also exhibit cellular apoptosis. The creation of an *in vitro* system that recapitulates *in vivo* Slc25a12 KO astrocyte apoptosis will be essential for identifying metabolic abnormalities that may contribute to cell death and for testing small molecules or other therapeutics for their effects on preventing cell death. The lack of astrocyte cell death *in vitro* may be attributed to known differences between cultured and *in vivo* astrocytes, or the high availability of glucose and additional glycolytic substrates in the culture media. Future experiments include culturing Slc25a12 KO astrocytes in low glucose, low oxygen conditions, both of which have been demonstrated to have effects on astrocyte survival (Paquet et al., 2013).

Astrocyte apoptosis: Patient profile

Astrocytic abnormalities have not been reported in patients with Slc25a12 loss of function mutations, and it is not known whether astrocytes from these patients undergo apoptosis. We tested this question by generating astrocytes from patient-derived iPSCs and transplanting them into wild type (NOD-SCID) neonatal mouse cortex. Our preliminary experiments suggest that patient astrocytes do not undergo apoptosis, even after 3 weeks *in vivo*. However, it has been well documented that human astrocytes have uniquely hominid features that differentiate them from those of other mammals (Oberheim et al., 2009). These features include enhanced morphological complexity resulting in overlapping patterning, phenotypic diversity of GFAP expression, as well the existence of novel astrocyte population, which may contribute to or account for the phenotypic discrepancy observed between patient and Slc25a12 KO astrocytes. The discrepancy also seems to suggest that astrocyte cell death may be a cell non-autonomous effect, since the genotypic *in vivo* microenvironment patient astrocytes were transplanted in was wild type. We plan to use Slc25a12 KO mice as transplant recipients in future experiments to further explore this question.

Another possible reason for the survival of patient astrocytes *in vivo* is the difference in Slc25a12 protein functionality between patients and the knockout mouse. Unlike the mouse model, which by virtue of being a protein knockout, results in 0% protein functionality, the patients (from whom the iPSCs used in this study were generated) harbor mutations that confer only a partial loss of function that results in 15% protein functionality compared to wild type Slc25a12. It is possible that the retention of some, albeit limited, protein functionality is able to sustain

astrocyte metabolism enough to promote cell survival. A separate case study identified patients with a different mutation in Slc25a12 that conferred 0% protein functionality (Wibom et al., 2009). Future studies using derived astrocytes from these patients may be able to shed light on this issue.

Finally, an important caveat to consider is the heterogeneity of astrocytes; a multitude of different astrocyte cell types have been identified that differ with respect to their morphologies, localization, and transcriptomes (Matyash and Kettenmann, 2010; Chaboub and Deneen, 2012; Zhang et al., 2014). Using a previously published differentiation protocol (Krencik et al., 2011), we were able to differentiate patient-derived iPSCs into cells that expressed glutamine synthetase and GFAP (not shown). However, the current state of not only identification of astrocytic subtypes, but also methods for their differentiation from iPSCs is not as advanced as it is for neurons, for which there are published subtype specific markers and protocols for differentiation into excitatory, motor, and even inhibitory neuron subtypes with fine specificity. Though the cells we generated were astrocytic in nature, it is unclear what type of astrocyte was generated. Upon transplantation, patient astrocytes did not demonstrate localization specificity. Rather, they migrated to every brain region, consistent with previous published reports on human astrocyte transplants (Windrem et al., 2014). The vast heterogeneity of astrocytes and the current challenge of differentiating subtype specific astrocytes from iPSCs must be kept in mind in the interpretation of these experiments.

Concluding Remarks

In healthy individuals, mitochondria function optimally to provide energy to sustain the metabolic needs of all cell types. In the brain, mitochondria are especially important as the brain uses 20% of the body's basal metabolism. Thus, it is not surprising that encephalomyopathy is the most common symptom of mitochondrial disease. The diversity of mitochondrial diseases yields heterogeneity in the resulting encephalomyopathies. The first step in therapeutic development for seizures resulting from mitochondrial disease is identifying and understanding changes in the development and function of neural cell types. To this end, the findings described in this Chapter provide novel insight on astrocytic contributions to dysregulated glutamatergic neurotransmission and seizures in a particular mitochondrial disease resulting from Slc25a12 loss of function. In addition, this work underscores the importance of studying astrocytes in disease and suggests that cell-targeted therapeutics may be a beneficial avenue to explore in treating this disease.

Experimental Procedures

Animals

Slc25a12 heterozygous mice were re-derived from sperm (a gift from the Joseph Buxbaum lab) and out-bred once onto a CD1 genetic background. Heterozygous mice were bred with each other to generate homozygous Slc25a12 KO mice, which were viable until approximately P22 and born in expected Mendelian ratios. For preparation of brain tissue, animals were transcardially perfused with phosphate buffer saline (PBS) followed by 4% paraformaldehyde (PFA). Brains were removed from the skull, immersed in 4% PFA overnight, washed three times with PBS at room temperature. Brains were then mounted in 4% low-melt agarose and sectioned at 50 μm using a Leica vibratome. All experiments described in this study were performed in accordance with an approved institutional animal care and use committee protocol.

Immunohistochemistry

Brain sections were blocked for 1 hour at room temperature (5% BSA in 0.1% PBS-Triton) and probed in blocking buffer with antibodies recognizing Slc25a12 (Thermo Scientific, PA5-23778, 1:100), PV (Swant, PV 235, 1:2500), GFP (Abcam, ab13970, 1:1000), GABA (Swant, GABA 3A12, 1:500), S100β (Sigma, S2657, 1:100), cleaved caspase 3 (Cell Signaling, 9664S, 1:400), cleaved PARP (Cell Signaling, 9544S, 1:400), CD44 (BD Biosciences, 550538, 1:50), or ADK (gift from Boison Detlev, 1:500) overnight at 4°C. The following secondary antibodies were used: Alexa-568 goat anti-rabbit (Life Technologies, A-11011, 1:1000), Alexa-488

goat anti-mouse (Life Technologies, A-11001, 1:1000), Alexa-488 goat anti-chicken (Life Technologies, A-11039, 1:1000), Alexa-568 goat anti-mouse (Life Technologies, A-11034, 1:1000).

For differentiated patient-derived iPSCs, cells were fixed for 20 minutes at room temperature with 4% PFA, washed three times with PBS, blocked blocked for 1 hour at room temperature (5% BSA in 0.1% PBS-Triton) and probed in blocking buffer with an antibody recognizing Nkx2.1 (Abcam, ab72876, 1:100). The secondary antibody used was Alexa-568 goat anti-rabbit (Life Technologies, A-11011, 1:1000).

TUNEL assay

Floating 50 μm sections were treated with 50 μl of 10 μg/ml Proteinase K in 10 mM Tris-HCl, pH 7.5 for 5 minutes at 37°C, washed three times in PBS, and then incubated in *In Situ* Cell Death Detection Kit TUNEL reaction mixture (Roche, 11684795910) according to the manufacturer's instructions. Positive controls were achieved by incubating wild type sections in 3000 U/ml DNase I recombinant (Roche 4716728001) in 50 mM Tris-HCl, pH 7.5, 1 mg/ml BSA for 10 minutes at room temperature.

Imaging and phenotypic analysis

Images were acquired using a Photometrics CoolSNAP ES2 camera attached to a Nikon Eclipse Ni microscope with NIS Elements AR imaging software. Images were processed using Adobe Photoshop and scored using ImageJ Cell Counter tool. When counting cells, a cell was considered to be apoptotic or GABAergic if the

fluorescent signal was pervasive throughout the cell body or nucleus (representing cells on the top plane of the tissue), with nuclear DAPI present. Cells were counted only in the hippocampal hilus and did not extend to the region beyond the fork of the dentate gyrus. For pixel area quantification in CD44 experiment, thresholding was achieved by first calculating the mean and standard deviation (σ) for three randomly selected background staining ROIs. Three times the standard deviation above the mean was established as the positive detection threshold.

Patient-derived iPSC interneuron differentiation

Patient-derived iPSCs were maintained on 5% extracellular matrix (Sigma, E6909) in DMEM/F-12 media until confluency. Once confluent, cells were re-plated into ECM-coated 24-well plates for differentiation. For differentiation, iPSCs were treated with KnockOut Serum Replacement media (Life Technologies, 10828-028) supplemented with LDN-193189 (Stemgent, 04-0074, 100 nM), SB431542 (Stemgent, 04-0010, 10 μM), and XAV939 (Stemgent, 04-00046, 2 μM), hereafter referred to as "LSX" media, from differentiation days (Zhang et al.) 0-4. From DD4-5, iPSCs were treated with 3:1 LSX:N2 media (N2 media consists of DMEM/F-12 with 0.75 g D-glucose (EM Science, DX0156), 1% glutamax (Gibco, 35050), 1% N2 supplement B (Stemgent, 07156), 0.1% beta-mercaptoethanol (Life Technologies, 21985-023), and 0.2% primocin (Life Technologies, Ant-pm-2)). From DD6-7, iPSCs were treated with 1:1 LSX:N2 media, and from DD8-9, with 1:3 LSX:N2 media. From DD10-18, iPSCs were subject to ventral cell patterning by being treated with N2+B27 media containing human Shh (R&D, 1845-SH-0251, 100 ng/mL) and

purmorphamine (Stemgent, 04-009, 1 μM). From DD18 onwards, iPSCs were treated with Neurobasal media (Gibco, 21103) with B27 supplement (Life Technologies, 17504).

Video behavioral seizure monitoring

P7 to P16 age Slc25a12 KO mice and wild type littermates were placed in cage compartment on top of a heated pad for 1 hour. Behavioral seizures were recorded with a digital video camera (Stellate Systems; Harmonie, version 5.0b).

Western assay

To generate hippocampal protein lysates, brains were quickly dissected on dry ice and hippocampus was isolated from the overlying cortex. Tissues were placed in pre-weighed Eppendorf tubes, and 1 ml RIPA lysis buffer with protease inhibitor (Sigma, P8340, 1:100) was added per 200 mg tissue. Tissues were homogenized using a handheld tissue homogenizer, agitated for 2 hours at 4°C, then centrifuged at 12,000 RPM for 20 minutes. 5, 10, and 40 μg protein for the detection of GLT-1, GLAST, and ADK respectively, were loaded into 4-12% Bis-Tris Plus Gels (Life Technologies, BG04120BOX), electrophoresed for 40-60 minutes at 80V, then transferred onto nitrocellulose membranes using the iBlot dry blotting system (Life Technologies, IB1001). Membranes were incubated for 1 hour at room temperature in Odyssey blocking buffer (Licor, 927-50000), washed three times in PBS with 0.1% Tween (PBS-T), then incubated overnight at 4° in with antibodies recognizing GLT-1 (Jeffrey Rothstein lab, 1:5000), GLAST (Miltenyi Biotec, 130-095-822, 1:50), and

ADK (Detlev Boisson lab, 1:6000). After washing membranes three times with PBS-T, membranes were incubated with Licor Odyssey secondary antibodies according to the manufacturer's instructions, and developed and quantified using the Odyssey CLx Infrared Imaging System (Licor) and Image Studio Lite software (Licor).

Electrophysiology

Mice aged P13-P17 were anesthetized with isoflurane and decapitated. Brains were dissected out placed immediately in bubbled ice cutting solution (2.5 mM KCl, 1.25 mM NaH_2PO_4, 218 mM sucrose, 26 mM $NaHCO_3$, 10 mM D-glucose, 0.5 mM $CaCl_2$, 10 mM $MgSO_4$, with 95% O_2 and 5% CO_2 and 285 mOsM). Brains were bisected down the midline and mounted on a cutting stage angled at 12-15 degrees to produce 350 μm thick hippocampal entorhinal cortex sagittal slices. Slices were placed in bubbled artificial cerebrospinal fluid (130 mM NaCl, 2.75 mM KCl, 1.1 mM NaH_2PO_4, 28.82 mM $NaHCO_3$, 11.1 mM D-glucose, 2.5 mM $CaCl_2$, 1.43 mM $MgSO_4$ with 315 mOsM) for 30 minutes at 37°C, then at room temperature for 1 hour prior to recording. For mEPSC and sIPSP recordings, pyramidal cells in CA3 were patched with an internal pipette solution consisting of 5 mM KCl, 135 mM K-gluconate, 2 mM NaCl, 10 mM HEPES, 4 mM EGTA, 4 mM MgATP, 0.3 mM Na_3GTP, with a pH of 7.2 and osmolarity of 285 mOsM. Cells were held at -60 mV in the presence of 0.5 μM tetrodotoxin (mEPSC) and -40 mV (sIPSP). After recording, cells were filled with neurobiotin (Vector Labs, SP-1120) for post-recording processing.

ADK inhibitor treatment

ABT-702 (Tocris, 2372) was reconstituted in sterile DMSO. Mice will be given daily intraperitoneal injections of 10 mg/kg ABT-702 in sterile PBS (Tocris, 2372) from P10-P16, 12 hours before prior to the assessment of behavioral seizures by video monitoring.

Figure 3.1. Slc25a12 (AGC) is localized to the inner mitochondrial membrane where it is a part of the malate aspartate shuttle.

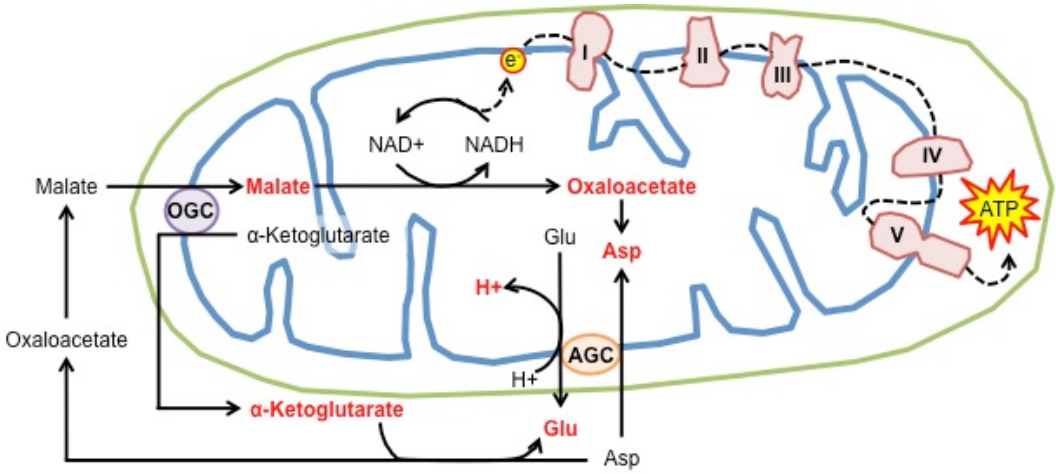

Figure 3.1. Slc25a12 (AGC) is localized to the inner mitochondrial membrane where it is a part of the malate aspartate shuttle.

As part of the malate-aspartate shuttle with the oxoglutarate carrier (OGC), Slc25a12 (shown here as AGC) catalyzes the exchange of intramitochondrial aspartate and cytosolic glutamate plus a proton. This process brings NADH from the cytosol to the mitochondria, where its electrons participate in the electron transport chain to generate ATP for the cell.

Figure 3.2. Slc25a12 is expressed in neurons, interneurons, and astrocytes

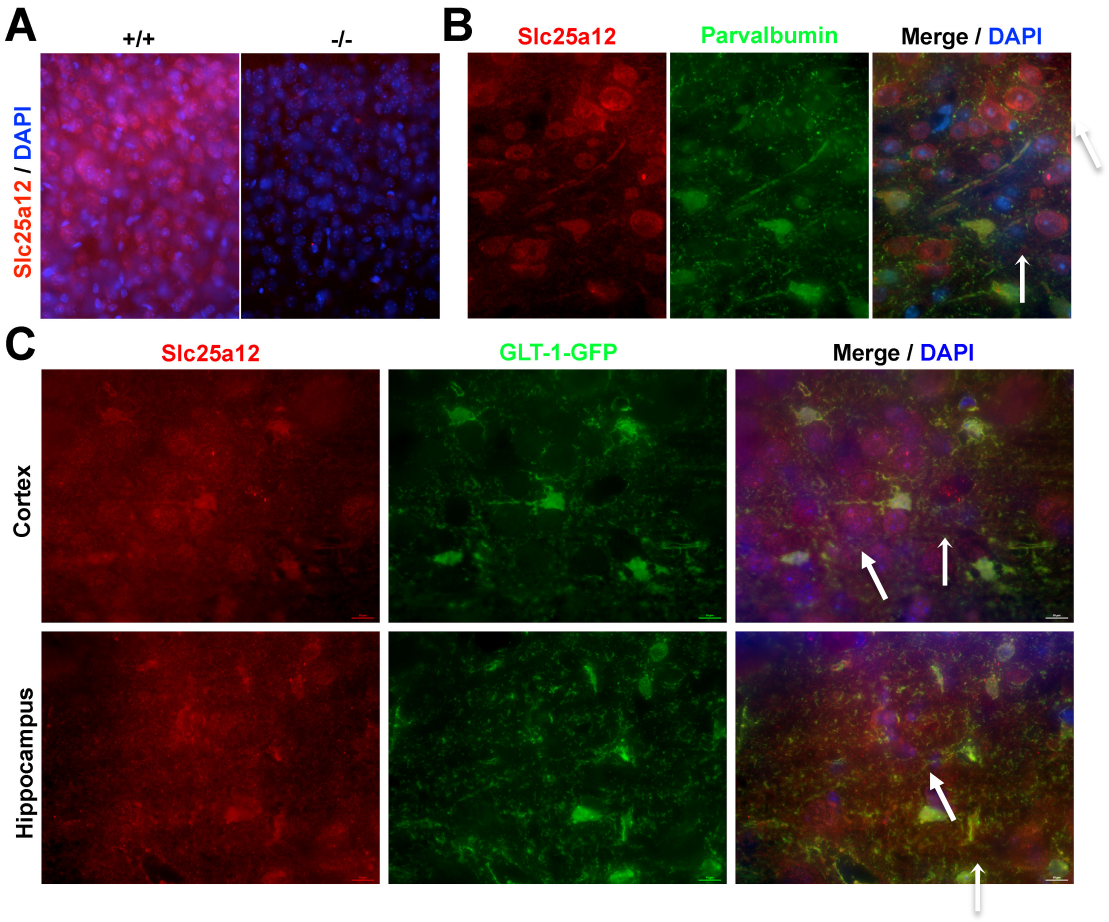

Figure 3.2. Slc25a12 is expressed in neurons, interneurons, and astrocytes

A) Fluorescence immunohistochemistry for Slc25a12 (red) in P16 wild type (left) and Slc25a12 KO (right) mouse cortex. Dorsal is up.

B) Fluorescence immunohistochemistry for Slc25a12 (red) and parvalbumin (green) in P16 wild type mouse brain. Open arrowhead indicates cells that co-express Slc25a12 and parvalbumin. Closed arrowheads show cells that express only Slc25a12.

C) Fluorescence immunohistochemistry for Slc25a12 (red) and GFP (green, driven by GLT-1/BAC). Open arrowhead indicates cells that co-express Slc25a12 and GFP. Closed arrowheads show cells that express only Slc25a12.

Figure 3.3. Loss of Slc25a12 does not adversely impact interneuron development and differentiation

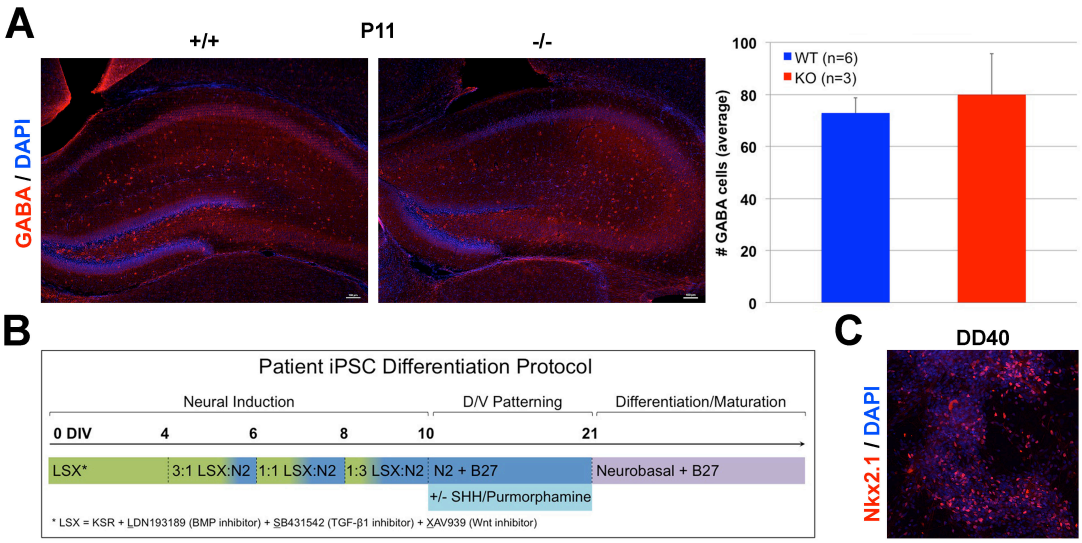

Figure 3.3. Loss of Slc25a12 does not adversely impact interneuron development and differentiation

A) Fluorescence immunohistochemistry for GABA (red) and DAPI (blue) of P11 wild type and Slc25a12 KO hippocampus (left). Quantification of GABA cell counts (right). Data were analyzed by two-tailed Student's t-test. Error bars indicate SEM.

B) Patient-derived induced pluripotent stem cell protocol for differentiation into putative interneurons.

C) Fluorescence immunocytochemistry for the putative interneuron marker Nkx2.1 (red) and DAPI (blue) on Slc25a12 loss of function patient-derived induced pluripotent stem cells differentiated into ventralized, putative interneurons after 40 days of differentiation.

Figure 3.4. Slc25a12 KO results in hippocampal selective astrocyte apoptosis.

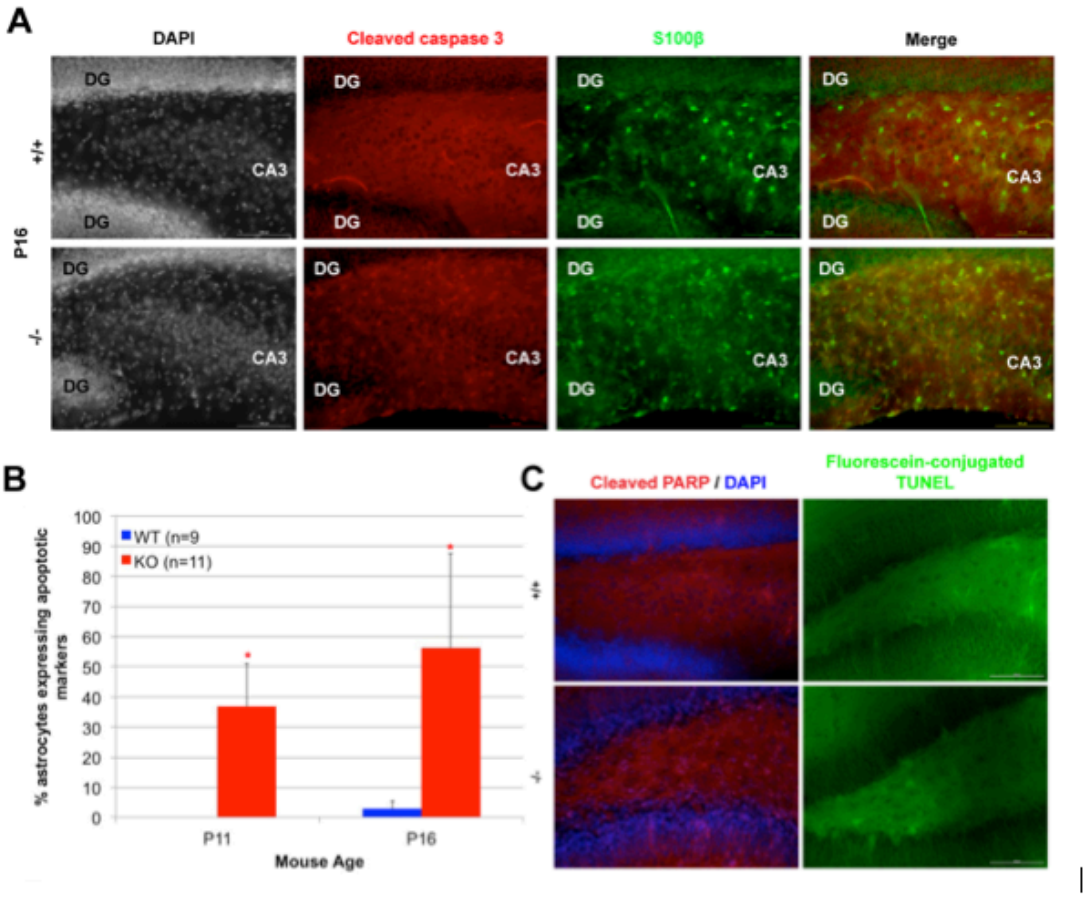

Figure 3.4. Slc25a12 KO results in hippocampal selective astrocyte apoptosis.

A) Fluorescence immunohistochemistry for the apoptotic marker cleaved caspase 3 (red) and S100β (green) in P16 wild type (top panel) and Slc25a12 KO (bottom panel) hippocampus. DG indicates dentate gyrus.

B) Quantification of the astrocytes expressing apoptotic markers cleaved caspase 3 or cleaved PARP. Data were analyzed by two-tailed Student's t-test. * indicates $p<0.05$ compared to wild type. Error bars indicate SEM.

C) Fluorescence immunohistochemistry for the apoptotic marker cleaved PARP (red), on left, and fluorescein-conjugated TUNEL reaction (green), on right.

Figure 3.5. Astrocyte apoptosis is accompanied by compensatory increase in astrocyte numbers and precedes the onset of behavioral seizures.

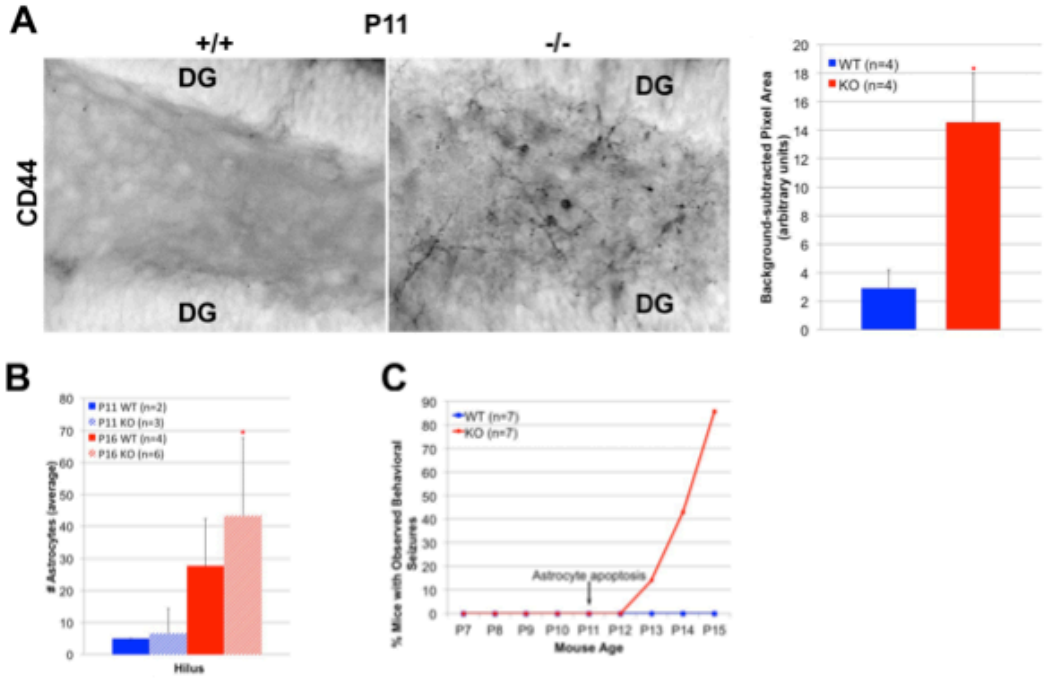

Figure 3.5. Astrocyte apoptosis is accompanied by compensatory increase in astrocyte numbers and precedes the onset of behavioral seizures.

A) Inverted image of fluorescence immunohistochemistry for CD44 (dark) in P11 wild type and Slc25a12 KO hippocampus (left). Quantification of pixel area (right). Thresholding for CD44 signal was achieved by first calculating the mean and standard deviation (σ) for three randomly selected background staining ROIs. Three times the standard deviation above the mean became the positive detection threshold. DG indicates dentate gyrus. Data were analyzed using two-tailed Student's t-test. * indicates $p<0.05$. Error bars indicate SEM.

B) Quantification of hippocampal astrocyte number at P11 (blue) and P16 (red). Solid bars indicate wild type, and hatched bars indicate Slc25a12 KO. Data wre analyzed using two-tailed Student's t-test. * indicates $p<0.05$. Error bars indicate SEM.

C) Line chart illustrating time of onset for astrocyte apoptosis and behavioral seizures in wild type and Slc25a12 KO mice.

Figure 3.6. Hippocampal astrocyte apoptosis is not apparent in mice deficient in the transcription factor Arx.

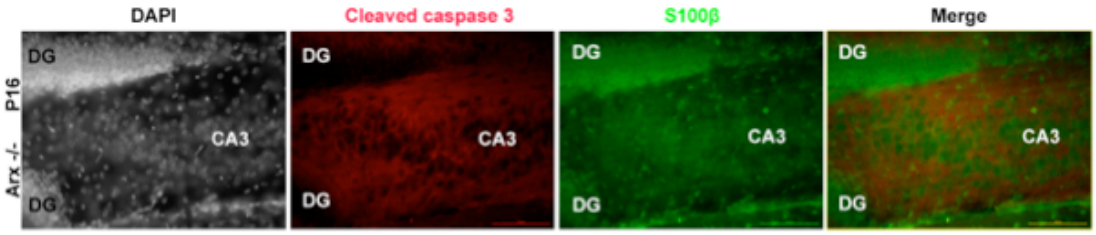

Figure 3.6. Hippocampal astrocyte apoptosis is not apparent in mice deficient in the transcription factor Arx.

Fluorescence immunohistochemistry for the apoptotic marker cleaved caspase 3 (red) and S100β (green) in P16 *Arx*$^{(GCG)10+7}$ mice (n=2).

Figure 3.7. Slc25a12 KO astrocytes down-regulate expression of glutamate transporters GLT-1 and GLAST.

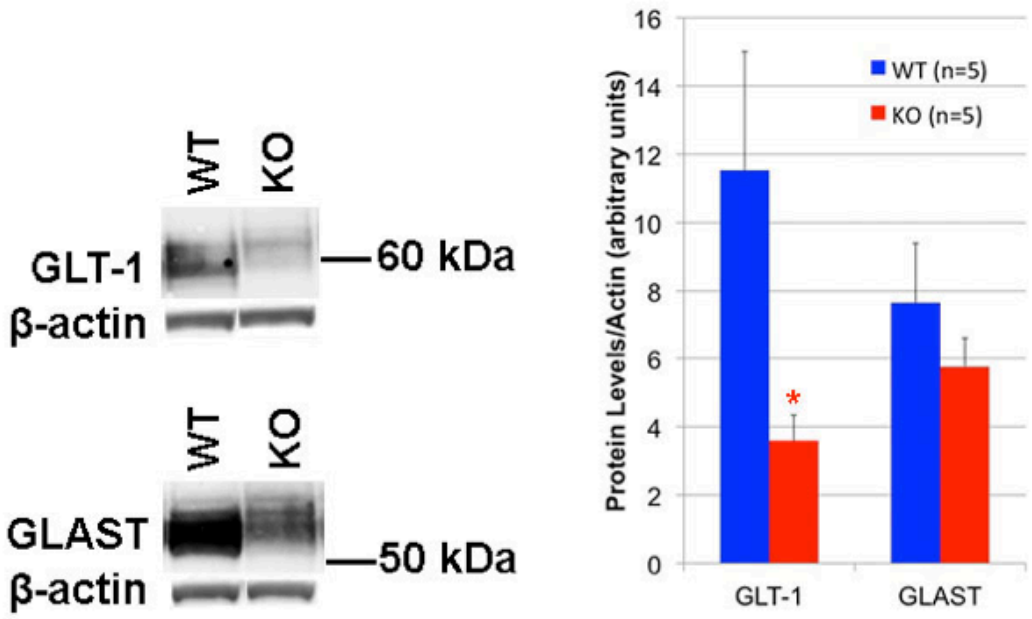

Figure 3.7. Slc25a12 KO astrocytes down-regulate expression of glutamate transporters GLT-1 and GLAST.

Representative blots for GLT-1 and GLAST are shown on the left panel.

Quantification of blot intensity on right. Data were analyzed with two-tailed Student's t-test. * indicates $p<0.05$. Error bars indicate SEM.

Figure 3.8. Electrophysiology of Slc25a12 KO pyramidal cells indicate evidence of synaptic glutamate retention.

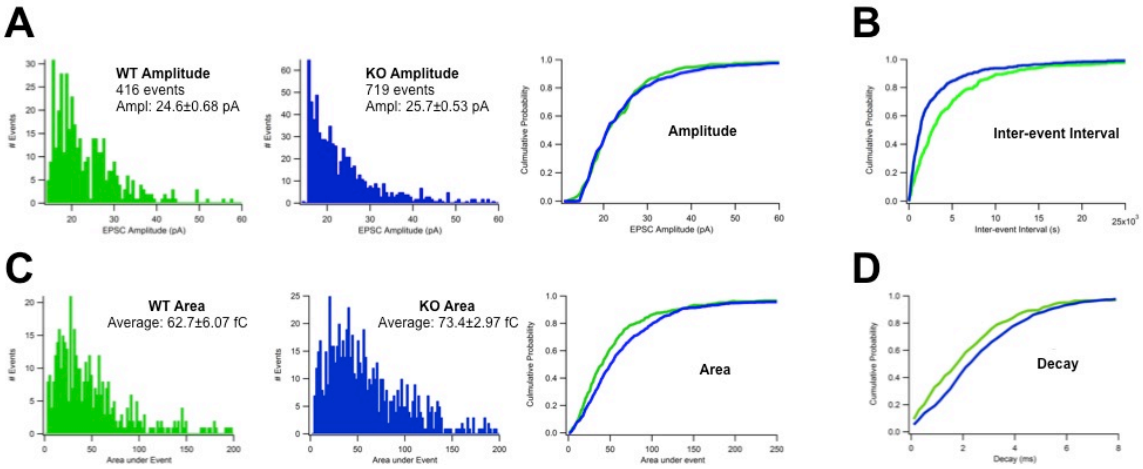

Figure 3.8. Electrophysiology of Slc25a12 KO pyramidal cells indicate evidence of synaptic glutamate retention.

A) Histogram depicting the number of events for a bin of amplitudes for wild type (green) and Slc25a12 KO (blue) on left, followed by cumulative probability K-S curve for amplitude, on right.

B) Inter-event interval cumulative probability K-S curve for wild type (green) and Slc25a12 KO (green).

C) Histogram depicting the number of events for a bin of mEPSP areas for wild type (green) and Slc25a12 KO (blue) on left, followed by cumulative probability K-S curve for mEPSP area, on right.

D) mEPSP decay cumulative probability K-S curve for wild type (green) and Slc25a12 KO (green).

Figure 3.9. Slc25a12 KO astrocytes up-regulate expression of the neuromodulatory kinase ADK.

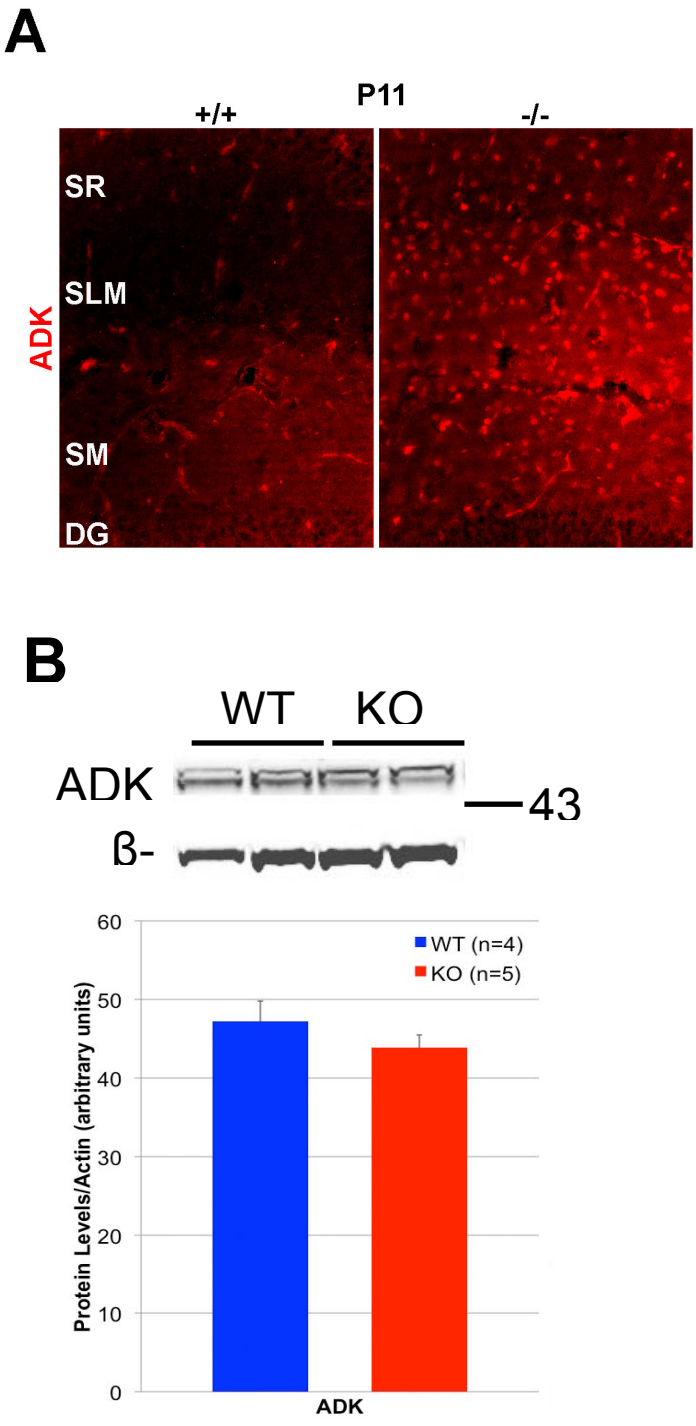

Figure 3.9. Slc25a12 KO astrocytes up-regulate expression of the neuromodulatory kinase ADK.

A) Fluorescence immunohistochemistry for ADK (red) in hippocampus of P16 wild type and Slc25a12 KO mice. SR, SLM, SM, DG indicate stratum radiatum, stratum lacunosum moleculare, stratum moleculare, and dentate gyrus respectively.

B) Representative blots for ADK are shown on the top panel. Band intensity was quantified for both long and short isoforms, and was not significantly different between wild type and KO. The quantification of total band intensity is shown on the bottom panel. Data were analyzed with two-tailed Student's t-test. Error bars indicate SEM.

References

Airaksinen AM, Hekmatyar SK, Jerome N, Niskanen JP, Huttunen JK, Pitkanen A, Kauppinen RA, Grohn OH (2012) Simultaneous BOLD fMRI and local field potential measurements during kainic acid-induced seizures. Epilepsia *53*:1245-1253.

Aito H, Aalto KT, Raivio KO (2002) Biphasic ATP depletion caused by transient oxidative exposure is associated with apoptotic cell death in rat embryonal cortical neurons. Pediatric research *52*:40-45.

Altman BJ, Rathmell JC (2012) Metabolic stress in autophagy and cell death pathways. Cold Spring Harbor perspectives in biology *4*:a008763.

Anitha A, Nakamura K, Thanseem I, Yamada K, Iwayama Y, Toyota T, Matsuzaki H, Miyachi T, Yamada S, Tsujii M, Tsuchiya KJ, Matsumoto K, Iwata Y, Suzuki K, Ichikawa H, Sugiyama T, Yoshikawa T, Mori N (2012) Brain region-specific altered expression and association of mitochondria-related genes in autism. Molecular autism *3*:12.

Blasi F, Bacchelli E, Carone S, Toma C, Monaco AP, Bailey AJ, Maestrini E, International Molecular Genetic Study of Autism C (2006) SLC25A12 and CMYA3 gene variants are not associated with autism in the IMGSAC multiplex family sample. European journal of human genetics : EJHG *14*:123-126.

Bordey A, Sontheimer H (1998) Properties of human glial cells associated with epileptic seizure foci. Epilepsy research *32*:286-303.

Buono RJ, Lohoff FW, Sander T, Sperling MR, O'Connor MJ, Dlugos DJ, Ryan SG, Golden GT, Zhao H, Scattergood TM, Berrettini WH, Ferraro TN (2004) Association between variation in the human KCNJ10 potassium ion channel gene and seizure susceptibility. Epilepsy research *58*:175-183.

Bushong EA, Martone ME, Ellisman MH (2004) Maturation of astrocyte morphology and the establishment of astrocyte domains during postnatal hippocampal development. International journal of developmental neuroscience : the official journal of the International Society for Developmental Neuroscience *22*:73-86.

Campbell SL, Hablitz JJ (2008) Decreased glutamate transport enhances excitability in a rat model of cortical dysplasia. Neurobiology of disease *32*:254-261.

Chaboub LS, Deneen B (2012) Developmental origins of astrocyte heterogeneity: the final frontier of CNS development. Developmental neuroscience *34*:379-388.

Chien WH, Wu YY, Gau SS, Huang YS, Soong WT, Chiu YN, Chen CH (2010) Association study of the SLC25A12 gene and autism in Han Chinese in Taiwan. Progress in neuro-psychopharmacology & biological psychiatry *34*:189-192.

Cobos I, Calcagnotto ME, Vilaythong AJ, Thwin MT, Noebels JL, Baraban SC, Rubenstein JL (2005) Mice lacking Dlx1 show subtype-specific loss of interneurons, reduced inhibition and epilepsy. Nature neuroscience *8*:1059-1068.

Corradetti R, Lo Conte G, Moroni F, Passani MB, Pepeu G (1984) Adenosine decreases aspartate and glutamate release from rat hippocampal slices. European journal of pharmacology *104*:19-26.

Correia C, Coutinho AM, Diogo L, Grazina M, Marques C, Miguel T, Ataide A, Almeida J, Borges L, Oliveira C, Oliveira G, Vicente AM (2006) Brief report: High frequency of biochemical markers for mitochondrial dysfunction in autism: no association with the mitochondrial aspartate/glutamate carrier SLC25A12 gene. Journal of autism and developmental disorders *36*:1137-1140.

Das A, Wallace GCt, Holmes C, McDowell ML, Smith JA, Marshall JD, Bonilha L, Edwards JC, Glazier SS, Ray SK, Banik NL (2012) Hippocampal tissue of patients with refractory temporal lobe epilepsy is associated with astrocyte activation, inflammation, and altered expression of channels and receptors. Neuroscience *220*:237-246.

de Lanerolle NC, Kim JH, Robbins RJ, Spencer DD (1989) Hippocampal interneuron loss and plasticity in human temporal lobe epilepsy. Brain research *495*:387-395.

del Arco A, Morcillo J, Martinez-Morales JR, Galian C, Martos V, Bovolenta P, Satrustegui J (2002) Expression of the aspartate/glutamate mitochondrial carriers aralar1 and citrin during development and in adult rat tissues. European journal of biochemistry / FEBS *269*:3313-3320.

del Arco A, Satrustegui J (1998) Molecular cloning of Aralar, a new member of the mitochondrial carrier superfamily that binds calcium and is present in human muscle and brain. The Journal of biological chemistry *273*:23327-23334.

Dennis SC, Lai JC, Clark JB (1977) Comparative studies on glutamate metabolism in synpatic and non-synaptic rat brain mitochondria. The Biochemical journal *164*:727-736.

Dudek FE (2002) Selective Inhibitory Interneuron Loss Produces Chronic Hippocampal Hyperexcitability. Epilepsy currents / American Epilepsy Society *2*:21-22.

Dutuit M, Touret M, Szymocha R, Nehlig A, Belin MF, Didier-Bazes M (2002) Decreased expression of glutamate transporters in genetic absence epilepsy rats before seizure occurrence. Journal of neurochemistry *80*:1029-1038.

Eid T, Thomas MJ, Spencer DD, Runden-Pran E, Lai JC, Malthankar GV, Kim JH, Danbolt NC, Ottersen OP, de Lanerolle NC (2004) Loss of glutamine synthetase in the human epileptogenic hippocampus: possible mechanism for raised extracellular glutamate in mesial temporal lobe epilepsy. Lancet *363*:28-37.

Faherty CJ, Xanthoudakis S, Smeyne RJ (1999) Caspase-3-dependent neuronal death in the hippocampus following kainic acid treatment. Brain research Molecular brain research *70*:159-163.

Falk MJ, Li D, Gai X, McCormick E, Place E, Lasorsa FM, Otieno FG, Hou C, Kim CE, Abdel-Magid N, Vazquez L, Mentch FD, Chiavacci R, Liang J, Liu X, Jiang H, Giannuzzi G, Marsh ED, Guo Y, Tian L, Palmieri F, Hakonarson H (2014) Erratum to: AGC1 Deficiency Causes Infantile Epilepsy, Abnormal Myelination, and Reduced N-Acetylaspartate. JIMD reports *14*:119.

Fedele DE, Gouder N, Guttinger M, Gabernet L, Scheurer L, Rulicke T, Crestani F, Boison D (2005) Astrogliosis in epilepsy leads to overexpression of adenosine kinase, resulting in seizure aggravation. Brain : a journal of neurology *128*:2383-2395.

Friocourt G, Kanatani S, Tabata H, Yozu M, Takahashi T, Antypa M, Raguenes O, Chelly J, Ferec C, Nakajima K, Parnavelas JG (2008) Cell-autonomous roles of ARX in cell proliferation and neuronal migration during corticogenesis. The Journal of neuroscience : the official journal of the Society for Neuroscience *28*:5794-5805.

Gouder N, Scheurer L, Fritschy JM, Boison D (2004) Overexpression of adenosine kinase in epileptic hippocampus contributes to epileptogenesis. The Journal of neuroscience : the official journal of the Society for Neuroscience *24*:692-701.

Gulyas AI, Buzsaki G, Freund TF, Hirase H (2006) Populations of hippocampal inhibitory neurons express different levels of cytochrome c. The European journal of neuroscience *23*:2581-2594.

Henshall DC (2007) Apoptosis signalling pathways in seizure-induced neuronal death and epilepsy. Biochemical Society transactions *35*:421-423.

Henshall DC, Schindler CK, So NK, Lan JQ, Meller R, Simon RP (2004) Death-associated protein kinase expression in human temporal lobe epilepsy. Annals of neurology *55*:485-494.

Kang HC, Lee YM, Kim HD (2013) Mitochondrial disease and epilepsy. Brain & development *35*:757-761.

Khurana DS, Salganicoff L, Melvin JJ, Hobdell EF, Valencia I, Hardison HH, Marks HG, Grover WD, Legido A (2008) Epilepsy and respiratory chain defects in children with mitochondrial encephalopathies. Neuropediatrics *39*:8-13.

Khurana DS, Valencia I, Goldenthal MJ, Legido A (2013) Mitochondrial dysfunction in epilepsy. Seminars in pediatric neurology *20*:176-187.

Kim SJ, Silva RM, Flores CG, Jacob S, Guter S, Valcante G, Zaytoun AM, Cook EH, Badner JA (2011) A quantitative association study of SLC25A12 and restricted repetitive behavior traits in autism spectrum disorders. Molecular autism *2*:8.

Krencik R, Weick JP, Liu Y, Zhang ZJ, Zhang SC (2011) Specification of transplantable astroglial subtypes from human pluripotent stem cells. Nature biotechnology *29*:528-534.

Lepagnol-Bestel AM, Maussion G, Boda B, Cardona A, Iwayama Y, Delezoide AL, Moalic JM, Muller D, Dean B, Yoshikawa T, Gorwood P, Buxbaum JD, Ramoz N, Simonneau M (2008) SLC25A12 expression is associated with neurite outgrowth and is upregulated in the prefrontal cortex of autistic subjects. Molecular psychiatry *13*:385-397.

Li B, Hertz L, Peng L (2012) Aralar mRNA and protein levels in neurons and astrocytes freshly isolated from young and adult mouse brain and in maturing cultured astrocytes. Neurochemistry international *61*:1325-1332.

Li X, Zou H, Brown WT (2012) Genes associated with autism spectrum disorder. Brain research bulletin *88*:543-552.

Maroof AM, Keros S, Tyson JA, Ying SW, Ganat YM, Merkle FT, Liu B, Goulburn A, Stanley EG, Elefanty AG, Widmer HR, Eggan K, Goldstein PA, Anderson SA, Studer L (2013) Directed differentiation and functional maturation of cortical interneurons from human embryonic stem cells. Cell stem cell *12*:559-572.

Mathern GW, Mendoza D, Lozada A, Pretorius JK, Dehnes Y, Danbolt NC, Nelson N, Leite JP, Chimelli L, Born DE, Sakamoto AC, Assirati JA, Fried I, Peacock WJ, Ojemann GA, Adelson PD (1999) Hippocampal GABA and glutamate transporter immunoreactivity in patients with temporal lobe epilepsy. Neurology *52*:453-472.

Matyash V, Kettenmann H (2010) Heterogeneity in astrocyte morphology and physiology. Brain research reviews *63*:2-10.

McManus MF, Golden JA (2005) Neuronal migration in developmental disorders. Journal of child neurology *20*:280-286.

Miller HP, Levey AI, Rothstein JD, Tzingounis AV, Conn PJ (1997) Alterations in glutamate transporter protein levels in kindling-induced epilepsy. Journal of neurochemistry *68*:1564-1570.

Narkilahti S, Pirttila TJ, Lukasiuk K, Tuunanen J, Pitkanen A (2003) Expression and activation of caspase 3 following status epilepticus in the rat. The European journal of neuroscience *18*:1486-1496.

Nixdorf-Bergweiler BE, Albrecht D, Heinemann U (1994) Developmental changes in the number, size, and orientation of GFAP-positive cells in the CA1 region of rat hippocampus. Glia *12*:180-195.

Oberheim NA, Takano T, Han X, He W, Lin JH, Wang F, Xu Q, Wyatt JD, Pilcher W, Ojemann JG, Ransom BR, Goldman SA, Nedergaard M (2009) Uniquely hominid features of adult human astrocytes. The Journal of neuroscience : the official journal of the Society for Neuroscience *29*:3276-3287.

Pardo B, Rodrigues TB, Contreras L, Garzon M, Llorente-Folch I, Kobayashi K, Saheki T, Cerdan S, Satrustegui J (2011) Brain glutamine synthesis requires neuronal-born aspartate as amino donor for glial glutamate formation. Journal of cerebral blood flow and metabolism : official journal of the International Society of Cerebral Blood Flow and Metabolism *31*:90-101.

Petr GT, Sun Y, Frederick NM, Zhou Y, Dhamne SC, Hameed MQ, Miranda C, Bedoya EA, Fischer KD, Armsen W, Wang J, Danbolt NC, Rotenberg A, Aoki CJ, Rosenberg PA (2015) Conditional Deletion of the Glutamate Transporter GLT-1 Reveals That Astrocytic GLT-1 Protects against Fatal Epilepsy While Neuronal GLT-1 Contributes Significantly to Glutamate Uptake into Synaptosomes. The Journal of neuroscience : the official journal of the Society for Neuroscience *35*:5187-5201.

Prandini P, Pasquali A, Malerba G, Marostica A, Zusi C, Xumerle L, Muglia P, Da Ros L, Ratti E, Trabetti E, Pignatti PF, Italian Autism N (2012) The association of rs4307059 and rs35678 markers with autism spectrum disorders is replicated in Italian families. Psychiatric genetics *22*:177-181.

Price MG, Yoo JW, Burgess DL, Deng F, Hrachovy RA, Frost JD, Jr., Noebels JL (2009) A triplet repeat expansion genetic mouse model of infantile spasms syndrome, Arx(GCG)10+7, with interneuronopathy, spasms in infancy, persistent seizures, and adult cognitive and behavioral impairment. The Journal of neuroscience : the official journal of the Society for Neuroscience *29*:8752-8763.

Proper EA, Hoogland G, Kappen SM, Jansen GH, Rensen MG, Schrama LH, van Veelen CW, van Rijen PC, van Nieuwenhuizen O, Gispen WH, de Graan PN (2002) Distribution of glutamate transporters in the hippocampus of patients with pharmaco-resistant temporal lobe epilepsy. Brain : a journal of neurology *125*:32-43.

Rabionet R, McCauley JL, Jaworski JM, Ashley-Koch AE, Martin ER, Sutcliffe JS, Haines JL, DeLong GR, Abramson RK, Wright HH, Cuccaro ML, Gilbert JR, Pericak-Vance MA (2006) Lack of association between autism and SLC25A12. The American journal of psychiatry *163*:929-931.

Raichle ME, Gusnard DA (2002) Appraising the brain's energy budget. Proceedings of the National Academy of Sciences of the United States of America *99*:10237-10239.

Ramos M, del Arco A, Pardo B, Martinez-Serrano A, Martinez-Morales JR, Kobayashi K, Yasuda T, Bogonez E, Bovolenta P, Saheki T, Satrustegui J (2003) Developmental changes in the Ca2+-regulated mitochondrial aspartate-glutamate carrier aralar1 in brain and prominent expression in the spinal cord. Brain research Developmental brain research *143*:33-46.

Ramoz N, Reichert JG, Smith CJ, Silverman JM, Bespalova IN, Davis KL, Buxbaum JD (2004) Linkage and association of the mitochondrial aspartate/glutamate carrier SLC25A12 gene with autism. The American journal of psychiatry *161*:662-669.

Regan MR, Huang YH, Kim YS, Dykes-Hoberg MI, Jin L, Watkins AM, Bergles DE, Rothstein JD (2007) Variations in promoter activity reveal a differential expression and physiology of glutamate transporters by glia in the developing and mature CNS. The Journal of neuroscience : the official journal of the Society for Neuroscience *27*:6607-6619.

Sakurai T, Ramoz N, Barreto M, Gazdoiu M, Takahashi N, Gertner M, Dorr N, Gama Sosa MA, De Gasperi R, Perez G, Schmeidler J, Mitropoulou V, Le HC, Lupu M, Hof PR, Elder GA, Buxbaum JD (2010) Slc25a12 disruption alters myelination and neurofilaments: a model for a hypomyelination syndrome and childhood neurodevelopmental disorders. Biological psychiatry *67*:887-894.

Sarac S, Afzal S, Broholm H, Madsen FF, Ploug T, Laursen H (2009) Excitatory amino acid transporters EAAT-1 and EAAT-2 in temporal lobe and hippocampus in intractable temporal lobe epilepsy. APMIS : acta pathologica, microbiologica, et immunologica Scandinavica *117*:291-301.

Segurado R, Conroy J, Meally E, Fitzgerald M, Gill M, Gallagher L (2005) Confirmation of association between autism and the mitochondrial aspartate/glutamate carrier SLC25A12 gene on chromosome 2q31. The American journal of psychiatry *162*:2182-2184.

Setkowicz Z, Pawlinski R, Ziaja M, Janeczko K (1999) Spatiotemporal pattern of the postnatal astrogliogenesis in the rat hippocampal formation. International journal of

developmental neuroscience : the official journal of the International Society for Developmental Neuroscience *17*:215-224.

Shen HY, Sun H, Hanthorn MM, Zhi Z, Lan JQ, Poulsen DJ, Wang RK, Boison D (2014) Overexpression of adenosine kinase in cortical astrocytes and focal neocortical epilepsy in mice. Journal of neurosurgery *120*:628-638.

Sicca F, Imbrici P, D'Adamo MC, Moro F, Bonatti F, Brovedani P, Grottesi A, Guerrini R, Masi G, Santorelli FM, Pessia M (2011) Autism with seizures and intellectual disability: possible causative role of gain-of-function of the inwardly-rectifying K+ channel Kir4.1. Neurobiology of disease *43*:239-247.

Silverman JM, Buxbaum JD, Ramoz N, Schmeidler J, Reichenberg A, Hollander E, Angelo G, Smith CJ, Kryzak LA (2008) Autism-related routines and rituals associated with a mitochondrial aspartate/glutamate carrier SLC25A12 polymorphism. American journal of medical genetics Part B, Neuropsychiatric genetics : the official publication of the International Society of Psychiatric Genetics *147*:408-410.

Sloviter RS (1987) Decreased hippocampal inhibition and a selective loss of interneurons in experimental epilepsy. Science *235*:73-76.

Studer FE, Fedele DE, Marowsky A, Schwerdel C, Wernli K, Vogt K, Fritschy JM, Boison D (2006) Shift of adenosine kinase expression from neurons to astrocytes during postnatal development suggests dual functionality of the enzyme. Neuroscience *142*:125-137.

Takahashi DK, Vargas JR, Wilcox KS (2010) Increased coupling and altered glutamate transport currents in astrocytes following kainic-acid-induced status epilepticus. Neurobiology of disease *40*:573-585.

Tanaka K, Watase K, Manabe T, Yamada K, Watanabe M, Takahashi K, Iwama H, Nishikawa T, Ichihara N, Kikuchi T, Okuyama S, Kawashima N, Hori S, Takimoto M, Wada K (1997) Epilepsy and exacerbation of brain injury in mice lacking the glutamate transporter GLT-1. Science *276*:1699-1702.

Turunen JA, Rehnstrom K, Kilpinen H, Kuokkanen M, Kempas E, Ylisaukko-Oja T (2008) Mitochondrial aspartate/glutamate carrier SLC25A12 gene is associated with autism. Autism research : official journal of the International Society for Autism Research *1*:189-192.

van der Hel WS, Notenboom RG, Bos IW, van Rijen PC, van Veelen CW, de Graan PN (2005) Reduced glutamine synthetase in hippocampal areas with neuron loss in temporal lobe epilepsy. Neurology *64*:326-333.

Vermeiren C, Hemptinne I, Vanhoutte N, Tilleux S, Maloteaux JM, Hermans E (2006) Loss of metabotropic glutamate receptor-mediated regulation of glutamate transport in chemically activated astrocytes in a rat model of amyotrophic lateral sclerosis. Journal of neurochemistry *96*:719-731.

Wallraff A, Kohling R, Heinemann U, Theis M, Willecke K, Steinhauser C (2006) The impact of astrocytic gap junctional coupling on potassium buffering in the hippocampus. The Journal of neuroscience : the official journal of the Society for Neuroscience *26*:5438-5447.

Wibom R, Lasorsa FM, Tohonen V, Barbaro M, Sterky FH, Kucinski T, Naess K, Jonsson M, Pierri CL, Palmieri F, Wedell A (2009) AGC1 deficiency associated with global cerebral hypomyelination. The New England journal of medicine *361*:489-495.

Windrem MS, Schanz SJ, Morrow C, Munir J, Chandler-Militello D, Wang S, Goldman SA (2014) A competitive advantage by neonatally engrafted human glial progenitors yields mice whose brains are chimeric for human glia. The Journal of neuroscience : the official journal of the Society for Neuroscience *34*:16153-16161.

Zhang G, Raol YS, Hsu FC, Brooks-Kayal AR (2004) Long-term alterations in glutamate receptor and transporter expression following early-life seizures are associated with increased seizure susceptibility. Journal of neurochemistry *88*:91-101.

Zhang LX, Smith MA, Li XL, Weiss SR, Post RM (1998) Apoptosis of hippocampal neurons after amygdala kindled seizures. Brain research Molecular brain research *55*:198-208.

Zhang Y, Chen K, Sloan SA, Bennett ML, Scholze AR, O'Keeffe S, Phatnani HP, Guarnieri P, Caneda C, Ruderisch N, Deng S, Liddelow SA, Zhang C, Daneman R, Maniatis T, Barres BA, Wu JQ (2014) An RNA-sequencing transcriptome and splicing database of glia, neurons, and vascular cells of the cerebral cortex. The Journal of neuroscience : the official journal of the Society for Neuroscience *34*:11929-11947.

Chapter 4
Future Directions

The first part of my thesis research found an unprecedented association between the human papillomavirus type 16 oncoprotein E6 and human focal cortical dysplasia type IIB (FCDIIB) through the detection of E6 DNA, mRNA, and protein in FCDIIB brain specimens that is not detected in controls. Additionally, my research established a functional link between E6 expression and the development of cortical malformations in an acute mouse model of focal cortical malformations. Several questions on how HPV can infect the brain remain unanswered, including the mode of HPV transmission to the brain and the putative unique tropism of HPV for epithelial cells. In addition, my thesis work raised several broader questions, including whether these findings are reproducible and what they mean for the general population and the incidence of epilepsy and HPV.

The second part of my research uncovered a novel, hippocampal astrocyte apoptosis phenotype accompanied by increased astrocyte turnover, down-regulation of the glutamate reuptake transporter GLT-1, and up-regulation of adenosine kinase, resulting from Slc25a12 knockout. Because of the role astrocytes play in modulating excitatory glutamatergic neurotransmission, these findings suggest that excitotoxic glutamatergic neurotransmission preceded by astrocyte abnormalities is the root of seizures in the Slc25a12 KO mouse model. This work raises interesting questions about developmental and compensatory astrocyte homeostasis, such as whether astrocyte maturation is delayed and whether the astrocytic expression of apoptotic

markers is a definitive indicator of cellular apoptosis. In this chapter, I will discuss experimental approaches to answer these questions.

Part 1

HPV mode of transmission

Because it is believed that FCDIIB forms during embryonic brain development, the question of how HPV infection is acquired or transmitted remains. One highly appealing possibility is transplacental HPV16 infection of neuroglial progenitor cells *in utero* during brain development. The transplacental HPV transmission rate has been reported as 12.2% (Rombaldi et al., 2008), and as the prevalence of HPV infection is estimated at 26.8% (Dunne et al., 2007) in the United States, transplacental transmission of HPV16 is a plausible mechanism for entry into the brain (Figure 4.1). Alternatively, it is conceivable that the effects of HPV16 E6 could lead to FCDIIB formation in the early neonatal period.

Unfortunately, there is no easy experimental model to validate transplacental transmission. *In vitro* models, such as the mouse vaginal challenge model, are insufficient since real human papillomaviruses are dangerous to work with and not readily isolatable. One possibility is to conduct a retrospective correlational study on the HPV status of the parents of FCDIIB patients. However, this would be speculative at best, since there is no effective means of knowing whether a parent was infected with HPV before or after the birth of an FCDIIB patient. Since the advent of the HPV vaccine, prospective studies on the incidence of FCDIIB are now possible.

The tropism of human papillomavirus: Can HPV infect the brain?

Human papillomavirus type 16 is widely known as the virus that causes cervical cancer, and it is generally believed that HPV displays unique tropism for

epithelial cells. However, recent research has yielded an increasing body of evidence indicating that this may not be this case. HPV has been detected in peripheral nerves adjacent to oropharyngeal cancers and in spermatozoa (Füle et al., 2006; Foresta et al., 2011). Additionally, the detection of HPV genomic elements and oncoproteins in human FCDIIB brain provides further evidence for the widespread tropism of HPV.

HPV infection has been demonstrated *in vitro* and *in vivo* to occur through the binding of viral capsid protein L1 to cell surface HSPGs (Giroglou et al., 2001; Horvath et al., 2010; Schiller et al., 2010). Additional studies have specified syndecan-1 as the critical HSPG needed for HPV binding and infection (Shafti-Keramat et al., 2003; Knappe et al., 2007). Syndecan-1, a type I transmembrane HSPG and a member of the syndecan proteoglycan family is highly expressed in neuroglial progenitor cells in the ventricular zone of the developing brain, but not in mature neurons (Nakanishi et al., 1997), suggesting that neuroglial progenitor cells may be susceptible to infection by HPV during development.

One experiment that can answer the question of whether neuroglial progenitor cells can be infected by HPV is to culture murine neuroglial progenitor cells (mNPCs) with HPV pseudoviruses. Pseudoviruses are commonly used in HPV research as they do not contain viral genomes and are considered biologically safe reagents. They are generated by introducing two plasmids into 293TT cells: one encoding both viral capsid proteins L1 and L2; and the other, which serves as the viral "pseudogenome," encoding E6-GFP under the control of the SV40 origin of replication. Viral capsid proteins assemble *in vitro* and encapsulate the pseudogenome. The resultant pseudoviruses can then be extracted by detergent lysis

and purified using density gradient ultracentrifugation.

mNPC infectability can be assayed by co-culturing with HPV pseudoviruses. Infection is achieved when the pseudogenome containing GFP is transmitted to the host cell. The necessity of syndecan-1 for HPV pseudovirus infection can be tested by stably knocking down syndecan-1 in mNPCs and assaying for infection. The ability of syndecan-1 to facilitate HPV pseudovirus infection on its own can also be tested by transiently transfecting syndecan-1 into K562 cells (which do not normally express syndecan-1).

It is possible that L1 may bind syndecan-1, but mNPCs may not be infected. As pseudoviruses have been demonstrated to be agents of infection in other cell types that express syndecan-1, this suggests that perhaps other proteins may be involved in facilitating pseudovirus infection that may not be expressed in mNPCs, but may be expressed in cells of an earlier developmental time point, such as neural stem cells. Additionally, L1 may not bind syndecan-1, but mNPCs may become infected. However, given that the dissociation constant of L1 to heparan sulfate groups is in the range of 10^{-5}-10^{-7} M *in vitro* (Sun et al., 2010), the possibility that L1 will not bind syndecan-1 is very low. However, if there is no binding, it would suggest that HPV pseudoviruses use other proteins to facilitate infection in mNPCs and that the mechanism of HPV infection in neural cell types is unique and different from that which governs epithelial cells.

Lastly, L1 may not bind syndecan-1 in any neural cell type suggesting that there may be species-specific interactions inhibiting HPV pseudovirus binding and infection or neural cell types are unable to be infected by HPV. In the case of the

former, a reasonable follow-up experiment would be to test HPV pseudovirus infectability in human neuroglial progenitor cells, which are commercially available. In the case of the latter, it is possible that HPV can enter the brain by virtue of somatic genome integration when an infected sperm fertilizes an oocyte.

Reproducibility of results

Since the publication of the data in Chapter 2, three independent groups have repeated this study to varying results. The first of these published reports, published in 2014 (Liu et al., 2014), conducted PCR and immunohistochemistry for HPV on 27 FCDIIA and 20 FCDIIB specimens. Their data indicate that HPV16 was detected in 90% of FCDIIB and 22.2% of FCDIIA specimens. My thesis research indicated that HPV16 E6 was present in balloon cells of FCDIIB, making its detection in FCDIIA, a focal malformation disorder without balloon cells, an interesting finding. In addition to detecting HPV, Liu and colleagues also detected four other common intrauterine infection-related viruses – cytomegalovirus (19.1%), human herpes virus-6B (12.7%), and herpes simplex virus-1 (31.9%) in non-specified FCD specimens. Of 36 normal brain specimens examined, only 2 were positive for viral expression (not specified). While their data support the findings of Chapter 2, the discovery of additional viruses in FCD specimens detracts from the hypothesized causal association between HPV and FCDIIB, as it is not known how the other viruses affect mTOR signaling and brain development. Cytomegalovirus in particular, and herpes simplex virus-1 to a lesser extent, have both been associated with seizures in a number of reports (Jay et

al., 1995; Suzuki et al., 2008), suggesting that viral infection and propagation may be a common denominator in the alteration of early brain development.

The other two reports, both published in 2015, were unable to replicate our findings. In the first (Shapiro et al., 2015), 14 distinct FCDIIB specimens obtained from one surgical center were tested for HPV using PCR, *in situ* hybridization, chromogenic *in situ* hybridization, and immunohistochemistry. HPV was not detected by PCR, *in situ* hybridization, or chromogenic *in situ* hybridization. They expressed concern about degraded DNA quality from tissue specimens, citing that 7 of the 14 specimens failed to generate an adequate amplicon, leaving the amplicons detected in the other 7 samples subject to investigation. No mention was made as to the size of the amplicons detected, or whether sequencing analysis was conducted. Shapiro and colleagues conducted immunohistochemistry for p16INK4a, a cyclin-dependent kinase inhibitor that is highly associated with HPV infection and used as a surrogate marker of HPV infection, and found that 3 of 10 cases examined exhibited immunoreactivity in balloon cells. HPV16 E6 immunohistochemistry was not conducted. The discrepancy between the findings of Shapiro and colleagues and the findings presented in Chapter 2 may be due to the variability in the rate of HPV infection in various populations. The cohort used in this study came from a single surgical center, which may be located in an area with low HPV exposure. The authors are quick to point out that the animal model in our study did not contain dysmorphic neurons and balloon cells. It is possible that the temporal expression of E6 (5 days) was too short to result in morphological cellular deficits. Future studies will need to

be conducted on postnatal mice to determine whether extended expression of E6 will result in cytopathic effects concomitant with eventual seizures.

The third and last published report on FCDIIB and HPV probed 14 FCDIIB specimens using 4 PCR primers for HPV DNA and antibodies against E6 (Coras et al., 2015). Interestingly, all 14 specimens did not yield amplicons for HPV DNA, and immunohistochemistry for E6 revealed weak staining in FCDIIB specimens as well as in TSC specimens, attributed to a non-specific antibody and technical pitfalls when using formalin-fixed paraffin-embedded brain tissues. No antibody controls were conducted.

The lack of HPV detection by PCR by two of three research groups is puzzling. It is possible that HPV DNA can exist as an episome or as an integrated genome in the host cell nucleus. Perhaps HPV DNA that has successfully integrated is more amenable to amplification by PCR. In the case of the former, detection would be more likely using *in situ* hybridization, which Shapiro and colleagues conducted, with no detection. Considering these differing findings, it is clear that the association between HPV16 and FCDIIB is highly contested and will not be resolved without more replication and research.

Part 2

Region-specific astrocyte apoptosis/mechanism of astrocyte apoptosis

In human temporal lobe epilepsy as well as many seizure models, neuronal cell death is evident in the hippocampus. For astrocytes, however, the literature on apoptosis is very sparse. Since the time of Santiago Ramon y Cajal, astrocytes have garnered a reputation for being hardier than neurons. Thus, our finding that astrocytes undergo apoptosis in the hippocampus before the onset of behavioral seizures is both novel and unprecedented. However, the mechanism underlying how loss of Slc25a12 leads to astrocyte cell death is still unknown.

Though we have made every effort to be rigorous in the analysis of the timeline of the onset of both astrocyte apoptosis and behavioral seizures, one possibility that we must consider is that seizure-like electroencephalographic (EEG) abnormalities can be present without, and possibly before, the onset of behavioral manifestations. However, measuring EEG in mouse pups under 2 weeks of age remains a challenge due to the non-availability of small electrode devices and set ups that accommodate the small size of pups. This limitation is reflected in the current studies on Slc25a12 KO mice, which have not examined EEGs earlier than P15 (Gómez-Galán et al., 2012). However, even current studies raise more questions than answers. Analyzing local field potentials (LFP) from hippocampus of wild type and Slc25a12 KO mice aged P16 to P22, one group reported reduced LFP power in Slc25a12 KO (Gómez-Galán et al., 2012), which is inconsistent with LFPs recorded from other seizure models (Queiroz et al., 2009; Keller et al., 2010). They argued that their LFPs are generated from hippocampal inhibitory interneurons by citing a deficit

in gamma oscillations (waveforms propagated by GABAergic interneurons) as well as a reduction in glutamic acid decarboxylase in Slc25a12 KO animals. Their evidence suggests that Slc25a12 KO mice are deficient in GABA, implicating GABAergic interneurons as the major driver of seizure genesis in Slc25a12 KO animals. We submit that there may be global network deficiencies in Slc25a12 KO mice, including contributions from GABAergic interneurons. However, our analyses have pointed us toward the astrocyte as the major contributor in seizure genesis, as GABAergic interneurons are largely unaffected by Slc25a12 KO.

To account for astrocytic cell death, one possibility to consider is the role of astrocytic metabotropic glutamate receptor 5 (mGluR5). Astrocytic mGluR5 has a demonstrated role in neuron-glia interactions, including the regulation of glutamate reuptake (Vermeiren et al., 2006), and the expression of mGluR5 has also been shown to be up-regulated in some models of epilepsy (Ferraguti et al., 2001; Aronica et al., 2003). Additionally, in one study of murine primary cortical astrocyte cultures, enhanced astrocytic mGluR5 expression resulting from oxygen glucose deprivation resulted in the activation of phospholipase C and release of intracellular calcium stores, leading to subsequent astrocyte cell death (Paquet et al., 2013). Though this mechanism of astrocyte cell death has not been demonstrated *in vivo,* it is possible that Slc25a12 KO cells experience partial glucose and oxygen deprivation by virtue of their inability to maximally utilize glucose and oxygen (Pardo et al., 2011). This partial deprivation may also explain the localized specificity of astrocyte cell death, as brain regions vary in their metabolic demands, lending those regions with higher

demands, such as the hippocampus, to be increasingly susceptible to perturbations in glucose utilization.

One possibility that is appealing to speculate upon is that the expression of cleaved caspase 3 and cleaved PARP in Slc25a12 KO astrocytes are not actually indicators of cellular apoptosis, but rather, are expressed proteins that are used for other cellular processes. Indeed, in addition to the role of apoptotic executioner proteins in morphogenesis, cellular maturation, and differentiation, apoptotic executioner proteins have also been demonstrated to be critical in compensatory cellular proliferation and regeneration in many species, including mouse (Carlile et al., 2004; Sztiller-Sikorska et al., 2009; Khalil et al., 2012; Miura, 2012). It is worth noting that it is the *uncleaved* isoforms of these executioner caspases that are involved in these various cellular processes. Therefore, given that the astrocytes in Slc25a12 KO hippocampus exhibit robust cleaved caspase 3 and cleaved PARP, proteins in the final common pathway of apoptosis, it is very likely the astrocytes in Slc25a12 KO are undergoing apoptosis, and not facilitating the regulation of another cellular process.

Astrocyte maturation

The increased expression of the immature astrocyte marker CD44 begs the question of whether astrocytes are truly undergoing compensatory cell turnover or whether astrocytes simply fail to mature properly. In support of the failure to achieve maturation hypothesis, immature astrocytes consistently express reduced levels of glutamate reuptake transporter GLT-1 in comparison to mature astrocytes (Furuta et

al., 1997; Kugler and Schleyer, 2004). The fact that we see down-regulated levels of GLT-1 in Slc25a12 KO hippocampus supports this hypothesis. However, it is worth noting that we have also observed GLT-1 reduction in cortical protein lysates of Slc25a12 KO brains (data not shown). The expression of CD44 in Slc25a12 KO mouse brain, however, is restricted to the hippocampus. The presence of astrocyte precursor cells in the region of the hippocampus where astrocyte apoptosis is occurring is not coincident, and suggests that astrocytes undergo cell turnover in the hippocampus to account for dying cells. Since it had been previously demonstrated that astrocytes undergo local proliferation (Ge et al., 2012), this hypothesis is likely to be a possibility.

Nuclear sequestration of ADK in Slc25a12 KO astrocytes

Our finding of enhanced localization of ADK-L in astrocytic nuclei is not consistent with previous findings in mouse seizure models of increased ADK-S localization in astrocytic cytoplasm. Furthermore, the discrepancy between the immunohistochemical and Western data is puzzling. It is possible that putative increases in nuclear ADK levels may be masked by the total amount of protein present. The differential functions of the two ADK isoforms have not been elucidated to date. So far, there is evidence to suggest that cytoplasmic ADK (ADK-S) may be responsible for maintaining the balance of extracellular adenine nucleotides, while nuclear ADK (ADK-L) contributes to epigenetic functions related to cell proliferation (Cui et al., 2009). It is unclear whether nuclear localization of ADK shares the same linkage to seizures as the previously established cytoplasmic ADK. Western assays

on proteins from nuclear and cytoplasmic fractionation may help us resolve the true extent of ADK expression and localization. However, it is appealing to speculate that enhanced nuclear ADK-L in astrocytes may play a role in the enhancement of astrocyte numbers we observed at P16, due to its putative effects on cell proliferation. More studies, such as an astrocyte-specific ADK knockdown need to be conducted in order to establish a mechanism of action linking nuclear ADK and astrocyte proliferation.

ADK inhibition and treating seizures

Our data suggesting a link between astrocytes, ADK, and glutamate on seizures prompted us to investigate whether reinstating adenosine-modulated inhibitory tone would ameliorate behavioral seizures. To this extent, we plan to treat Slc25a12 KO mice with the ADK inhibitor 4-amino-5-(3-bromophenyl)-7-(6-morpholino-pyridin-3-yl)pyrido[2,3-d]pyrimidine, (ABT-702) and monitor them for behavioral seizures, as described previously. ADK inhibitors have been used to effectively treat and prevent seizures in animal models (Li et al., 2008). ABT-702 is 9-fold more potent than other ADK inhibitors such as 5-iodotubercidin (5-IT), and works by binding to the phosphorylation site on adenosine where ADK would normally bind, preventing it from interacting with ADK (Jarvis et al., 2000). It is highly selective for this region, as it has not been demonstrated to bind to other sites of adenosine interaction, such as with the A_1, A_{2A}, A_3 receptors and the adenosine transporter and deaminase binding regions, and its binding affinity for this site is high ($K_i = 1.4 \pm 0.8$ nM) (Jarvis et al., 2000). Though structure-activity relationships and

computational modeling indicate that the half-life of ABT-702 is short at 2.42 hours, it is longer than that of 5-IT and its high binding affinity suggests that though free ABT-702 may be degraded in a short amount of time, the effects of bound ABT-702 are long lasting (Zheng et al., 2001).

Inhibiting the activity of ADK can result in sedation due to its effects on increasing bioavailable adenosine. In a pilot study, we determined that 10 µg/kg (i.p.) daily for young mouse pups resulted in minimal sedation that resolved itself within 12 hours. We will be administering this dose to mouse pups from P10-P16 and monitoring for behavioral seizures using video recording. As previously speculated, the link between ADK and seizures in Slc25a12 KO is tenuous considering its nuclear localization. Furthermore, the ability of ABT-702 to cross the nuclear membrane is unknown. If ABT-702 treatment results in minimal seizure amelioration, other avenues such as activators of glutamate reuptake transporters or apoptotic inhibitors can be explored. Evidence in the human and animal models of epilepsy literature cites the efficacy of the ketogenic diet for ameliorating seizures related to metabolic deficiencies (Beniczky et al., 2010; Noh et al., 2003; Yudkoff et al., 2005). In Slc25a12 KO mice however, we have found that the ketogenic diet given to Slc25a12 KO pups through consumption by the dam, caused both pups and dams to lose weight and may have contributed to premature pup death. There is evidence to suggest that implementing the ketogenic diet during gestation alters brain structure and embryonic organ growth leading to postnatal dysfunction (Sussman et al., 2013a; Sussman et al., 2013b). Because the brain is still developing in neonatal mice, it is possible that neonatal administration of ketogenic diet may contribute to altered brain structure and

metabolic status as seen in pups treated *in utero*. In light of the astrocyte pathology observed in Slc25a12 KO mice, we submit that a more astrocyte-centric approach to therapy, such as ADK inhibitors, may be beneficial in treating seizures.

Other effects of Slc25a12 loss of function

Though most studies in the literature have focused on the role of Slc25a12 on generating ATP, loss of Slc25a12 affects other cellular processes as well. As mentioned previously, the role of Slc25a12 in cells is to shuttle reducing equivalents (NADH), which are otherwise unable to cross the inner mitochondrial membrane, into the mitochondria. When the ratio of NADH to NAD+ becomes high in the cytosol, as it would if Slc25a12 was not functioning properly, glycolysis, which uses NAD+ as an intermediate, will shut down. This results in a metabolic "double-hit," where the cell with deficient Slc25a12 is not only deficient in oxidative phosphorylation, but also in the secondary mechanism of energy production, glycolysis. This may result in a build up of lactate, which can be toxic to cells. However, in our preliminary analysis, we (and others) did not observe an increase in lactate production *in vivo* by magnetic resonance spectroscopy (Pardo et al., 2011) or *in vitro* using conditioned media from mixed and astrocyte only cultures (data not shown), indicating that there may be compensatory shuttling of reducing equivalents by other transporters such as the glycerol-3-phosphate shuttle.

Another often over-looked function of Slc25a12 is its calcium-binding N-terminal. Slc25a12 requires the binding of calcium to facilitate its transporter capabilities; in situations where Slc25a12 protein function or expression is reduced, it

is possible that the cell may experience a build-up of intra-mitochondrial calcium, which can affect many processes, including cellular excitability. Imaging mitochondria using calcium dyes would enable us to determine whether an increase in intra-mitochondrial calcium is occurring, and additional experiments to determine the morphology and localization of mitochondria would shed light on whether Slc25a12 loss of function results in additional mitochondrial dysfunction.

Figure 4.1. Hypothesized model of HPV infection *in utero.*

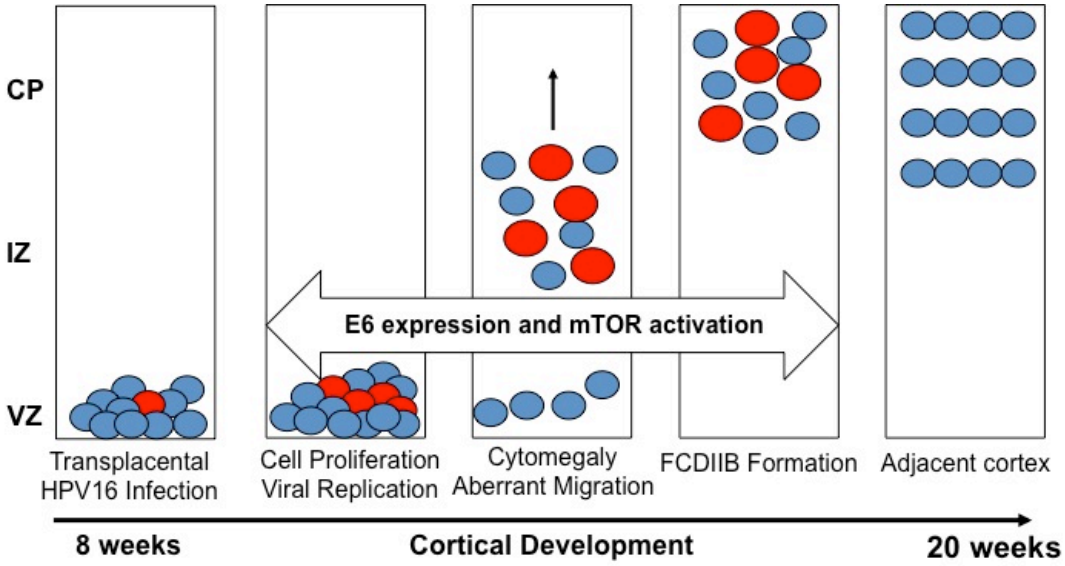

Figure 4.1. Hypothesized model of HPV infection *in utero.*

A single cell is infected transplacentally, where it proliferates and passes the viral load on to its daughter cells. The infected cells activate the mTOR signaling cascade and become cytomegalic,, leading to a focal malformation, surrounded by healthy cells.

References

Aronica E, Gorter JA, Jansen GH, van Veelen CW, van Rijen PC, Ramkema M, Troost D (2003) Expression and cell distribution of group I and group II metabotropic glutamate receptor subtypes in taylor-type focal cortical dysplasia. Epilepsia *44*:785-795.

Beniczky S, Jose Miranda M, Alving J, Heber Povlsen J, Wolf P (2010) Effectiveness of the ketogenic diet in a broad range of seizure types and EEG features for severe childhood epilepsies. Acta neurologica Scandinavica *121*:58-62.

Carlile GW, Smith DH, Wiedmann M (2004) Caspase-3 has a nonapoptotic function in erythroid maturation. Blood *103*:4310-4316.

Coras R, Korn K, Bien CG, Kalbhenn T, Rossler K, Kobow K, Giedl J, Fleckenstein B, Blumcke I (2015) No evidence for human papillomavirus infection in focal cortical dysplasia IIb. Annals of neurology *77*:312-319.

Cui XA, Singh B, Park J, Gupta RS (2009) Subcellular localization of adenosine kinase in mammalian cells: The long isoform of AdK is localized in the nucleus. Biochemical and biophysical research communications *388*:46-50.

Dunne EF, Unger ER, Sternberg M, McQuillan G, Swan DC, Patel SS, Markowitz LE (2007) Prevalence of HPV infection among females in the United States. Jama *297*:813-819.

Ferraguti F, Corti C, Valerio E, Mion S, Xuereb J (2001) Activated astrocytes in areas of kainate-induced neuronal injury upregulate the expression of the metabotropic glutamate receptors 2/3 and 5. Experimental brain research *137*:1-11.

Foresta C, Patassini C, Bertoldo A, Menegazzo M, Francavilla F, Barzon L, Ferlin A (2011) Mechanism of human papillomavirus binding to human spermatozoa and fertilizing ability of infected spermatozoa. PloS one *6*:e15036.

Fule T, Mathe M, Suba Z, Csapo Z, Szarvas T, Tatrai P, Paku S, Kovalszky I (2006) The presence of human papillomavirus 16 in neural structures and vascular endothelial cells. Virology *348*:289-296.

Furuta A, Rothstein JD, Martin LJ (1997) Glutamate transporter protein subtypes are expressed differentially during rat CNS development. The Journal of neuroscience : the official journal of the Society for Neuroscience *17*:8363-8375.

Ge WP, Miyawaki A, Gage FH, Jan YN, Jan LY (2012) Local generation of glia is a major astrocyte source in postnatal cortex. Nature *484*:376-380.

Giroglou T, Florin L, Schafer F, Streeck RE, Sapp M (2001) Human papillomavirus infection requires cell surface heparan sulfate. Journal of virology *75*:1565-1570.

Gomez-Galan M, Makarova J, Llorente-Folch I, Saheki T, Pardo B, Satrustegui J, Herreras O (2012) Altered postnatal development of cortico-hippocampal neuronal electric activity in mice deficient for the mitochondrial aspartate-glutamate transporter. Journal of cerebral blood flow and metabolism : official journal of the International Society of Cerebral Blood Flow and Metabolism *32*:306-317.

Jarvis MF, Yu H, Kohlhaas K, Alexander K, Lee CH, Jiang M, Bhagwat SS, Williams M, Kowaluk EA (2000) ABT-702 (4-amino-5-(3-bromophenyl)-7-(6-morpholinopyridin-3-yl)pyrido[2, 3-d]pyrimidine), a novel orally effective adenosine kinase inhibitor with analgesic and anti-inflammatory properties: I. In vitro characterization and acute antinociceptive effects in the mouse. The Journal of pharmacology and experimental therapeutics *295*:1156-1164.

Jay V, Becker LE, Otsubo H, Cortez M, Hwang P, Hoffman HJ, Zielenska M (1995) Chronic encephalitis and epilepsy (Rasmussen's encephalitis): detection of cytomegalovirus and herpes simplex virus 1 by the polymerase chain reaction and in situ hybridization. Neurology *45*:108-117.

Keller CJ, Truccolo W, Gale JT, Eskandar E, Thesen T, Carlson C, Devinsky O, Kuzniecky R, Doyle WK, Madsen JR, Schomer DL, Mehta AD, Brown EN, Hochberg LR, Ulbert I, Halgren E, Cash SS (2010) Heterogeneous neuronal firing patterns during interictal epileptiform discharges in the human cortex. Brain : a journal of neurology *133*:1668-1681.

Khalil H, Peltzer N, Walicki J, Yang JY, Dubuis G, Gardiol N, Held W, Bigliardi P, Marsland B, Liaudet L, Widmann C (2012) Caspase-3 protects stressed organs against cell death. Molecular and cellular biology *32*:4523-4533.

Knappe M, Bodevin S, Selinka HC, Spillmann D, Streeck RE, Chen XS, Lindahl U, Sapp M (2007) Surface-exposed amino acid residues of HPV16 L1 protein mediating interaction with cell surface heparan sulfate. The Journal of biological chemistry *282*:27913-27922.

Kugler P, Schleyer V (2004) Developmental expression of glutamate transporters and glutamate dehydrogenase in astrocytes of the postnatal rat hippocampus. Hippocampus *14*:975-985.

Li T, Ren G, Lusardi T, Wilz A, Lan JQ, Iwasato T, Itohara S, Simon RP, Boison D (2008) Adenosine kinase is a target for the prediction and prevention of epileptogenesis in mice. The Journal of clinical investigation *118*:571-582.

Liu S, Lu L, Cheng X, Xu G, Yang H (2014) Viral infection and focal cortical dysplasia. Annals of neurology *75*:614-616.

Miura M (2012) Apoptotic and nonapoptotic caspase functions in animal development. Cold Spring Harbor perspectives in biology *4*.

Nakanishi T, Kadomatsu K, Okamoto T, Ichihara-Tanaka K, Kojima T, Saito H, Tomoda Y, Muramatsu T (1997) Expression of syndecan-1 and -3 during embryogenesis of the central nervous system in relation to binding with midkine. Journal of biochemistry *121*:197-205.

Noh HS, Kim YS, Lee HP, Chung KM, Kim DW, Kang SS, Cho GJ, Choi WS (2003) The protective effect of a ketogenic diet on kainic acid-induced hippocampal cell death in the male ICR mice. Epilepsy research *53*:119-128.

Paquet M, Ribeiro FM, Guadagno J, Esseltine JL, Ferguson SS, Cregan SP (2013) Role of metabotropic glutamate receptor 5 signaling and homer in oxygen glucose deprivation-mediated astrocyte apoptosis. Molecular brain *6*:9.

Pardo B, Rodrigues TB, Contreras L, Garzon M, Llorente-Folch I, Kobayashi K, Saheki T, Cerdan S, Satrustegui J (2011) Brain glutamine synthesis requires neuronal-born aspartate as amino donor for glial glutamate formation. Journal of cerebral blood flow and metabolism : official journal of the International Society of Cerebral Blood Flow and Metabolism *31*:90-101.

Queiroz CM, Gorter JA, Lopes da Silva FH, Wadman WJ (2009) Dynamics of evoked local field potentials in the hippocampus of epileptic rats with spontaneous seizures. Journal of neurophysiology *101*:1588-1597.

Rombaldi RL, Serafini EP, Mandelli J, Zimmermann E, Losquiavo KP (2008) Transplacental transmission of Human Papillomavirus. Virology journal *5*:106.

Schiller JT, Day PM, Kines RC (2010) Current understanding of the mechanism of HPV infection. Gynecologic oncology 118:S12-17.

Shafti-Keramat S, Handisurya A, Kriehuber E, Meneguzzi G, Slupetzky K, Kirnbauer R (2003) Different heparan sulfate proteoglycans serve as cellular receptors for human papillomaviruses. Journal of virology *77*:13125-13135.

Shapiro KA, McGuone D, Deshpande V, Sadow PM, Stemmer-Rachamimov A, Staley KJ (2015) Failure to detect human papillomavirus in focal cortical dysplasia type IIb. Annals of neurology.

Sun J, Yu JS, Jin S, Zha X, Wu Y, Yu Z (2010) Interaction of synthetic HPV-16 capsid peptides with heparin: thermodynamic parameters and binding mechanism. The journal of physical chemistry B *114*:9854-9861.

Sussman D, Ellegood J, Henkelman M (2013a) A gestational ketogenic diet alters maternal metabolic status as well as offspring physiological growth and brain structure in the neonatal mouse. BMC pregnancy and childbirth *13*:198.

Sussman D, van Eede M, Wong MD, Adamson SL, Henkelman M (2013b) Effects of a ketogenic diet during pregnancy on embryonic growth in the mouse. BMC pregnancy and childbirth *13*:109.

Suzuki Y, Toribe Y, Mogami Y, Yanagihara K, Nishikawa M (2008) Epilepsy in patients with congenital cytomegalovirus infection. Brain & development *30*:420-424.

Sztiller-Sikorska M, Jakubowska J, Wozniak M, Stasiak M, Czyz M (2009) A non-apoptotic function of caspase-3 in pharmacologically-induced differentiation of K562 cells. British journal of pharmacology *157*:1451-1462.

Vermeiren C, Hemptinne I, Vanhoutte N, Tilleux S, Maloteaux JM, Hermans E (2006) Loss of metabotropic glutamate receptor-mediated regulation of glutamate transport in chemically activated astrocytes in a rat model of amyotrophic lateral sclerosis. Journal of neurochemistry *96*:719-731.

Yudkoff M, Daikhin Y, Nissim I, Horyn O, Lazarow A, Luhovyy B, Wehrli S, Nissim I (2005) Response of brain amino acid metabolism to ketosis. Neurochemistry international 47:*119*-128.

Zheng GZ, Lee C, Pratt JK, Perner RJ, Jiang MQ, Gomtsyan A, Matulenko MA, Mao Y, Koenig JR, Kim KH, Muchmore S, Yu H, Kohlhaas K, Alexander KM, McGaraughty S, Chu KL, Wismer CT, Mikusa J, Jarvis MF, Marsh K, Kowaluk EA, Bhagwat SS, Stewart AO (2001) Pyridopyrimidine analogues as novel adenosine kinase inhibitors. Bioorganic & medicinal chemistry letters *11*:2071-2074.